Some optical properties of the alkali halides containing divalent impurities

B. K. Ridley

SOME OPTICAL PROPERTIES OF THE ALKALI HALIDES CONTAINING DIVALENT IMPURITIES

by

B. K. Ridley,

Ph.D. Thesis, 1957.

ABSTRACT

The investigation was limited mainly to $NaCl.Mn^{++}$ and $NaCl.Ca^{++}$, and was concerned with colour centres in single crystals of these materials. The crystals were grown by the Kyropoulis technique and optical absorption measurements were made with a grating spectrophotometer. The emphasis of the work was placed on the production of Z-bands in $NaCl.Ca^{++}$ but the effects of optical and thermal bleaching and of quenching were investigated in all crystals.

The results of the work on $NaCl.Mn^{++}$ confirmed the model of Schneider and Caffyn (1955) in which the Mn^{++} ions and positive ion vacancies are deposited at dislocations and become more uniformly distributed after quenching. In particular, it was found that quenched crystals were luminescent after being X-rayed, indicating the presence of dispersed Mn^{++} ions; a similar result was found in $NaCl.Ni^{++}$. A short study of the distribution of Mn^{++} in crystals was also made.

It was found that Mn^{++} and Ni^{++} gave rise to characteristic bands in the ultra violet, a weak band at 275 mμ with Mn^{++}, a strong band at 247 mμ with Ni^{++}. The presence of a band at 255 mμ in $NaCl.Cu^{++}$ was confirmed. No evidence was obtained for the formation of Z-bands by Mn^{++}, Ni^{++} or Cu^{++}.

Calcium was found to be much more soluble in NaCl than manganese, and enhanced the colouribility proportionately less, pointing to a close relationship between solubility, mis-match, and the production of negative ion vacancies. Analysis of the F-band in coloured $NaCl.Ca^{++}$ crystals indicated that Z-centres were formed by X-rays. Quenching enhanced the number of Z-centres, indicating a deposition at dislocations similar to that found for manganese. Evidence for the formation of both Z_1- and Z_2-centres by X-irradiation was found. In crystals containing a high proportion of Ca^{++} a band at 345 mμ, which is probably to be associated with Ca^{++}-positive ion vacancy complexes, was prominent.

The results of an investigation of the effect of concentration of Ca^{++} on the growth of the F- and Z-bands indicated that a Ca^{++} ion introduced about ten negative ion vacancies into the crystal. On the basis of a statistical mechanical model of the formation of Z-centres it was inferred that of the Ca^{++} ions producing Z-centres no more than 2% were associated with positive ion vacancies, confirming the work of Etzel (1952). It was also inferred that the activation energy associated with the liberation of Ca^{++} ions from dislocations to form incipient Z-centres was 1.9 eV, a value which agreed well with an estimated value.

Factors influencing the width of the F-band are also discussed.

CONTENTS

1 INTRODUCTION

1.1 Introduction

Many of the properties of certain solid materials which in the past have been thought to be intrinsic properties of the pure material are now regarded as manifestations of small quantities of impurity resident in the base material. Notably, it has been found that many, but not all, substances owe their semiconducting properties to this cause, and these properties can be profoundly modified by the choice of impurity added. Further, it has become evident that the effect of an impurity is out of all proportion to the quantity present: one impurity atom for every 10^5 atoms of the base material is ample to provide an observable effect. Since impurity concentrations of this order are prevalent in ordinary "pure" materials manufactured in bulk it becomes difficult, if not impossible, to differentiate between intrinsic properties and properties due to impurities; and until purer materials are generally available, this difficulty will not be resolved. While a claim that a particular property of a solid is an intrinsic one must be viewed with caution, there are many properties which are obviously not intrinsic but due to impurities, and it is with these that this work is concerned in the main.

The alkali halides, with their simple cubic lattice crystal structure, make an ideal base material not only for this type of study but for the broader study of the structure of solids in general. The model of an ideal alkali halide single crystal is the repetition throughout the volume of the crystal of a cube which has at its corners alternately metal and halogen ions. There is every reason to suppose that this picture is a correct one providing the size of the crystal is drastically limited to the order of 100Å cubed, but for sizes of crystals used in practice it must be regarded as only a first approximation to the truth, for during growth imperfections of many types are formed and frozen into the crystal. Notable among these are dislocations, areas of strain within the crystal, produced by the existence of extra planes of ions each extra plane producing an edge-dislocation, or by the twisting of planes of ions to give screw-dislocations; and vacancies in the lattice, produced by ions migrating to the surface giving Schottky defects, or by ions migrating to interstitial positions giving Frenkel defects, (see Wagner and Schottky, 1930, and Frenkel, 1926). In the current theory these imperfections are responsible for many of the properties of the crystal.

Lattice defects and associations of lattice defects can form colour centres under conditions where free electrons and holes are present in the crystal, and these give rise to optical absorption bands in the visible and the near ultra violet and

Fig. 1 COLOUR CENTRES.

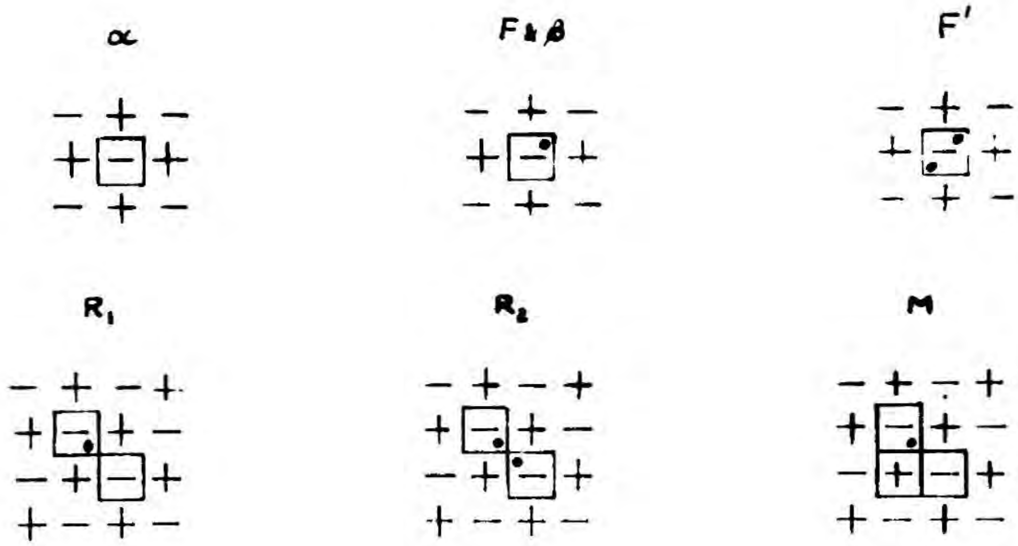

(a) F-type Centres

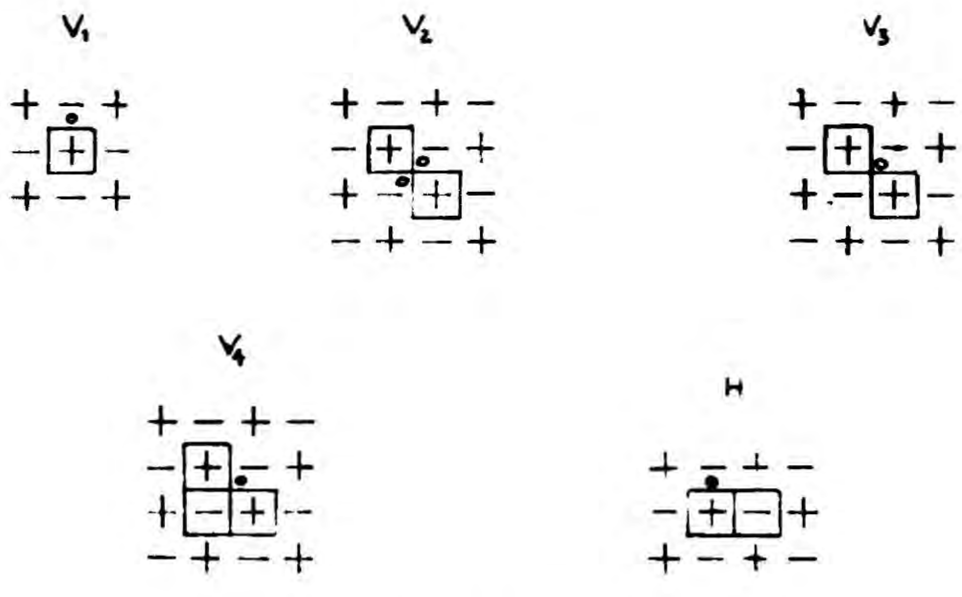

(b) V-type Centres

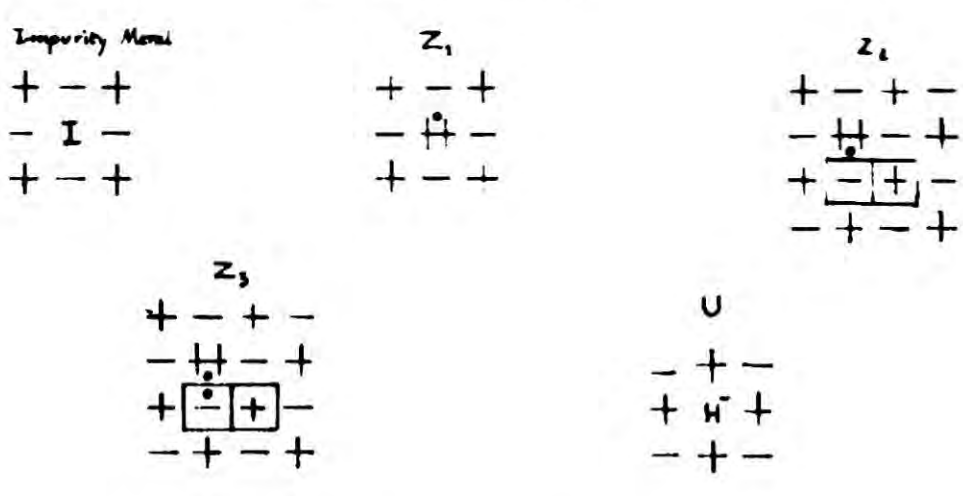

(c) Impurity Centres

infra red; consequently, measurement of absorption spectra has yielded much information about colour centres. Impurity ions, themselves imperfections, also modify the absorption spectrum. In particular, the modifications produced by certain divalent impurities is the subject of this research.

To appreciate the effect of an impurity on a property it is essential to know something about the property it is modifying. Before reviewing the work already done on alkali halides containing impurities it is necessary, therefore, to outline briefly the information regarding colour centres.

1.2 Electron Traps in the Alkali Halides.

(a) The Negative Ion Vacancy.

Many polar salts, when heated in the vapour of one of their constituent elements, acquire a stoichiometric excess of that component. In the case of an alkali halide crystal heated in the vapour of the corresponding metal, the crystal acquires a stoichiometric excess of the metal and at the same time becomes deeply coloured - yellowish brown for NaCl, blue for KCl, and so on. Such coloured crystals are known as additively coloured crystals. Since their discovery by Goldstein (1896) the properties of coloured crystals have been studied in great detail by Pohl and his co-workers (see, for example R. W. Pohl, 1937, 1938, 1952), whose results enable a fairly complete picture of these phenomena to be built up.

Measurements of the absorption of coloured alkali halides have revealed that the colouration is due to an absorption band whose peak wavelength is characteristic of the alkali halide, moving from the blue to the red end of the spectrum in the series LiCl, NaCl, KCl, RbCl, CsCl. This band is known as the F-band (from the German Farbzentren, or colour centres) and the absorbing centres F-centres. De Boer (1937) suggested that F-centres were electrons trapped at negative ion vacancies, and there is appreciable evidence to support this model, notably, the density measurements on coloured crystals made by Estermann et al (1949).

The mechanism of the formation of F-centres in additively coloured crystals is probably as follows. The alkali atoms of the vapour ionize at the surface and become part of the lattice, forming a complimentary number of negative ion vacancies and free electrons. At the high temperature of the crystal these vacancies can diffuse into the body of the crystal and become uniformly dispersed. Since effectively, they are positively charged, they will attract and trap electrons from the ionized alkali atoms, and so become F-centres. Quanta of F-light (light absorbed by the F-centres) can then energize the trapped electron to the first excited level of the centre, and thus the crystal shows an absorption band.

There is a close analogy between the F-centre and the hydrogen atom, since both contain an electron trapped in a central Coulomb field, and this has been used to calculate the energy level scheme of the F-centre by Simpson (1949), Lehovac (1953), and others. The ground state of the trapped electron (the 1s state) is about 3.5 eV below the conduction band minimum in NaCl, while the first excited state (by analogy with the hydrogen atom, a 2p state) is about 1 eV below the conduction band minimum. The transition 1s to 2p is responsible for the F-band. Mott and Gurney (1940) suggested that transitions to higher levels were responsible for the short wavelength tail of the F-band, observed by Kleinschrod (1936).

F-centres can also be formed by exposing the crystal to ionizing radiation, indicating the existence of negative ion vacancies already present in the crystal. The radiation liberates electrons and holes which wander through the crystal until recombination or trapping occurs. The colour centre formed in this way is much more unstable than that formed additively, prolonged exposure to F-light destroying the colour completely, corresponding to the liberation of the trapped electrons by the light and their subsequent recombination with trapped holes.

It is possible for the F-centre to capture a second electron, and the resulting centre is known as an F'-centre, producing a broad adsorption band in the near infra red. The F'-band is formed over a limited temperature range when the F-band is bleached. In the case of KCl this range is from -130°C to -80°C. Above this range the F'-centre is thermally unstable; below, the F-centre remains unionized by the F-light. Normally, at room temperatures the F'-band is not formed.

The negative ion vacancy and the F-centre also give rise to bands in the long wavelength tail of the fundamental absorption, associated with transitions of electrons from neighbouring halogen ions to levels created by the imperfection. These bands are known as α and β bands, the α-band being associated with the vacancy, and the β-band being associated with the F-centre (see Pringsheim et al, 1950, 1953 and Duerig and Markham, 1952). In KBr these bands lie beyond 2000Å and become resolvable only at low temperatures (about -180°C).

(b) Associations of Vacancies.

When the F-band is bleached with F-light at room temperature the resulting absorption spectrum, if examined at low temperatures where the resolution is improved due to low temperature narrowing of bands, shows three bands on the long wavelength side of the F-band (in the red and near infra red for NaCl). Proceeding from the F-band the bands are designated R_1, R_2, and M, respectively. The R_1-band is thought to be due to centres of the type electron + negative ion vacancy pair, while R_2-centres are negative ion vacancy pairs which have captured two electrons (Seitz, 1946). The M-centre is believed to arise from the capture of an electron by an association of vacancies containing two negative ion vacancies and one positive ion vacancy (Seitz, 1946). On this model, the ground state of the M-centre has been computed to be 5.63 eV, and the first excited state 3.90 eV, below the conduction band minimum in NaCl (Inui et al, 1952). The difference in energy, 1.73 eV, agrees well with the optical data. A fourth band, the N-band, which appears further in the infra red, has also been discovered (Petroff, 1950, and Burstein and Oberly, 1950). Seitz (1954) has suggested that this band is also due to associations of vacancies which have captured electrons. All these bands appear both in additively coloured and X-rayed crystals.

Scott (e.g. 1953) has found that when additively coloured crystals, which contain R, M, and N, centres, are heated a broad, composite band appears in the R-band region. This band, the R'-band, is probably a combination of the aforementioned centres together with other similar aggregates, (Seitz, 1954). Further annealing at about 400°C produces the colloid band in the red or near infra red, due to the formation of colloidal specks of the excess alkali metal.

1.3 Hole Traps in the Alkali Halides.

Mollwo (1937) found that it was possible for KBr and KI to acquire a stoichiometric excess of halogen, and that crystals so treated showed a series of bands in the ultra violet, now known as the V-bands. These are due to positive ion vacancies which have captured holes, freed by the ionization of the halogen atoms. There is thus a close analogy to the formation of F-centres in excess alkali crystals. However, there is an important difference between the two processes, for whereas the concentration of excess alkali is proportional to the partial pressure of the monatomic alkali vapour, Mollwo found that the concentration of excess halogen was proportional to the partial pressure of the diatomic halogen gas, indicating that the V-bands were associated with pairs of positive ion vacancies.

V-bands may also be produced by irradiating the crystals with X-rays, indicating that positive, as well as negative, ion vacancies are present naturally in the crystal. Irradiation at room temperature produces the V_2, and V_3, bands (situated around 210 mμ in NaCl) which are poorly resolved. According to Seitz (1954) the V_2-band is to be associated with a pair of positive ion vacancies which have captured two holes (the analogue of the R_2-centre). Irradiation at liquid nitrogen temperatures produces also the V_1, and the V_4, bands, associated with the analogues of the F-, and M-, centres respectively. A fifth band, the H-band, has also been discovered, and may be due to a centre consisting of a hole trapped at a vacancy pair (positive ion vacancy + negative ion vacancy). (See Casler et al, 1950, and Dorendorf, 1951).

One piece of evidence which supports the view that V-centres contain trapped holes is obtained from bleaching experiments. When the F-band is exposed to F-light bleaching occurs, rapidly at first, then more slowly, and the V-band (V_2 + V_3) drops in intensity. R and M-centres are also formed. The bleaching of the V-band indicates that the V-centres act as centres of recombination for the electrons freed from the F-centres, and are therefore destroyed by electron capture.

1.4 The Effect of Impurities.

The F-type centres and the V-type centres described above are found even in the purest crystals, and therefore they may be regarded, at the present stage of our knowledge, as intrinsic properties of the alkali halides. It is known, however, that their concentrations can be greatly increased by the presence of some impurities.

Shulman (1953) has suggested that impurities influence the colouribility of crystals by

(a) accentuating mismatch in the lattice and increasing the density of dislocations, leading to an increase in the vacancy concentration;

(b) directly enhancing the density of vacancies, e.g. the presence of a divalent impurity metal enhancing the density of positive ion vacancies;

(c) acting as traps.

Seitz (1954) has also pointed out that the enhancing of the positive ion vacancy concentration by divalent metals will, at room temperature, assist the migration of the slow moving negative ion vacancies by forming mobile vacancy pairs. Since vacancies play an important role in the ionic conductivity it may be expected that divalent impurities would have a marked effect, and, indeed, it has been found that the presence of an alkaline earth metal increases the ionic conductivity of KCl (Kelting and Witt, 1949).

Apart from enhancing the density of colour centres impurities can effect the optical absorption in three other ways:

(a) If present in sufficient concentration the impurity will precipitate and render the normally transparent crystal opaque, or merely cloudy; or produce colloid bands.

(b) An enhancement of the long wave-length tail of the fundamental absorption band may occur.

(c) The impurity may introduce a characteristic band in the ultra violet.

The fundamental absorption band may be regarded as being due to transitions of electrons from the halogen ions to neighbouring alkali ions, the energy involved in the transition being a function of, among other things, the ionization potential of the alkali atom. Transitions to an impurity having ionization potential greater ~~smaller~~ than that of the alkali metal will involve less energy, and this will result in an enhancement of the long wavelength tail of the fundamental absorption (Mott and Gurney, 1940). This effect has been observed for many impurities.

The characteristic impurity bands are associated with transitions between levels within the impurity ion itself. Sometimes these levels are metastable, an excited electron remaining in an excited condition for some time after the exciting stimulus has been removed before falling back to the ground state. The crystal is then luminescent, e.g. $KCl.Tl^+$, (Seitz, 1938). Characteristic bands have been found in the cases of lead and thallium (Hilsch, 1927, 1928; and Arsenjewa, 1929), and silver and copper (Smakula, 1927). Silver produces three bands, associated with single Ag^+ centres and complexes of Ag^+ ions (Etzel et al, 1952); and lead, in NaCl, gives two poorly resolved bands near 280 mμ (Shulman et al, 1950). Arsenjewa (1929) found that X-irradiation had a marked effect on these bands. Electrons liberated by the X-rays may be trapped at the monovalent impurity centre, forming an atomic centre, thus destroying the characteristic bands. Reduction of characteristic band intensity by X-rays has been noticed in the cases of lead (Shulman et al, 1950), silver (Burstein et al, 1952) and Kats[a], 1952), and copper (Kats[b], 1952). Only in the latter case was it observed that complete conversion to atomic centres was impossible.

Crystals containing the alkali metal hydride are particularly interesting in that they display a prominent band in the ultra violet, attributed to transitions within H^- ions which occupy substitut~~u~~ionally the halogen ion positions, (Pohl, 1938). The band is known as the U-band, unique, at present, as the only characteristic impurity band produced by an electro-negative impurity.

1.5 The Z-bands.

The study of crystals containing divalent impurities has been of immense importance to the development of our knowledge of the properties of the alkali halides. Of particular interest is the influence of the alkaline earths on the optical properties of coloured crystals. Since calcium and magnesium are often present as the predominant impurities in normal "pure" crystals, the work in this sphere is of great value in helping to answer the question, which properties are intrinsic, and which are due to impurities?

It has been found that the introduction of alkaline earth ions into the alkali halides can give rise to a set of absorption peaks in the visible region of the spectrum, known as the Z-bands (Pick, 1939; Heiland and Kelting, 1949; Seitz, 1951; Camagni et al, 1954). When a KCl crystal containing these impurities is coloured, additively or X-rayed, only the F-band appears. If the F-band is now bleached, a band appears on its long wavelength side (at 590 mμ in KCl at $-215^{\circ}C$ compared with the F-band at 540 mμ). This is denoted the Z_1-band, and Seitz has proposed that it is due to the centre formed when a divalent ion, occupying substitutionally a positive ion position, captures an electron. The efficiency of F-Z_1 conversion is very low, and Bassani and Fumi (1954) have suggested that this is due to the presence of an excess number of negative ion vacancies. The non-appearance of the band during the initial colouring is presumably due to the relatively low concentration of the divalent ions. (see sections 7+8) Heating the additively coloured crystal to 110°C converts the Z_1-band into the Z_2-band, whose peak is at 610 mμ, which, Seitz suggests, is associated with the centre formed by the capture of a vacancy pair by a Z_1-centre. Further heating of the additively coloured crystal (over 200°C) destroys the Z-bands, and the F-band re-emerges. Both bands diminish if either are optically bleached at -90°C and a broad band appears on the short wavelength side of the Z_1-band. Seitz suggests that this band, the Z_3-band, is analogous to the F'-band, i.e. associated with a negatively charged centre, and proposes that the Z_3-centre is a Z_2-centre which has captured a second electron. NaCl, containing strontium or calcium, behaves in a slightly different way, in that additively coloured crystals show the Z_2-band as well as the F-band. Subsequent bleaching of the Z_2-band gives the Z_1-band. The Z_3-band is not stable at room temperature. X-rayed NaCl.Ca or NaCl.Sr behaves in the same way as the KCl crystals containing alkaline earths.

1.6 Conclusion

The present work on the optical properties of the alkali halides containing divalent impurities derived much of its stimulus from the study of the Z-centres, very briefly described above, since several questions seemed to be unanswered, e.g.

(1) Z-centres should be formed during the colouring process. Why are they absent in KCl and X-rayed NaCl? If this is due to the low concentration of divalent ions making the bands undetectable, is it possible to increase this concentration until Z-bands of detectable intensity are formed?

(2) The low F-Z_1 conversion efficiency has been put down to the presence of an excess number of negative ion vacancies in the additively coloured crystal, produced by the divalent chloride. If this is the case, how efficient are the divalent chlorides in producing vacancies; in fact, can this excess number be measured; and can light be thrown on the mechanism involved?

(3) Only the divalent ions of the alkaline earths have given Z-bands. Do other divalent ions, such as Mn^{++}, Cu^{++} and Ni^{++}, produce Z-type bands, and if not, why?

The question of the production of negative ion vacancies by the impurity is a particularly interesting one, since it probes into the whole question of intrinsic and extrinsic properties. What proportion of vacancies present in a normal "pure" crystal are due to impurities? Would an absolutely pure crystal colour at all under X-irradiation? Above absolute zero it almost certainly would; it is most unlikely that impurities account for all vacancies produced. In this respect, colouration, at least some of it, is an intrinsic property of the alkali halide. But until purer crystals are available it will be impossible to decide the degree to which impurities affect the properties, to any great accuracy, that is. We know they have an important effect. How deep this effect is remains to be answered with confidence.

2 THE ABSORPTION SPECTROPHOTOMETER

2.1 Thomas's Grating Spectrophotometer.

Through the kindness of Professor W. E. Curtis and Dr. E. E. Schneider of the Physics Department, King's College, Newcastle, a grating spectrophotometer, made by T. B. Thomas and described in his M.Sc. thesis (1952) was made available. It consisted essentially of a heavy iron baseplate on which was mounted the monochromator housing and a mumetal box containing the electrical detection unit, and there was provision made for mounting a tungsten lamp or a hydrogen lamp near a condensing mirror. External elements necessary for operation were power supplies for the detection unit and lamps, and a sensitive galvanometer. The instrument was designed for use in the wavelength range 200 mμ to 600 mμ, i.e. over the near ultra violet and most of the visible region, with a bandwidth of 10Å which was constant over the whole range.

The optical system is shown diagrammatically in figure 2. Light from the source is condensed by a concave mirror on to the slit and rendered parallel by the collimating mirror, a concave mirror of focal length 25 cm and diameter 6 cm, mounted so that its position can be adjusted by the manipulation of three screws. Since it is necessary to use the mirror in an off-axis

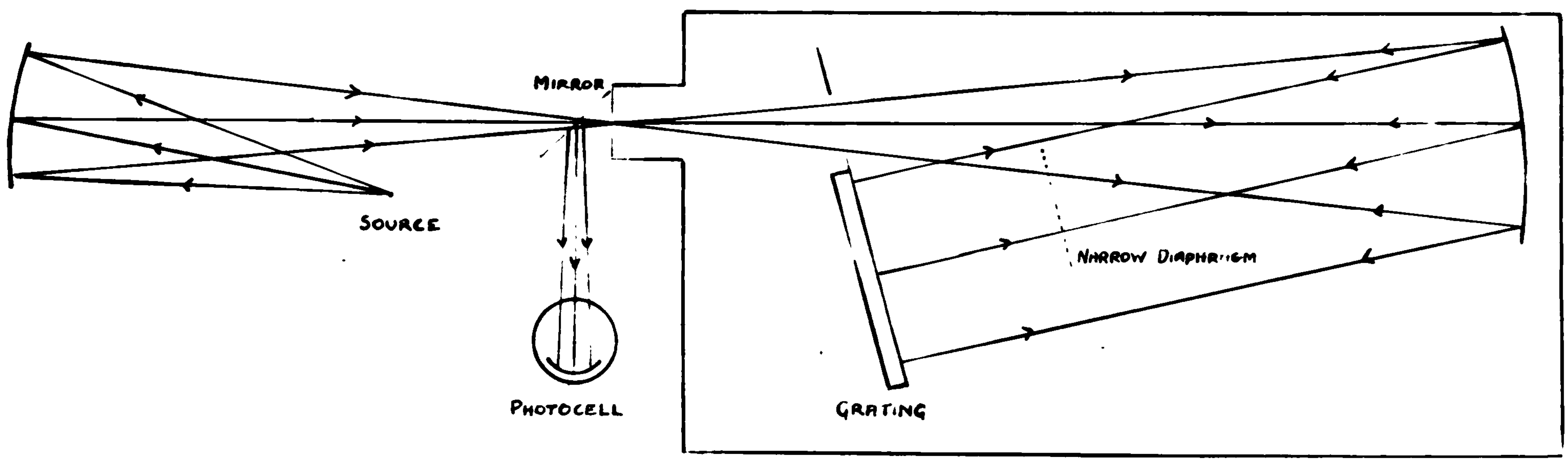

Fig. 2. THE OPTICAL SYSTEM.

position a certain amount of spherical aberration is inevitable. A single slit, divided in the middle, forms the exit and entrance slits, and is of width 0.007 cm. The parallel light from the collimator falls on a 4 cm x 3 cm replica reflection grating having 5,709 lines per cm. The grating mounting is shown in figure 3. Screws A, B and C are levelling screws. By them the small tilt to the vertical required to return the diffracted beam to the exit slit, and the small tilt necessary for rendering parallel the direction of the rulings to the slits, can be achieved. Once levelled, the platform is clamped by screws A', B' and C'. Loosening the wing-nuts allows the grating to be rotated for zero wavelength adjustments. The platform can rotate about a vertical axis, controlled rotation being effected by a micrometer pressing against a springed brass rod rigidly fixed to the platform. Readings of the micrometer can therefore be strictly correlated with the wavelengths of the light passing through the exit slit. The zero order reflected beam from the grating can be a serious source of scattered light for it may reach the grating again from the collimator when the grating is working at near normal incidence; consequently, a suitably placed diaphragm is necessary to eliminate this effect. A further source of scattered light is the light of longer wavelength than the chosen spectral band impinging on the area of the grating near the slit while

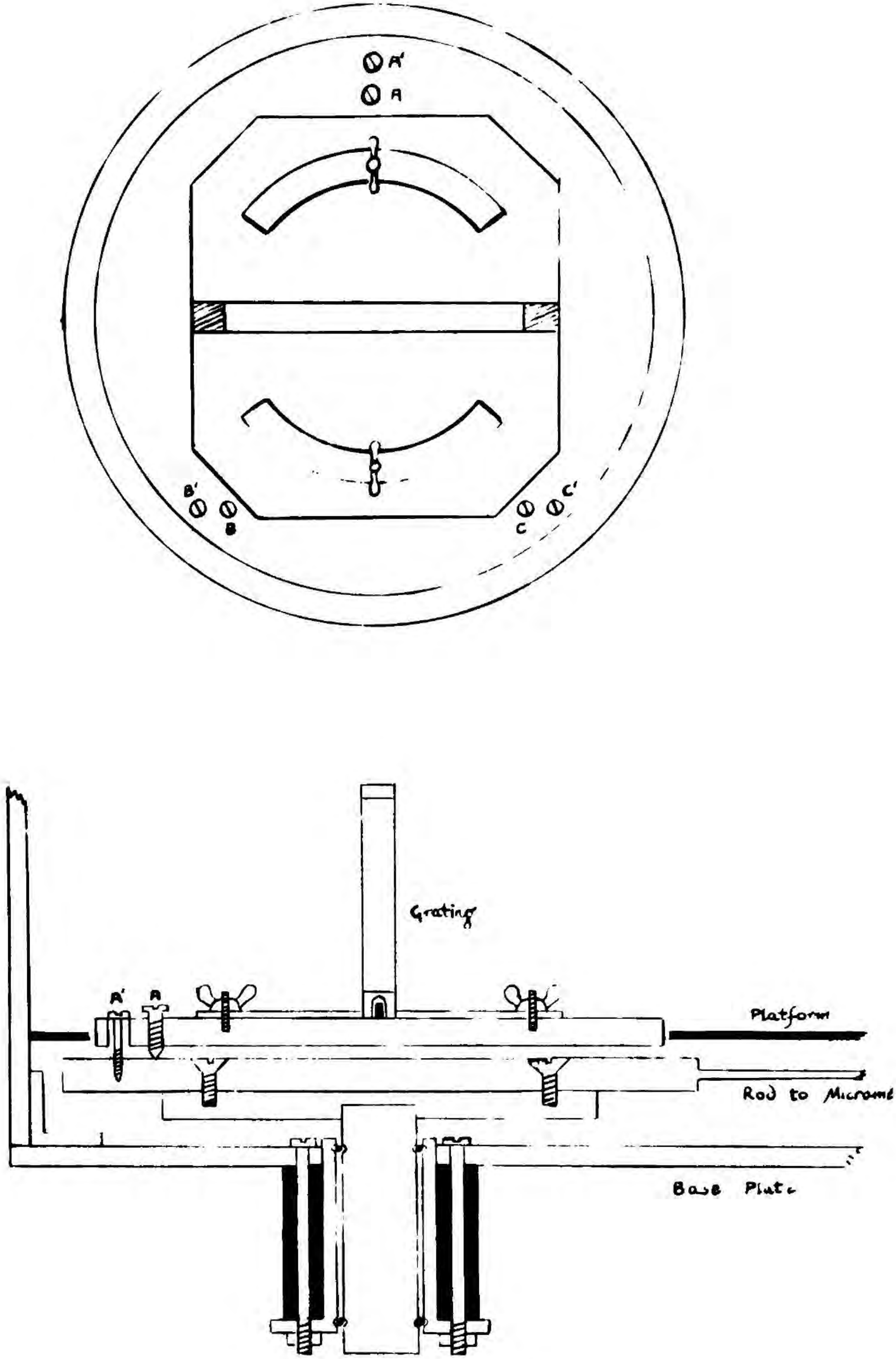

Fig. 3. THE GRATING TABLE

converging from the collimator to the focal plane. This beam converges to a thin horizontal strip as far in front of the grating as the slits are behind, and a baffle strip is placed in this position to eliminate this unwanted radiation.

The monochromator system just described was found to be quite satisfactory and was used throughout without any modifications. The remaining elements of the spectrophotometer, however, suffered some modification in the development of the instrument. These modifications will be dealt with later in this chapter.

The selected spectral band issuing through the exit slit in the original instrument is deflected by a plane mirror upwards into the specimen chamber which contains a sliding tray holding the specimen crystal. The tray pushed in, allows the exit beam to pass through the specimen; when pulled out the tray is completely outside the beam. The box containing the detection unit is connected to the specimen chamber by close-fitting brass rings through which the light passes to fall on to the cathode of the photoelectric cell.

To complete the description of the optical elements, the sources of light used may be mentioned. For visible radiation a 24 watt tungsten incandescent lamp with a straight vertical filament is used. This provides light from about 360 mμ upwards. The ultra violet source is a "Point Source" H.F.5 hydrogen arc of the Manufacturer's Supply Co. This lamp provides a continuous spectrum from 185 mμ to 350 mμ.

The electrical detection and measuring circuit is shown in figure 4. The photoelectric cell is an Osram Q.V.A. 39 with a blue-sensitive cathode of caesium-silver oxide and a quartz envelope. The working potential difference across the cell is derived from a 100 volt high tension battery. The output current from the cell flows through the 25 Kilomegohm resistor, which also serves as a grid leak for the electrometer valve. The high resistor can be short circuited by a switch consisting of a wire which can be rotated freely in air to make contact with the grid lead of the valve, so that when the switch is open the resistance between the wire and the grid is that of about a centimetre of air. An ordinary toggle switch used here would shunt the high resistance appreciably in the "open" position.

The electrometer valve is a General Electric Co. E.T.1, a triode, whose characteristics are cited elsewhere. It is supported on sponge rubber in order to reduce microphonics, derives its anode potential from three 2 volt accumulators, its filament current of 100 mA from one 2 volt accumulator, and its grid bias of 2 volts from

Weston Cadmium Standard Cells. Since the change in anode current to be measured, about 4 μA, is two orders of magnitude smaller than the anode current itself a backing-off circuit is employed to counter-balance exactly the quiescent anode current, i.e. the current with the grid leak shorted out. A Tinsley galvanometer, sensitivity 85 mm/μA at 1 m, then measures the change in anode current when the shorting switch is opened, and the deflection is directly proportional to the intensity of light falling on to the photocell since the E.T.1 is used in conditions where its characteristics are straight.

This circuit is an extremely simple one but is open to the serious criticism of being subject to battery drift, the main source of zero drift in D.C. amplifiers, although this is kept as low as possible by using high capacity accumulators. Even so for an 80 ampere-hour battery supplying 100 mA the voltage drift is of the order of 0.5 mV per hour if the battery is new, but can be ten times this and more for older cells, and this effect is serious in a circuit built to measure direct currents of 10^{-12} A and less. Consequently, a new measuring circuit was designed to counteract this effect and was subsequently built.

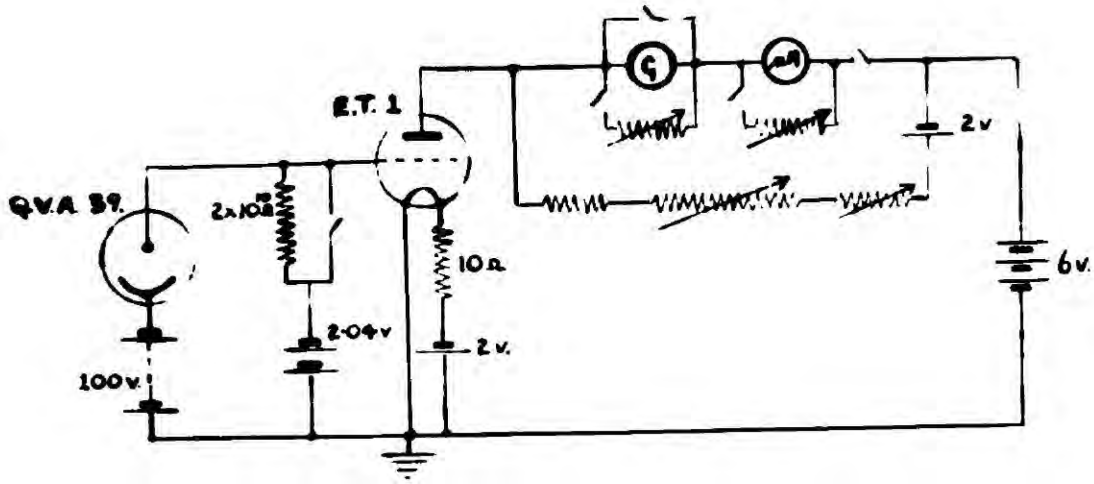

Fig. 4 THOMAS'S CIRCUIT

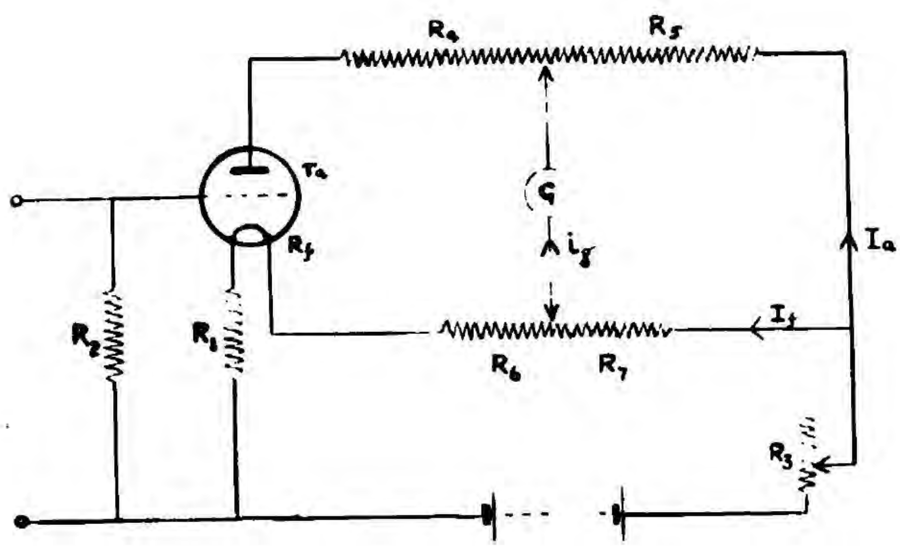

Fig. 5 MORTON'S CIRCUIT

2.2 The No-Drift Circuit

The circuit finally designed was based on a circuit used by Morton (1932) which is shown in figure 5. Essentially it is a Wheatstone Net whose arms are respectively $R_4 + r_a$, the anode slope resistance, R_5, R_7 and $R_6 + R_f$, the resistance of the filament. The potential drop across R_1 provides the grid bias, and it may be observed that there is only one source of power, providing, as well as the grid bias, the filament current and the potential difference across the valve. Battery drift is thus confined to one source and not three as in Thomas's circuit and can be eliminated by suitable choice of resistances, if the drift is not variable. Discharge curves quoted by manufacturers of accumulators, and personal experiments on the batteries actually used in the apparatus, show that the rate of drop of voltage is constant apart from short periods at the beginning and a similar period at the end of the discharge life of the battery.

Morton's treatment of the theory starts with the assumption that I_f is very much greater than I_a or i_G, which is usually the case. The condition for balance, i.e. no current through the galvanometer, may be obtained by applying Kirchhoff's Law

$$0 = R_7 I_f + i_G G - R_5(I_a - i_G) \quad . \quad (1)$$

$$i_G = 0 \text{ when } \frac{R_7}{R_5} = \frac{I_a}{I_f} \quad . \quad . \quad . \quad (2)$$

This condition corresponds to the backing-off in Thomas's circuit. Equation (1) may be written

$$(R_5 + G)\delta i_G = R_5 \delta I_a - R_7 \delta I_f$$

The condition for zero drift is then

$$\delta i_G = 0$$

$$\frac{R_7}{R_5} = \frac{\delta I_a}{\delta I_f} \quad . \quad . \quad . \quad (3)$$

The problem now is to find the change in anode current for a given change in filament current, due to battery drift.

Morton takes δI_a to be made up of two components:

(a) Change in potential difference across anode load and valve,

$$\text{whence } \delta I'_a = \frac{R_f + R_6 + R_7}{R_4 + R_5 + r_a} \delta I_f \quad . \quad (4)$$

(b) Change in grid bias acting as a signal of $R_1 \delta I_f$ volts to the grid.

To estimate the latter contribution let V_s be the resulting signal to the grid; this will be composed of the initial signal plus feed-back. Thus the amplified signal is μV_s, where μ is the amplification factor, and a fraction β is fed back, where

$$\beta = \frac{R_1}{R_4 + R_5 + r_a}$$

$$\therefore \quad V_s = V_g - \mu\beta V_s$$

$$\text{or} \quad V_s = \frac{V_g}{1 + \mu\beta}$$

The resultant output, V, is then

$$V = \frac{\mu V_g}{1 + \mu\beta}$$

$$= - \frac{\mu R_1 \delta I_f}{1 + \mu\beta}$$

Now $$\delta I_a'' = \frac{V}{R_4 + R_5 + r_a}$$

$$\therefore \quad \delta I_a'' = \frac{-\mu R_1}{R_4 + R_5 + r_a} \delta I_f \qquad . \qquad . \qquad (5)$$

The total change is obtained by adding 4 and 5. If R_1 is neglected in the denominator of 5 this is

$$\delta I_a' = \frac{R_f + R_6 + R_7 - \mu R_1}{R_4 + R_5 + r_a} \delta I_f'$$

Substitution in 3 gives the condition for zero drift to be

$$\frac{R_7}{R_5} = \frac{R_f + R_6 + R_7 - \mu R_1}{R_4 + R_5 + r_a} \qquad . \qquad . \qquad (6)$$

There is, however, yet another contribution to δI_a which Morton does not consider, yet which is quite as important as $\delta I_a'$ and $\delta I_a''$. It is the change in anode current due to change in emission from the filament: the $\delta I_a/\delta I_f$ characteristics of the valve. No reference in the literature has been found which takes this effect into account in this particular context.

Equation (6) should read:

$$\frac{R_7}{R_5} = \frac{R_f + R_6 + R_7 - \mu R_1}{R_4 + R_5 + r_a} + \left(\frac{\partial I_a}{\partial I_f}\right)_e \quad . \quad . \quad . \quad (7)$$

If equations (2) and (7) are combined the conditions of balance and zero drift are both fulfilled when

$$\frac{I_a}{I_f} = \frac{R_f + R_6 + R_7 - \mu R_1}{R_4 + R_5 - r_a} + \left(\frac{\partial I_a}{\partial I_f}\right)_e \quad . \quad . \quad . \quad (8)$$

The question then arose: Is the condition embodied by equation (8) attainable in practice when the valve in use is an electrometer valve, the E.T.1 manufactured by G.E.C? To answer this the characteristics of the valve at hand were determined and found not to differ greatly from the manufacturer's standard characteristics (see figure 6). By substituting values of I_a, I_f, etc. for various operating points and various battery voltages it was found that equation (8) could not be satisfied without diverging seriously from the normal working conditions of

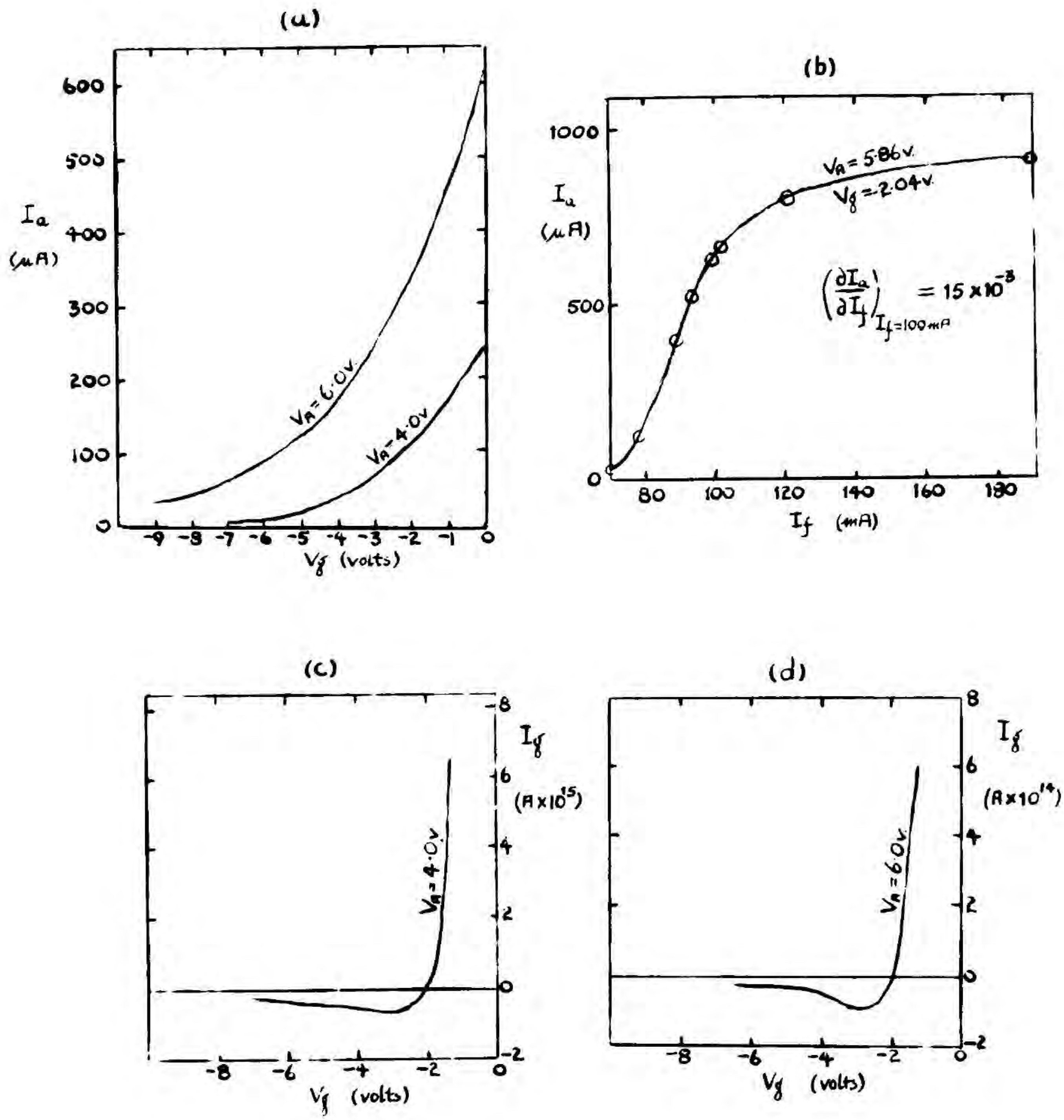

Fig 6. TYPICAL E.T.1. CHARACTERISTICS.

the valve. In other words, the conditions for balance and no-drift were found to be incompatible.

Even so, it may be observed that with the circuit just described, when the valve is working at optimum conditions and the condition for balance is satisfied, the rate of drift of i_G compared with Thomas's circuit is reduced by an order of magnitude.

In an attempt to improve this the circuit was slightly modified. It will be clear that in order to achieve compatibility in the conditions of balance and no-drift a further degree of freedom must be introduced into the circuit, and this can be obtained by including a battery in series with the galvanometer (figure 7). The condition for no-drift is unchanged if it is assumed that the voltage drift of the new battery is inappreciable; and the condition for balance becomes

$$e = \left(\frac{R_7}{R_5} - \frac{I_a}{I_f}\right) R_5 I_f \quad . \quad . \quad . \qquad (9)$$

where e is the battery voltage. The two conditions are now compatible if e is about 1.5 volts. The battery chosen was a Venner alkaline cell, of capacity 1.5 ampere-hours, having an open circuit voltage of 1.8 volts.

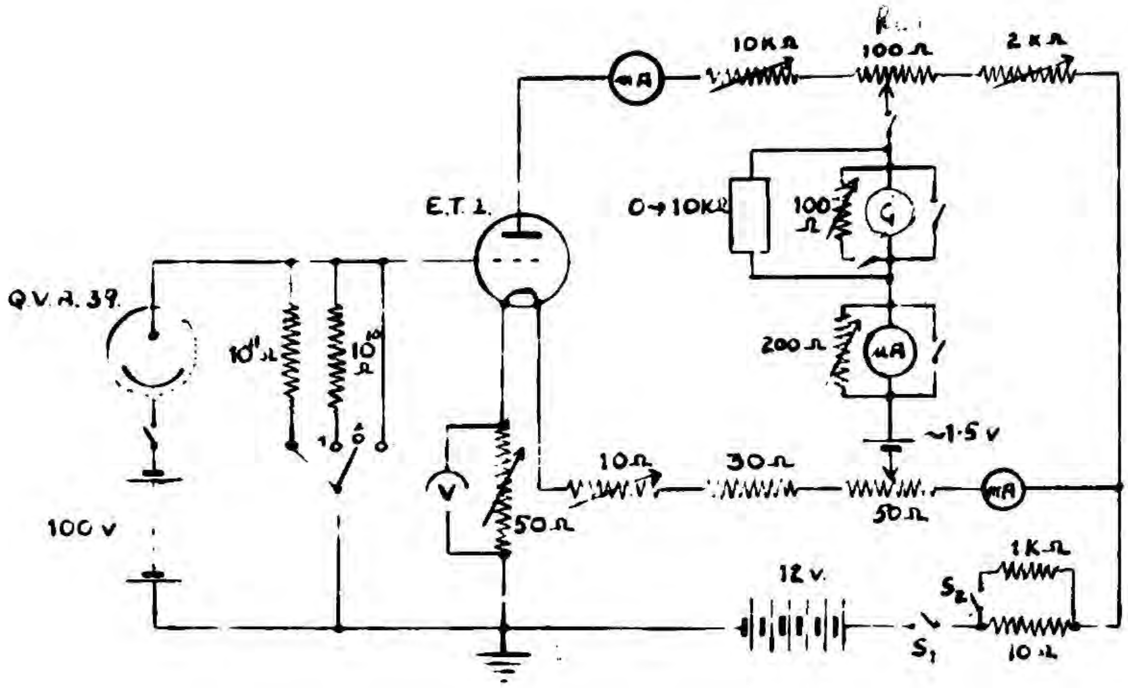

Fig 7. THE ZERO-DRIFT CIRCUIT.

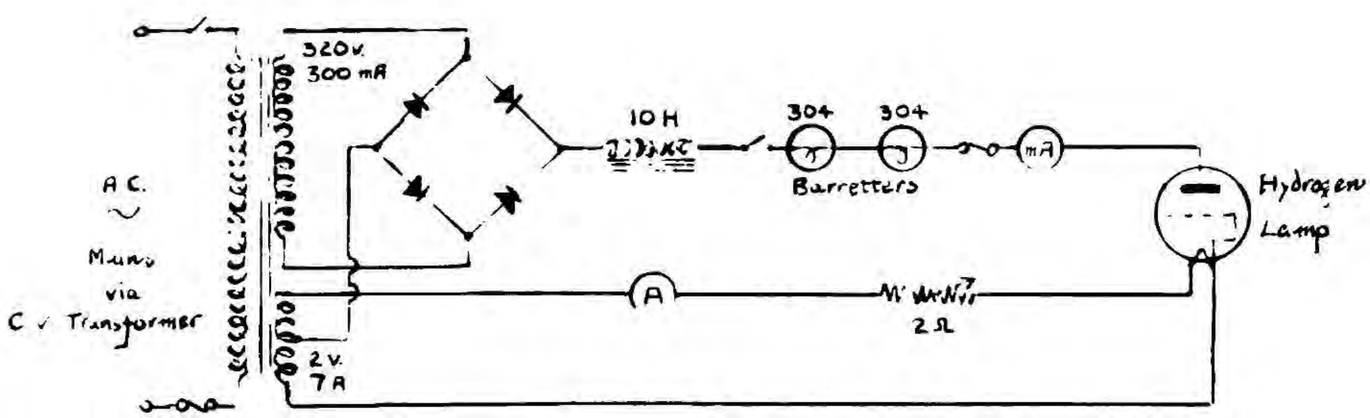

Fig 8. THE HYDROGEN LAMP POWER SUPPLY

This cell has an extremely flat discharge characteristic even at fairly high currents, an essential requirement for the purpose to which it was put.

Other details of the practical circuit will now be described. Since it was thought desirable to keep the circuit flexible two ammeters and a voltmeter to measure the anode and filament currents and grid bias voltage respectively were included; all were Weston sub-standard instruments. For stability, wire-bound resistors were used throughout; the variable resistors were Berco wire-wound potentiometers. The instrument used to measure the change in anode current produced by light falling on the photocell was a Tinsley galvanometer, sensitivity 300 mm per μA at 1 metre, and a less sensitive galvanometer was used for coarse balance. The elements S_2, R_2, R_3 provide a means for altering the filament current by 100 μA, this being achieved by the manipulation of the spring-loaded toggle switch, S_2, thereby making it possible to test for the no-drift condition. In the detection unit, two Victoreen high-stability resistors were present to give two sensitivity ranges; a higher, obtained by rotating the earthing switch half-way round from the "earth grid" position so that the higher resistor only is in circuit, and a lower range, obtained by full rotation so that the resistors are in parallel. The monochromator and detection unit were together enclosed in an earthed aluminium box and all electrical controls brought to a control panel forming one side of the box (see Plate I).

2.3 Balancing Procedure.

The description of the method used to balance the circuit at the condition for no-drift may be best given in instructional form:

(1) Before switching on check that the galvanometers are short-circuited.

(2) Switch on and adjust R_1 and R_6 (10Ω potentiometer) until the filament current ammeter registers 100 mA and the grid bias voltmeter 2.1 volts. Earth the grid.

(3) Set R_7 at about 25Ω and unshort the lower sensitivity shunt and adjust to obtain a suitable deflection.

(4) Balance by adjusting R_4 and R_5, keeping the anode current constant.

(5) Switch in the shunt of the sensitive galvanometer and unshort. Adjust the shunt to give a suitable sensitivity.

(6) Effect final balance by adjusting the R_4, R_5, 100Ω potentiometer with the first galvanometer short-circuited and the sensitive instrument unshunted.

(7) Test for the no-drift condition by depressing S_2. After an initial kick the galvanometer spot should return to zero when this condition holds.

(8) Repeat systematically with various values of R_7 until the condition is reached.

(9) Leave overnight to settle down.

(10) Small adjustments are usually necessary before use and during measurements to maintain the fine balance.

2.4 Sensitivity

The current sensitivity may be defined by

$$S_i = \frac{di_G}{di} \cdot S_G$$

where i_G is the current flowing in the galvanometer and i is the current flowing in the photocell. S_G is the current sensitivity of the galvanometer.

Now

$$S_G \frac{di_G}{di} = S_G \frac{di_G}{dI_a} \frac{dI_a}{dV_g} \frac{dV_g}{di} \quad . \quad . \quad (1)$$

where I_a is the plate current and V_g the grid bias.

From equation (1), section 3.2,

$$\frac{di_G}{dI_a} = \frac{R_5}{R_5 + G} \quad . \quad . \quad . \quad (2)$$

This is true when the compensating cell is present if G now includes the cell's internal resistance.

From ordinary valve theory

$$V_P = V_B - I_a (R_4 + R_5) + \mu V_g$$

where V_p is the anode potential, and V_B is the battery voltage.

Therefore

$$\frac{dV_p}{dV_g} = \mu - (R_4 + R_5) \frac{dI_a}{dV_g}$$

But

$$\frac{dV_p}{dI_a} = r_a,$$

Therefore

$$\frac{dI_a}{dV_g} = \frac{\mu}{r_a} - \frac{dI_a}{dV_g} \frac{(R_4 + R_5)}{r_a}$$

$$\frac{dI_a}{dV_g} = \frac{\mu}{r_a} \Big/ \left(1 + \frac{R_4 + R_5}{r_a}\right) \quad . \quad . \quad (3)$$

and this is the effective conductance, while μ/r_a is the mutual conductance, K_m.

Finally

$$\frac{dV_g}{di} = R \quad . \quad . \quad . \quad (4)$$

where R is the resistance of the grid leak. (True if there is no grid current).

Substitution of equations (2), (3) and (4) in 1 gives

$$S_i = \frac{\mu R}{r_a + R_4 + R_5} \cdot \frac{R_5}{R_5 + G} S_G \quad . \quad (5)$$

For typical working conditions $\mu = 0.5$, $R = 1 \times 10^{10}\ \Omega$ (low sensitivity) $r_a + R_4 + R_5 = 10\ K\Omega$, $R_5 = 2\ K\Omega$, $G = 500\Omega$, and $S_G = 300$ mm per μA, whence

$$S_i = 40 \text{ mm per } 10^{-12} \text{ amp.}$$

On the high sensitivity range $R = 1 \times 10^{11}\ \Omega$

$$S_i = 400 \text{ mm per } 10^{-12} \text{ amp,}$$

so that currents of the order of 10^{-13} amp can be comfortably detected.

2.5 The Light Sources.

The source for visible radiation is that of the original apparatus, a tungsten lamp of 24 watts, which derives its power from a constant voltage mains transformer feeding a step-down transformer. No elaborate precautions were taken to stabilise the lamp supply further, nor were they needed.

The ultra violet source is a Vitreosil hydrogen discharge lamp manufactured by Thermal Syndicate. This lamp has a quartz envelope and emits a continuous spectrum from 200 mμ to 370 mμ, and a line spectrum in the visible which is useful for checking the wavelength calibration of the spectrophotometer. A power supply for the lamp was built to the maker's recommendations and this was run off the constant voltage transformer supply. The circuit is shown in figure 8.

Both lamps are supported in a similar way: a platform on which the lamp is fixed is supported on two threaded rods fixed to a metal base-plate. This plate has a hole bored in its centre to take a positioning rod fixed ~~for~~ to the heavy base-plate of the spectrophotometer where the lamp must be placed when in use. Interchanging of lamps may therefore be facilitated and the time spent in re-focusing light on to the slit reduced to a minimum.

A lamp-housing of hard-board and aluminium was constructed to enclose the concave condensing mirror and lamp in order that stray light in the instrument enclosure may be cut down as much as possible.

2.6 The Cryostat.

In modifying the apparatus so that absorption spectra at low temperatures could be obtained the problem presented was one of keeping the specimen at 80°K, and providing means to move it in and out of a visible or ultra violet light beam. Further, it was thought desirable at the low temperature that provision be made for irradiating the crystal with X-rays.

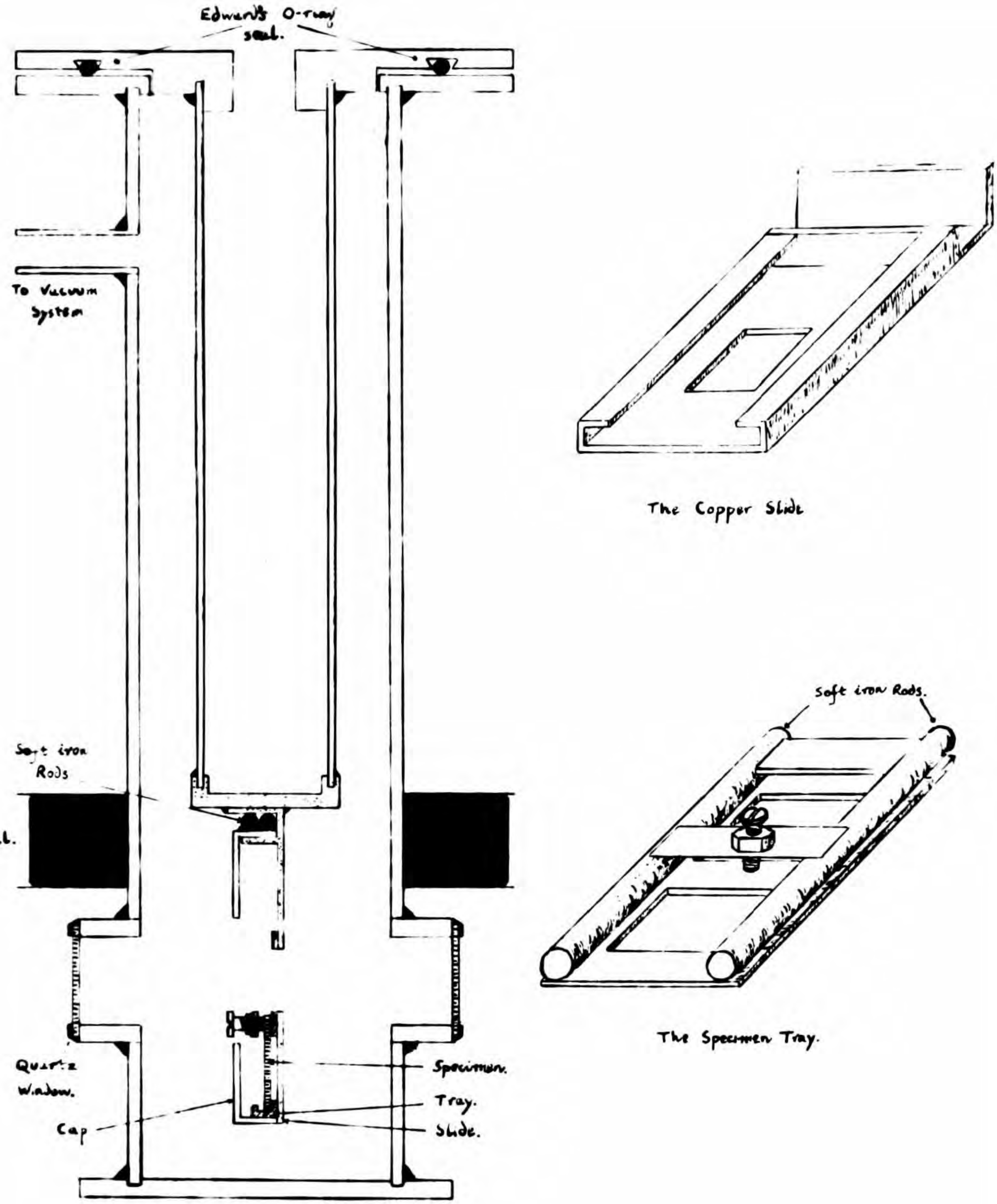

Fig 9. THE CRYOSTAT.

A successful cryostat was constructed to fill these requirements (figure 9). Essentially it is a metal Dewar flask consisting of two concentric tubes, an inner tube which holds the liquid air and to which is attached the crystal holder, and an outer tube which has diametrically opposed quartz windows with a beryllium window mid-way between them at one end and a vacuum connection at the other. Other workers (see for example Beale and Roe, 1951, and Mayence and Vadar, 1950) have used cryostats of broadly similar construction.

Methods described in the literature of moving the crystal in and out of the light beam have involved some purely mechanical process, such as rotation of the crystal holder. It was decided that the crystal holder should be constructed in such a way as to allow the movement of the crystal to be achieved magnetically, as this appeared to offer a great simplicity in the construction and operation.

The crystal holder is made of copper and has three components (figure 9): a tray, having two apertures and walls which are of soft iron on which the crystal is held, a slide soldered to the copper base of the inner tube, having one aperture slightly smaller than those in the crystal tray, and a cap which fits closely over the slide, having a large aperture and a tinned outer surface to induce any residual moisture to condense on it rather than on the crystal during cooling. The tray can slip up and down the copper slide so that when it is up, the lower aperture, over which the specimen lies, coincides with the fixed aperture of the slide, and when it is down the upper aperture coincides with the slide aperture. If a light beam is made to pass through the slide aperture the crystal can be placed in and out of the beam by moving the tray up and down respectively. The cap may be removed from the slide to allow the tray to be taken out when a new specimen is to be mounted.

The crystal tray is moved in the vacuum magnetically. A coil, of 400 turns of S.W.G.22 copper wire is wrapped around the outer brass tube just above the quartz windows so that when a current of sufficient strength flows, the tray, by virtue of its soft iron walls, moves to the top of the slide and falls when the current is switched off. Since, however, the current necessary to raise the tray is about 8 amps supplied from a 60 volt power pack, the energy dissipated per unit time is high (500 watts) and the coil will become very hot while the crystal is in the beam. To avoid this the circuit shown in figure 10 is used, its principle being merely the fact that although 8 amps are necessary to raise the tray, only 3 amps are required to hold it at the top. To raise the tray, S_1 and S_2 are closed and R_2 adjusted so that the tray is just pulled up.

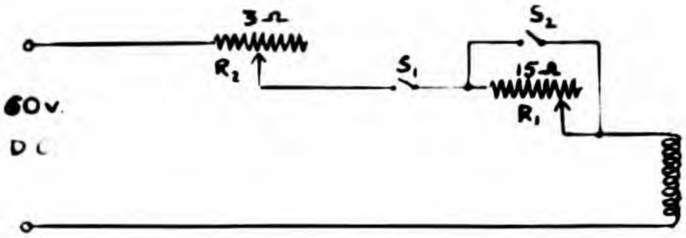

Fig 10. THE TRAY LIFTING CIRCUIT.

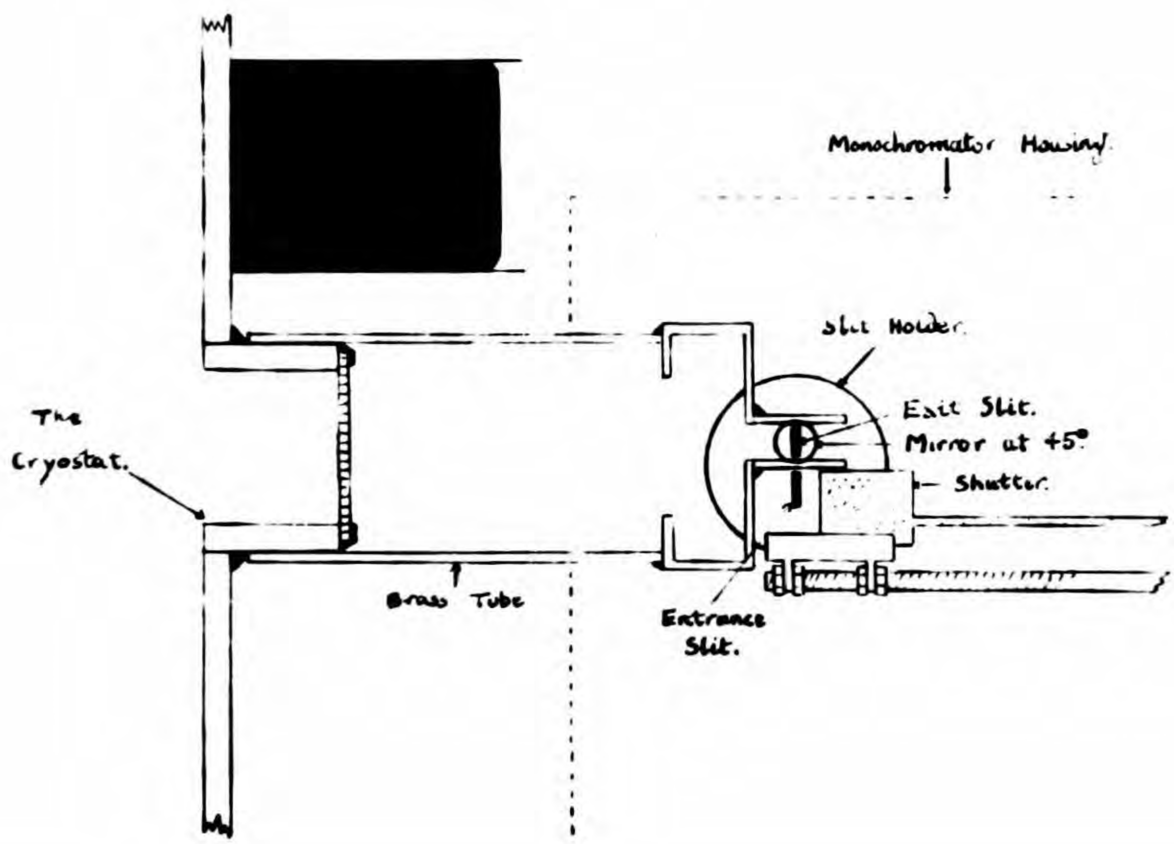

Fig. 11. THE CONNECTION BETWEEN THE CRYOSTAT AND THE MONOCHROMATOR.

S_2, a spring-loaded toggle, is released and R_1 is adjusted so that the tray just keeps up. The tray falls when S_1 is opened.

The vacuum is derived from an Edward's 2 S 20 "Speedivac" backing-pump, the pressure being indicated by an Edward's Macleod gauge. The vacuum circuitry is quite straightforward and merits no further description.

2.7 The Modified Optical System.

In order that the cryostat could be used with the monochromator it was necessary to make a small modification to the optical system dealing with the exit beam so that the beam would travel horizontally, and not vertically, through the crystal: a case of deflecting the beam by a mirror sideways instead of upwards. The old mirror was replaced by a galvanometer mirror. The beam emerging from the exit slit, on meeting the mirror supported at 45°, is now reflected sideways into a brass tube. This tube is long enough to project beyond the monochromator housing and wide enough to enclose one of the quartz windows of cryostat, (see figure 11). The other quartz window is enclosed by a short brass tube soldered to the photocell housing. The photocell housing and the cryostat itself stand on a table of adjustable height, and black-out

PLATE I.

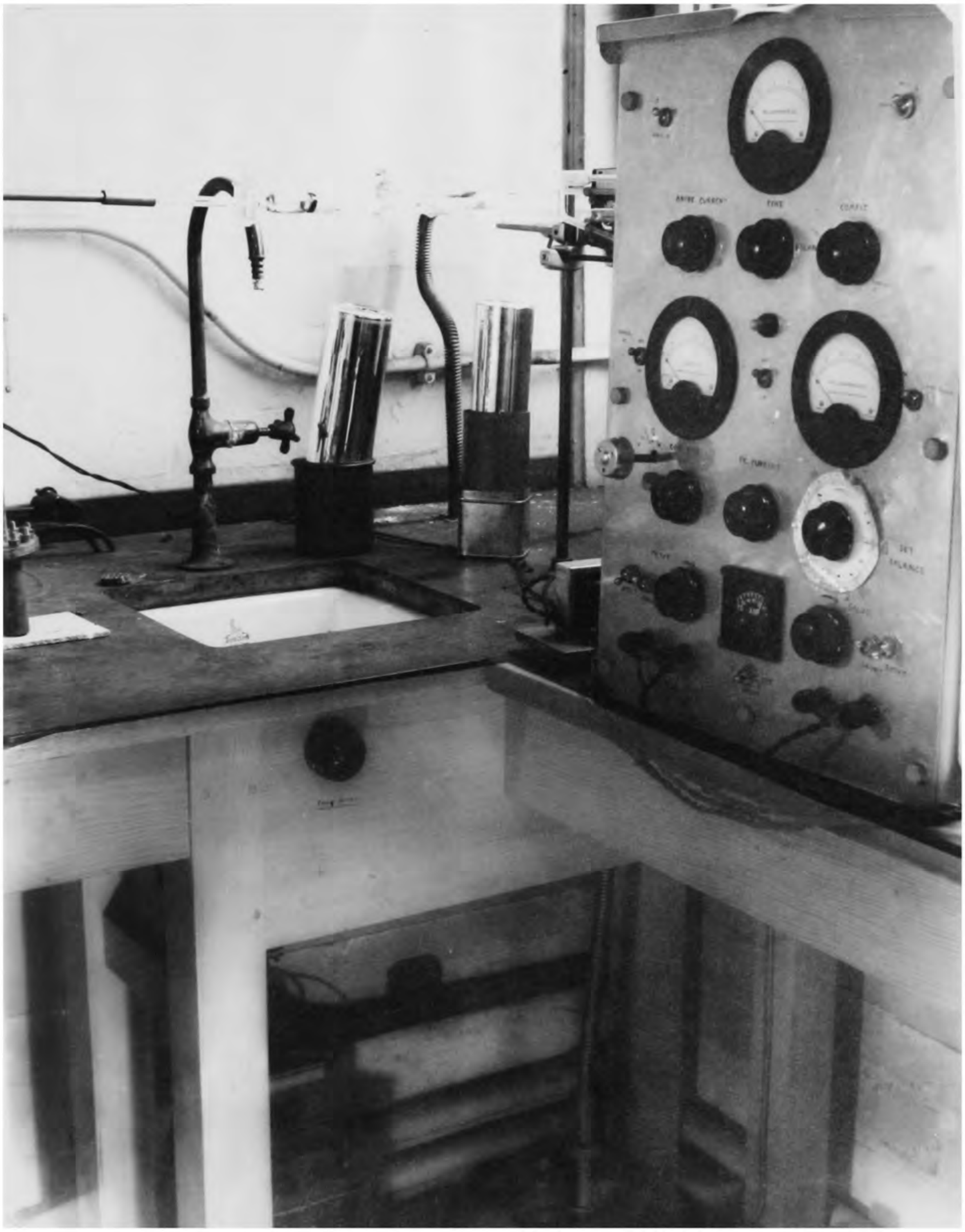

GENERAL VIEW OF APPARATUS.

PLATE II

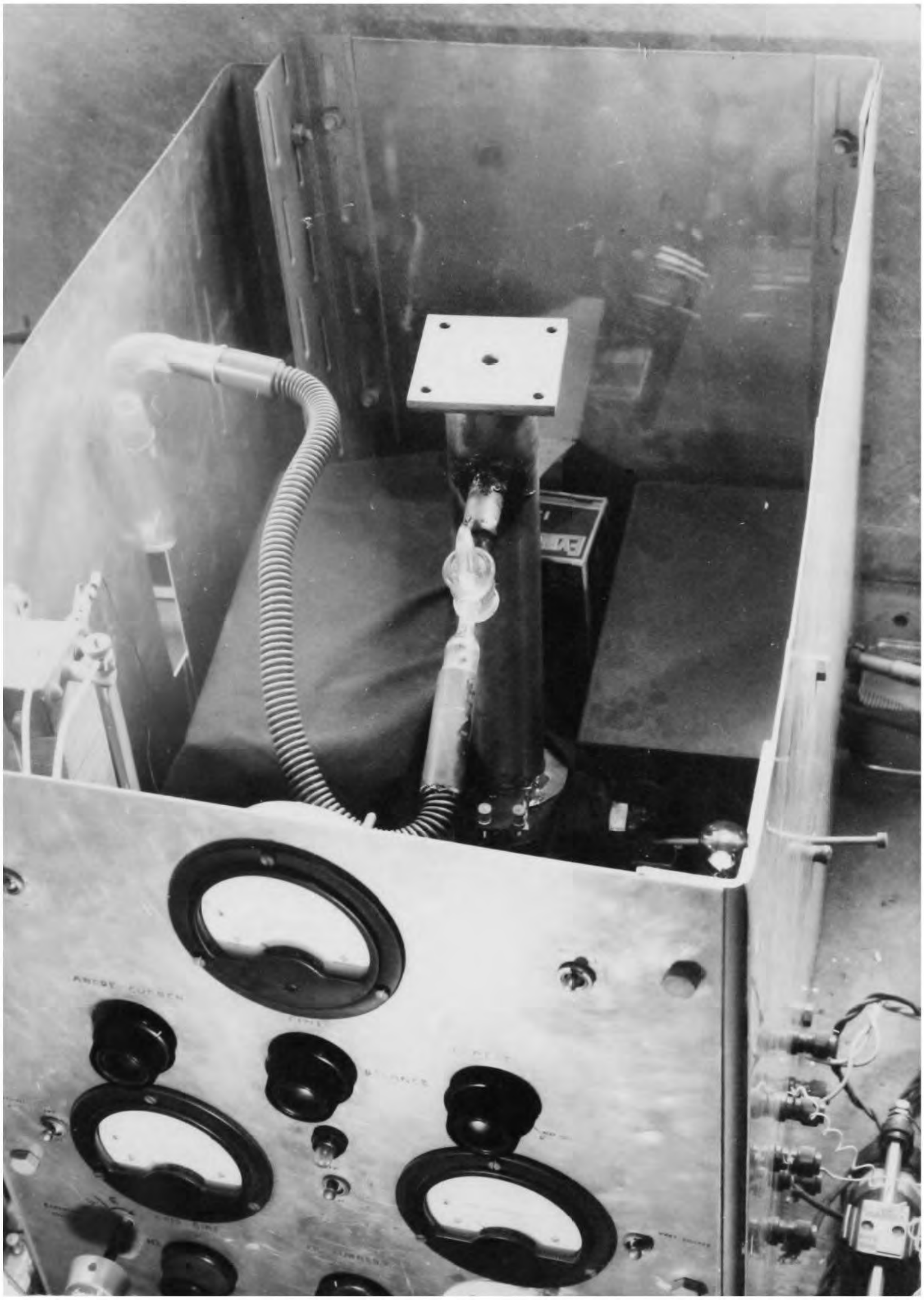

THE LOW-TEMPERATURE ABSORPTION SPECTROPHOTOMETER.

material is used to drape the "optical" joins to cut out stray light (see Plate II).

An important modification to the whole apparatus is the introduction of a shutter, a metal plate which can be moved across the entrance slit of the monochromator, an addition making for greater reliability in readings, as will be shown.

2.8 Operation

The specimen whose absorption spectrum is required is mounted, and if the measurement is to be made at $80^{\circ}K$ the cryostat is evacuated and liquid nitrogen is poured into the container until it is three-quarters full. The following procedure is now observed:-

(1) The balance is checked with the grid earthed.

(2) The tungsten lamp is switched on and the light is focused on the slit.

(3) With the shunt set at 100Ω and the micrometer reading about 12.00, the earthing switch is turned fully clockwise so that the low sensitivity range is used. A deflection of not more than 1 to 1.5 cm due to the photocell dark current plus stray light should be observed.

(4) To test the focusing, a swift run-through of the spectrum is performed. It should be necessary to reduce the shunt resistance to keep the galvanometer spot on the scale when the micrometer is reading from 21 to 24.

(5) The zero-wavelength setting of the micrometer is checked using the zero-order reflection from the grating.

(6) The micrometer is now set to give the required wavelength.

(7) Readings are taken when the shutter is closed, when it is opened, and when it is closed again. The last reading is a check to counteract any drifting which may have occurred, although this should not exceed 0.2 cm. The mean of the first and last readings subtracted from the second reading gives a value A, which is related to I_o by $I_o = A - S_o$, where S_o is the stray light correction.

(8) A value B is obtained in a similar way with the light passing through the crystal. Here $I = B - S$, where S is the stray light correction with the crystal in the beam.

(9) S_o and S are found by following the above procedure when the micrometer is reading about 12.00.

$$\text{Hence} \quad d = \log_{10} \frac{I_o}{I} ,$$

where d is the optical density of the specimen.

(10) To investigate the ultra violet spectrum, the filament current for the hydrogen lamp is switched on and 1½ minutes are allowed to pass before the H.T. is switched on; the light is then focused on the slit.

(11) The earthing switch is set to give the high sensitivity range.

(12) The procedure is then exactly the same as for the visible spectrum except that to find S_o and S the micrometer should be set at about 5.00 cm.

2.9 Maintenance

It was found that little maintenance work, above charging accumulators and renewing the silica gel in the detection unit housing, was necessary. The electrometer valve and the photocell were periodically cleaned with carbon tetrachloride, and it was found helpful to polish the slide of the crystal holder now and again to facilitate the lifting of the tray. Electrical maintenance consisted mainly of correcting large fluctuations which often appeared when the instrument had not been used for a period, due to either loose contacts or bad contact along a potentiometer wire.

2.10 Performance

A critical judgment of the performance of an absorption spectrophotometer rests on the appreciation of an ideal instrument and the comparison between the two, the ideal instrument in this case being one which is electrically stable, and has a monochromator combining constant intensity of light and an accurate wavelength calibration with good resolving power. Since the measurement of F-centre absorption is the main purpose of such an instrument here, the intensity of light passing through the crystal must be made low enough to make bleaching effects negligible. Since most of these factors are interdependent the practical instrument turns out to be some sort of compromise, and it is of interest to discover how the particular compromise effected in the instrument just described compares with the ideal.

Electrical instability manifests itself in random fluctuation and steady drifting; the former is related to the amount of light falling on the photocell cathode since if this is low the signal-to-noise ratio is low. The random fluctuations in the instrument are comparable to a signal fluctuation of the order of 10^{-14} amp but this is eliminated by increasing the response time of the galvanometer by reducing the shunt resistance to 500Ω or below. This also has the effect of reducing sensitivity. The drift is more variable. If the apparatus is left over-night the drift is about 10-20 cm scale deflection, i.e. about 1 cm per hour which is as good as may be hoped for, but the disturbance caused by taking measurements increases this rate almost tenfold, but this decreases to the negligible 1 cm per hour as measurements proceed. This drift is probably due to an inherent instability of the electrometer valve. Its effect, when appreciable, is greatly reduced by the method of measurement (see 2.8).

The necessity to counteract instability springs from maintaining a high resolving power, which requires a narrow slit and hence a weak illumination of the photocell cathode. The width of the slit is 0.007 cm giving a bandwidth of 1 mμ which, since a grating spectrum is linear, is constant over the whole wavelength range.

Although the light sources are only semi-stabilised, changes in light intensity are slow after an initial settling down period and are negligible during any one measurement of density.

Periodically, the wavelength calibration has been checked by using a mercury vapour lamp as a line source. The table is typical of the errors found:-

λ (calibration)	λ (mercury)	Error Å
2652	2652	0
2958	2967	-8
3133	3126	+7
3345	3342	+3
3660	3552 group	-2
4053	4047	+6
4356	4358	-2
5452	5461	-9
5785	5791 group	-6

The hydrogen lamp itself has been used as a check, since above 370 mμ it emits a line spectrum; in particular the 4861Å line is conveniently strong. Although not as refined a check on wavelength as a line spectrum, the F-band peak itself at 4650Å in NaCl provides a reference. All methods indicate a satisfactory calibration which is stable.

Figure 12 indicates the estimated error Δd which may be expected in one measurement of d, the density, as a function of wavelength, for three

Fig. 12. INSTRUMENT ERROR CURVES

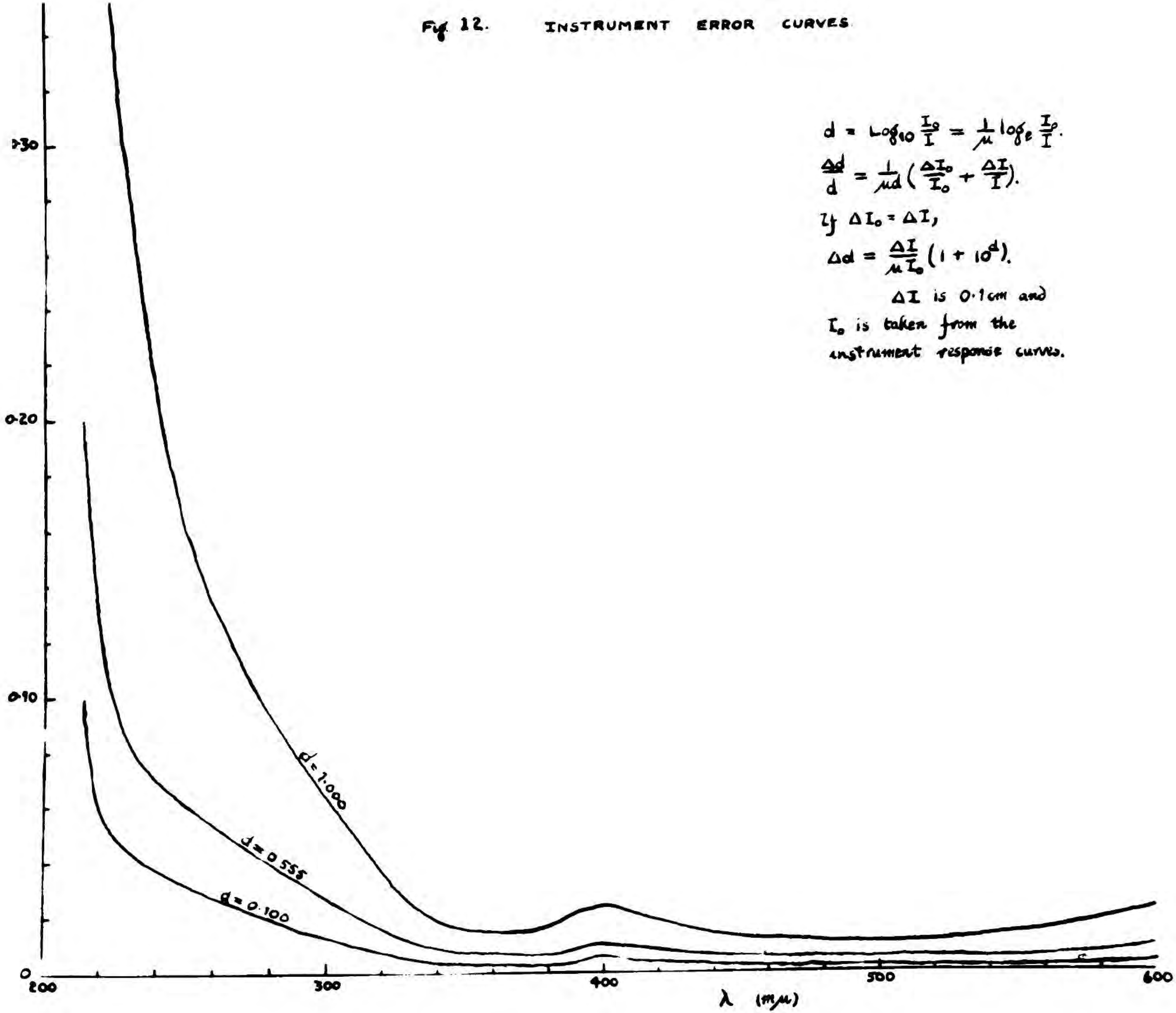

values of d. These curves were calculated on the assumption that I_o and I, the galvanometer scale readings, may be in error by 0.1 cm. I_o is a function of the emission spectrum of the source, and the response spectrum of the photocell. Typical total response curves are shown in figure 13 and I_o is taken from these curves to calculate Δd at various wavelengths. The accuracy is good in the visible but falls off with wavelength in the ultra violet, since the intensity of emission of ultra violet light from the hydrogen lamp becomes very low towards 200 mμ. The curves are unduly pessimistic in the region 200 mμ to 300 mμ, for when deflections are small the error in I_o is not above 0.05 cm; also the accuracy may be increased by replicate readings (a repeat reading is always taken even in the visible region) but a practical limit is set by the time factor and the limiting wavelength at which a useful value of d may be obtained is not much less than 240 mμ at moderate densities.

The greatest drawback of the apparatus is that of the time factor: it takes 2 to 3 hours to plot a spectrum throughout the range and it is laborious, exacting work. Future modifications should therefore be concerned with reducing the time to run through a spectrum.

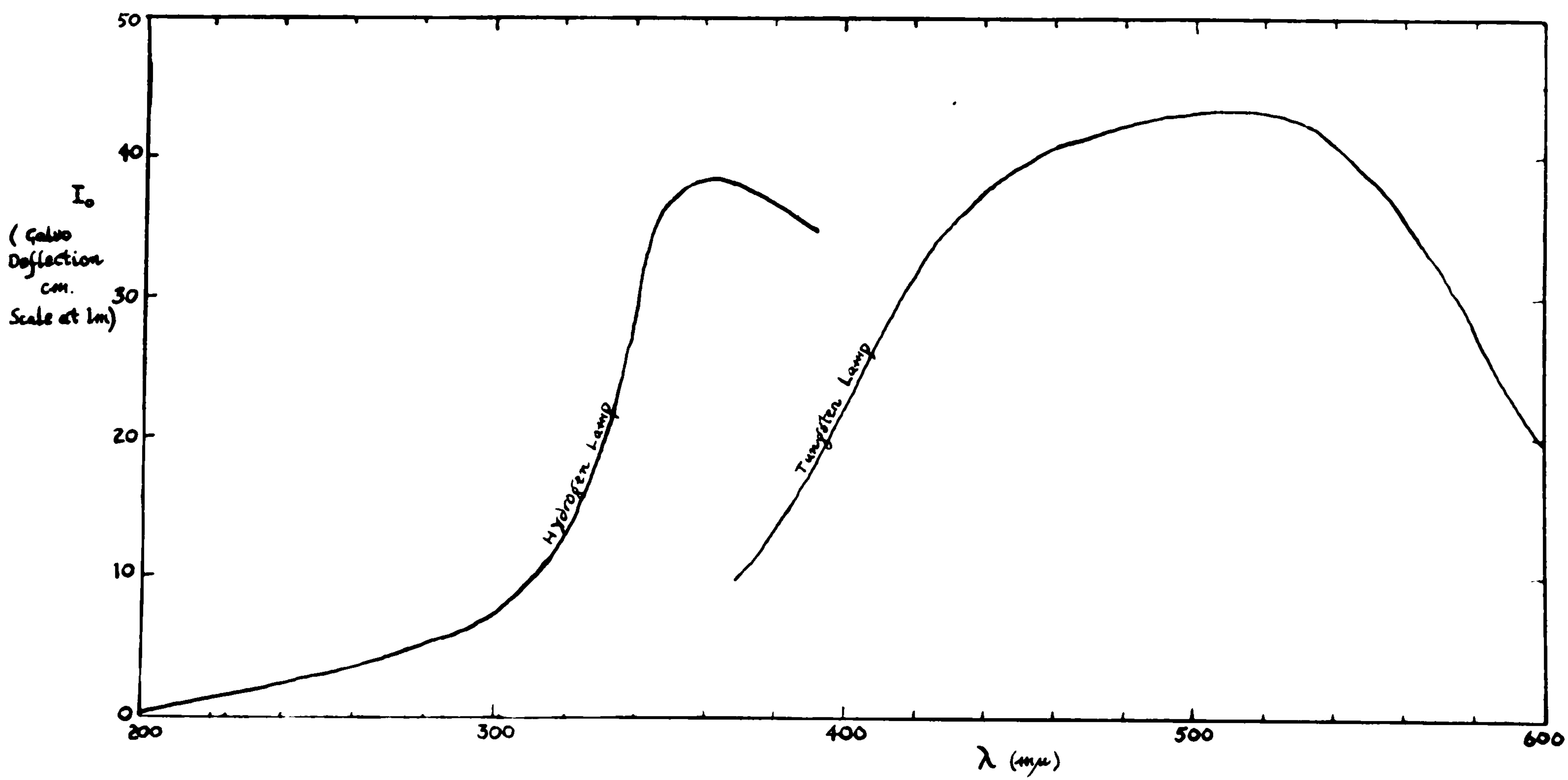

Fig. 13. TYPICAL INSTRUMENT RESPONSE CURVES

2.11 The Wavelength Calibration.

Micrometer Setting	Å	eV
8.50	1971	6.26
8.75	2028	6.08
9.00	2084	5.92
9.25	2141	5.76
9.50	2198	5.61
9.75	2255	5.47
10.00	2312	5.34
10.25	2368	5.21
10.50	2424	5.08
10.75	2480	4.97
11.00	2536	4.86
11.25	2594	4.75
11.50	2652	4.66
11.75	2709	4.55
12.00	2767	4.46
12.25	2823	4.37
12.50	2880	4.29
12.75	2937	4.20
13.00	2993	4.12
13.25	3053	4.04
13.50	3113	3.96
13.75	3173	3.88
14.00	3234	3.81
14.25	3289	3.75
14.50	3345	3.69
14.75	3401	3.63
15.00	3457	3.57

Micrometer Setting	Å	eV
15.25	3515	3.51
15.50	3573	3.45
15.75	3631	3.40
16.00	3689	3.35
16.25	3747	3.29
16.50	3807	3.24
16.75	3865	3.19
17.00	3925	3.14
17.25	3980	3.10
17.50	4035	3.06
17.75	4090	3.02
18.00	4146	2.98
18.25	4200	
18.50	4257	2.90
18.75	4312	
19.00	4368	2.83
19.25	4425	
19.50	4482	2.73
19.75	4539	
20.00	4597	2.68
20.25	4655	
20.50	4714	2.62
20.75	4772	
21.00	4831	2.55
21.25	4887	
21.50	4945	2.50
21.75	5001	
22.00	5059	2.44
22.25	5114	
22.50	5170	2.39

Micrometer Setting	Å	eV
22.75	5226	
23.00	5282	2.34
23.25	5338	
23.50	5394	2.29
23.75	5450	
24.00	5507	2.24
24.25	5564	
24.50	5624	2.19
24.75	5682	
25.00	5741	2.15
25.25	5797	
25.50	5854	
25.75	5910	
26.00	5967	2.07

3 THE GROWTH OF SINGLE CRYSTALS

3.1 The Kyropoulos Technique.

In recent years, the growing of single crystals has been stimulated by the need for such in investigations of the physical properties of the solid state, and there are many methods now available. The commonest and cheapest method is to grow from solution, but there are many disadvantages not the least of which is that the growing time is a matter of days rather than hours. Methods have been evolved for growing directly from the vapour (see Koref, 1922) and by electrolysis (see van Liempt, 1925), but these methods are usually used to magnify crystals which have been grown by some other method. In this respect, the zone-melting method developed by Pintsch (1918), and the cold work recrystallization method of Sauveur (1912), are similar. The most generally useful method for obtaining large single crystals in the laboratory is to grow from the melt, and many techniques based on this have been evolved, three of which are worthy of note. These are the "flame fusion process" developed by Verneuil (1904), by which crystals of ruby, rutile and sapphire have been successfully grown; the Stockbarger method (1938), which has been used extensively to grow crystals of metals; and, finally, the technique devised by Kyropoulos (1926, 1930), mainly used to grow crystals of the alkali halides. The choice of technique in a particular case depends on the properties, most important of which is the melting point, of the substance involved, but essentially they are the same in that they are methods of producing a temperature gradient at the melting point over a small portion of the melt.

In the Kyropoulis technique, a seed crystal is supported so that one end dips into the melt whilst the other is cooled by a stream of water. A temperature gradient is developed within the seed, and this can be varied by altering the rate of flow of the water. The rate at which heat is conducted away from the melt immediately surrounding the seed may therefore be controlled. When this exceeds the rate at which heat is received from the furnace solidification occurs on the seed until the rate of cooling of the surrounding melt becomes too low, when the growing stops. This equilibrium is disturbed if the seed is raised a little, and further solidification occurs. By slowly raising the seed so that only the lower surface is in contact with the melt a single crystal can be gradually drawn from the melt.

The size of crystal which can be grown by this method depends on the size of the furnace; this is common to all the methods mentioned. There is, however, a limitation peculiar to the Kyropoulis technique. The rate of growth is directly proportional to the rate at which heat is conducted away from the melt, and this is directly proportional to the temperature gradient in the growing crystal. As the crystal grows this gradient decreases and the rate of growth falls. There is thus a growing time which it is scarcely worth while to exceed. With the alkali halides this growing time is about three to four hours.

The technique is a convenient one for use with materials of fairly low thermal conductivity. Its advantages are that the necessary apparatus is comparatively simple, and that the actual growth can be directly observed and controlled easily. It is therefore an emminently suitable method for growing single crystals of the alkali halides.

3.2 The Growing Apparatus.

The growing apparatus was that used by T. L. Goodfellow (1955) who has given a full description of it. A brief summary of this will be given here.

The furnace consisted of a thermal alumina core around which the heating coil of nichrome wire was wrapped. The core was thermally insulated from its surroundings by a packing of diatomaceous earth around it. The furnace was run from the mains, and dissipated energy at the rate of 1.3/4 kilowatts. The temperature controller was essentially an A.C. bridge, one arm of which was a platinum resistance thermometer contained inside the core, and whose output was made to trigger a switch so that a resistance in series with the heating coil was short-circuited when the temperature fell below the required temperature, and vice versa. This unit proved to be a delicate controller of temperature in the range 500°C to 1000°C. The seed crystal was held in a nickel chuck brazed to a nickel tube which was supported vertically along the axis of the core. The supporting structure allowed the tube to be moved up and down by the manipulation of a screw. Inside the tube was a concentric tube through which water could flow. Side by side with the growing furnace was an identical furnace used for annealing the newly grown crystal. Its only temperature control was a rheostat in series with the heating coil, adjusted so that the rate of heating was equal to the rate of cooling at a temperature of about 700°C.

Throughout most of the work porcelain crucibles were used to contain the melt. During growth, a crucible rested in the furnace on the cylindrical refractory bricks which fitted loosely into the bottom of the core. Towards the end of the work a grant from the Royal Society was used to obtain a platinum crucible. Since the wall thickness of the crucible was only 0.006" the crucible rested in the furance in a refractory cement mould which gave the walls some mechanical support.

3.3 The Growing Technique.

The crucible was packed with the material say NaCl, and placed centrally in the furnace core. It was important to see that the bricks at the bottom of the core were also central, otherwise asymmetric cooling of the melt would occur and hence the crystal would not grow symmetrically. A seed of dimensions 3 cm x 0.6 cm was prepared and inserted into the chuck. The seed should be of the same material as the melt and be a single crystal. The material was melted and held at a temperature which was about $50^{\circ}C$ above its melting point.

The melting-back process is now begun. Cooled by a flow of water, the chuck was lowered into the furnace until the seed just dipped into the melt. It was then fixed in position, and subsequent movement was achieved by the manipulation of the screw. The flow of water was reduced until it was just boiling inside the nickel tube, and the seed was allowed to melt back for a while, care being taken to maintain contact between the seed and the melt by lowering the chuck when necessary. It was sufficient to melt back for about 5 minutes.

To initiate growth, the flow of water was increased until it emerged tepid and the furnace was cooled to a temperature just above the melting point. Crystallization was observed as an ever widening circle around the seed. By screwing up the chuck a little at 5 minute intervals this circle reached a maximum diameter of about 4 cm before vertical growth became important. When this stage was reached it was sufficient to lengthen the periods between adjustments to the height of the chuck to 15 or 20 minutes. When the crystal was grown it was transferred to the annealing furnace, which had been switched on prior to this and allowed to reach its equilibrium temperature. The crystal was cooled to room temperature in the annealing furnace over a period of 12 hours.

The only part of the process which was not directly observable was the melting-back and the initial growth; this was due to the chuck obscuring the seed. This stage was the most important one since, if the melting-back were insufficient, a polycrystal would result. The observational difficult was overcome by using a galvanometer lamp situated above the furnace to illuminate the area of the melt immediately surrounding the seed. When the seed was just in contact with the melt a meniscus was present which reflected the light clear of the chuck, so that a spot of light was visible. Growth was indicated by the spot moving away from the seed.

Caution had to be exercised when the furnace temperature was being reduced to induce growth, or over-cooling occurred, freezing the surface of the melt. Factors which had to be taken into account were the thermal lag of the growing crystal behind the attainment of the temperature set by the controller, and the width of the opening at the top of the furnace core. Usually, the top of the core was covered over except for a strip for observation. If this strip was too wide, freezing-over became difficult to avoid.

The resultant crystal, roughly cylindrical in shape, had a diameter of about 4 cm and a length of about 5 cm after four hours of growth. Crystals of this size have been grown of NaCl, NaBr, NaI, KCl, KBr, and Kl using this technique; and by mixing the appropriate halide of the impurity metal with the charge in the crucible, crystals have been grown containing Ca, Mn, Cr, Ni and Cu as divalent impurities.

4 EXPERIMENTAL PROCEDURES

4.1 Introduction

This chapter will deal with the techniques and experimental procedures employed in obtaining the results quoted in later chapters, so that when it is time to describe experiments carried out this can be done without a welter of detail which may obscure the principles involved. It will contain, therefore, descriptions of specimen preparation; of how the absorption measurements were performed; and of how the crystals were coloured, bleached and chemically analysed; and it will also point out the difficulties encountered and the precautions taken. Since the result of any experiment depends upon the procedure adopted, a critical appraisal of the methods used will be attempted in order that some evaluation of the results may be made.

4.2 The Specimen.

The size of specimen was governed, within limits, by the size of the specimen holder of the spectrophotometer. Two of these instruments were available - the one described in Chapter 2, which was mainly used for measurements at low temperatures, and a Unicam S.P.500, which was used for room temperature work. The first of these demanded specimens about 1 cm square, while the latter required specimen dimensions of about 1.5 cm x 0.7 cm.

The thickness of specimens used was 0.1 cm and under, but for quantitative work with X-rayed crystals, where uniformity of colouring was desirable, crystal thicknesses were 0.05 cm and less.

All specimens were cleaved from the parent crystal along the (100) plane with a sharp razor-blade. This method gave specimens of uniform thickness and having excellent surfaces, providing the crystal had been well-annealed; often, in cases where the crystal had been quenched, or merely poorly annealed, cleaving was difficult and specimens with poor surfaces resulted. The effect of surface quality on optical absorption is discussed in the next section, and it is sufficient here to assume that a good surface is desirable. Improvements, where necessary, were achieved by polishing the specimen. A thick glass plate covered with soft cloth formed a flat surface on which the crystal was rubbed, and alcohol soaked into the cloth, or a paste of finely powdered ZnO_2, was used as the abrasive. To protect the crystal from moisture from the hand finger stalls were used. Apart from this process finger stalls were not used in the general manipulation of the specimen since it was easy to hold the specimen by the sides and to avoid touching the surface; in any case, strict precautions of this nature are necessary only when measurements beyond 200 mμ are contemplated, where the surface effect is large.

4.3 Initial Absorption.

The alkali halides are transparent to light down to about 200 mμ, but there is an apparent absorption, which has virtually a constant value from 1000 mμ to about 200 mμ in NaCl, due to reflection of light at the surfaces. The optical density associated with this is about 0.05. Another source of apparent absorption is surface scattering which accounts for the rise of the absorption curve towards 200 mμ. It was necessary to determine this initial apparent absorption in each case before the specimen was irradiated so that the effect of the colouring treatment could be assessed. In the case of additively coloured crystals, where by nature of the colouring process it was impossible to measure initial absorption, it was important that specimens should have good surfaces from which scattering was negligible, so that the initial apparent absorption could be calculated from Fresnel's laws of reflection.

Since some slight deterioration of surface was inevitable during colouring and bleaching, it was important to find out the magnitude of the effect. Figure 14a shows the ultra violet absorption of specimens with a range of surface quality, and figure 14b shows the effect of scratching the surface intensively. Generally, it was found that deterioration raised the general level of absorption and steepened the curve near

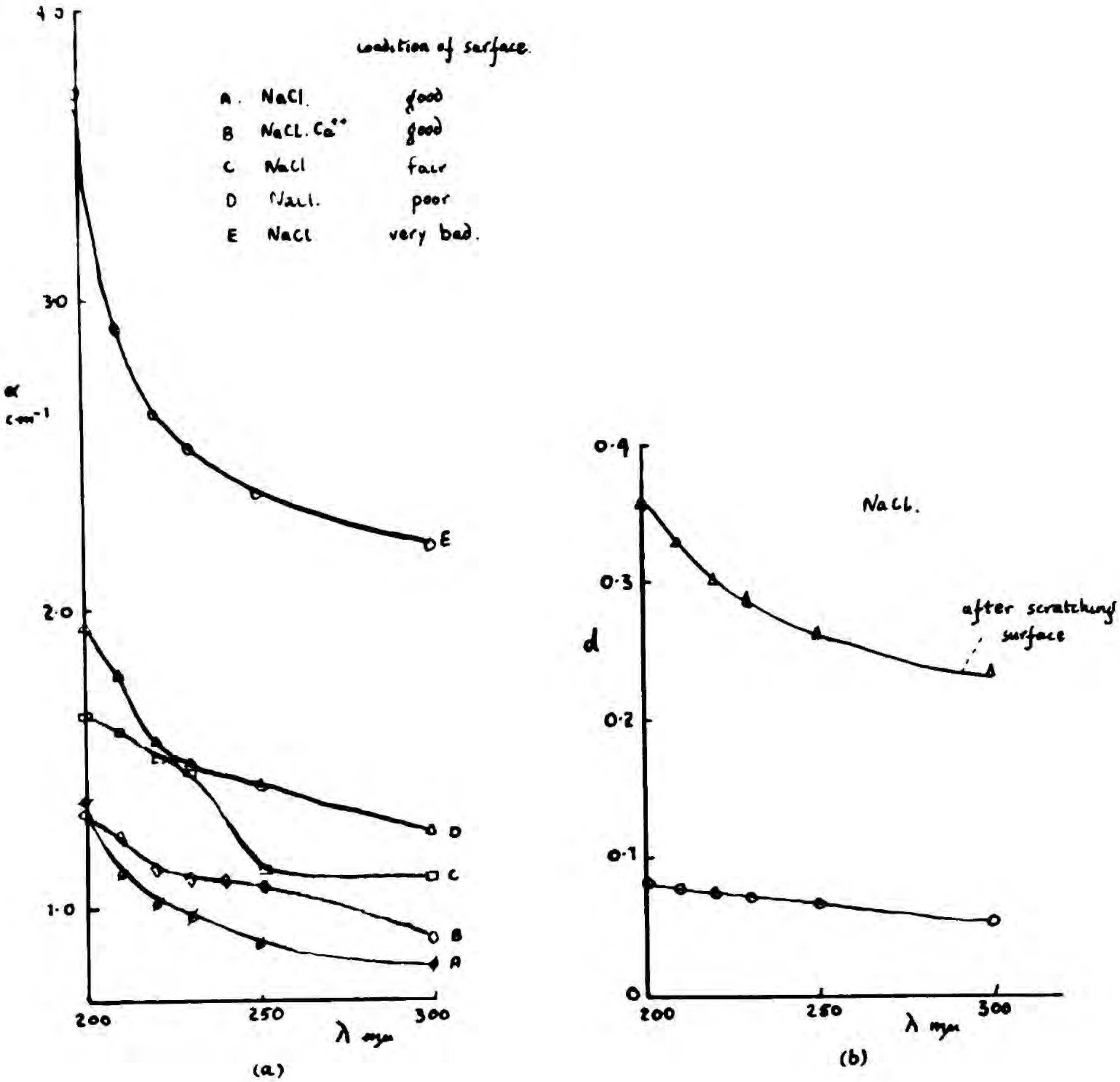

Fig. 14. EFFECT OF SURFACE CONDITIONS ON U.V. ABSORPTION.

200 $m\mu$, and the deterioration was always easily visible to the eye. The slight deterioration of a specimen during experiments produced only a negligible change in initial absorption.

Generally, then, it was advisable to use a specimen with a good surface so that the initial absorption in the ultra violet was low. A specimen which was inadvertently scratched during an experiment was discarded.

4.4 Measurement of Absorption.

In determining the absorption spectrum of a specimen the same general technique was used with both ~~either~~ instruments available. The coloured specimen was brought immediately from the colouring or bleaching site to the instrument to be used, so that thermal bleaching of the colouration (usually very slow at room temperature) was negligible; and optical bleaching was eliminated by carrying the specimen in a light-tight box. For the same reason the specimen was loaded into the spectrophotometer in semi-darkness. Ueta and Kanzig (1954) mention the precaution of waiting 10 minutes after optical bleaching before beginning measurements to allow the F'-band to decay, but attempts to observe this decay by making repeated measurements of optical density around 720 $m\mu$ from 5 to 10 minutes after bleaching have failed. It would appear that the F'-band, if formed at all at room temperature, has decayed within 10 minutes, so there is no danger in its manifesting itself as a broadening of the F-band.

Although the grating spectrophotometer and the Unicam had their own respective measuring procedures the underlying principles are the same. Absorption measuring instruments are based on the validity of de Beer's law, that is

$$I = I_o e^{-\alpha t}$$

where I_o is the intensity of light incident on an absorbing layer, I is the intensity after travelling t cm., and α is the absorption constant. The spectrophotometer is used to measure the ratio I_o/I. In the Unicam this ratio is expressed as the function $\log_{10} I_o/I$, which is the optical density, d. The relation between d and α is

$$\alpha = 2.303d/t \text{ cm}^{-1}.$$

Unless a comparison between specimens was desired it was convenient to display absorption measurements as plots of d against the wavelength, λ, otherwise it was necessary to measure t and convert to the absolute quantity α. The thickness of specimens was measured on completion of experiments as a matter of course, using a micrometer.

The wavelength interval between measurements of d was of some importance since if it was too large a narrow band could be missed. It was found that convenient, but by no means rigid, rules where coloured NaCl or KCl were concerned were to measure at intervals of 25 to 50 mμ in the near infra red, 10 to 20 mμ in the visible, and 10 mμ in the ultra violet.

4.5 Colouring by X-Rays.

Of the three methods used for colouring crystals, viz. heating with sodium vapour, exposure to α, β, and γ rays, and irradiation with X-rays, the latter was used most extensively. A machine manufactured by American Philips Company housed in a dark-room and having a tube with a copper target, was used as the source of X-rays, and it was operated at 40 kV and 20 mA. The apparatus is shown in figure 16. The crystal to be irradiated was held at a reproducible distance away from the source. This distance was about 12 cm and was sufficiently big to ensure uniform irradiation over the crystal surface by the slightly diverging X-ray beam.

When the tube was running it emits a dim glow and it was thought advisable to see if this had any effect on the resultant colouration. Two specimens from the same crystal were irradiated

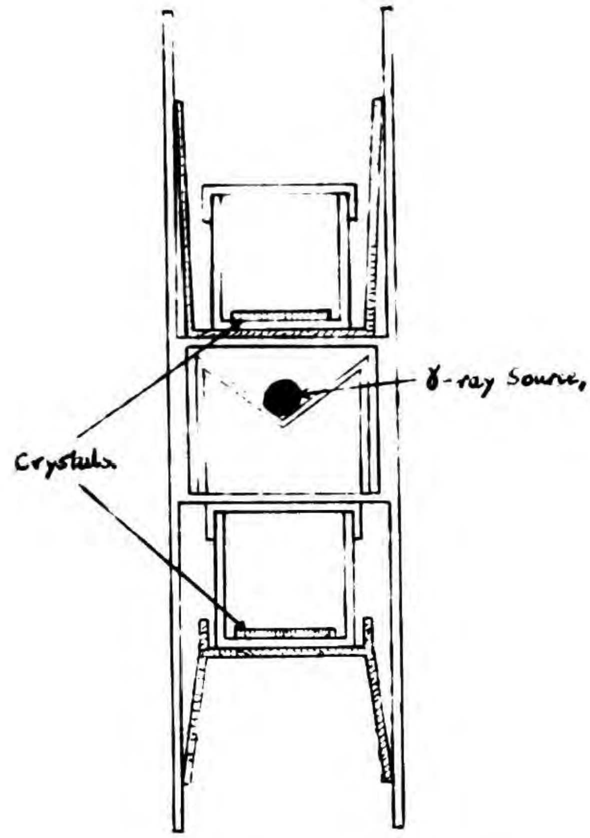

Fig. 15. APPARATUS FOR γ-IRRADIATION.

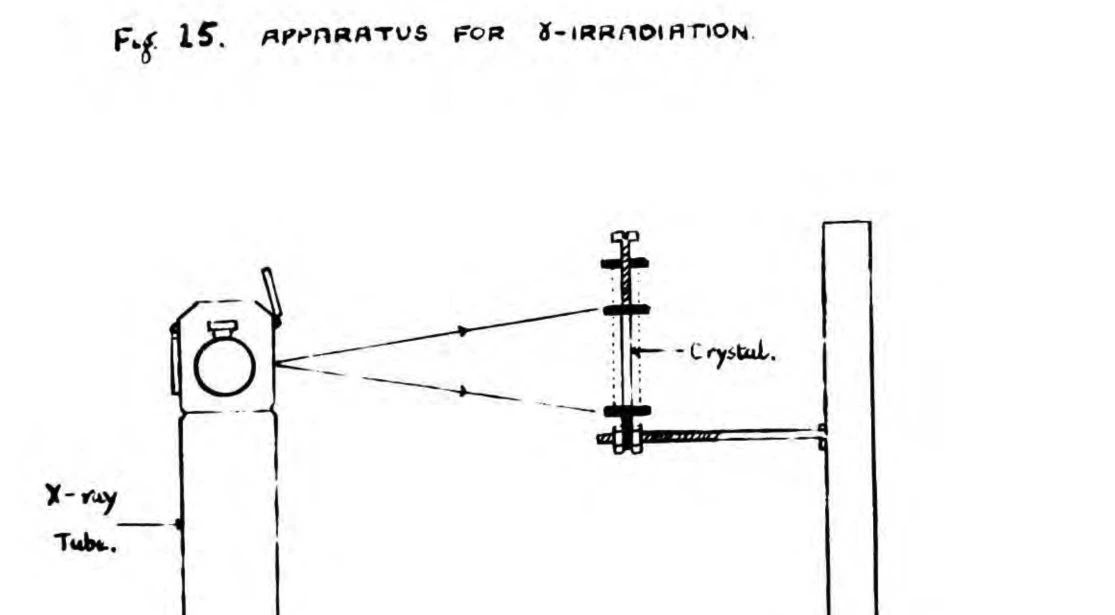

Fig. 16. APPARATUS FOR X-IRRADIATION

one being left uncovered, the other being covered with black paper. The resultant absorption spectra were identical, showing that the effect was negligible. Consequently, crystals were irradiated uncovered in general since the use of covering only increased the time of exposure necessary to give a given density of colouration. As it was, times of exposure ranged from 1 hour to 7 hours.

To achieve exposure times of this order it was necessary to dispense with a filter in the X-ray beam. Specimens were therefore exposed to a beam of heterogeneous X-rays, the full copper spectrum in fact, and this complicates any interpretation of the X-ray absorption of the crystal. The question of uniformity of colouration was not important where qualitative work such as the determination of band position or comparitive colouribility was concerned, but quantitative interpretation of results is vastly simplified if the colouration is uniform. A thick crystal was irradiated and cleaved into sections; the intensity of the F-band in each section was then measured. The results are given in figure 17. The experiment shows that the bulk of the colouration resides within 0.05 cm of the irradiated surface, but colouration falls of rapidly towards the interior of the crystal due to absorption of the X-rays. Although it was possible

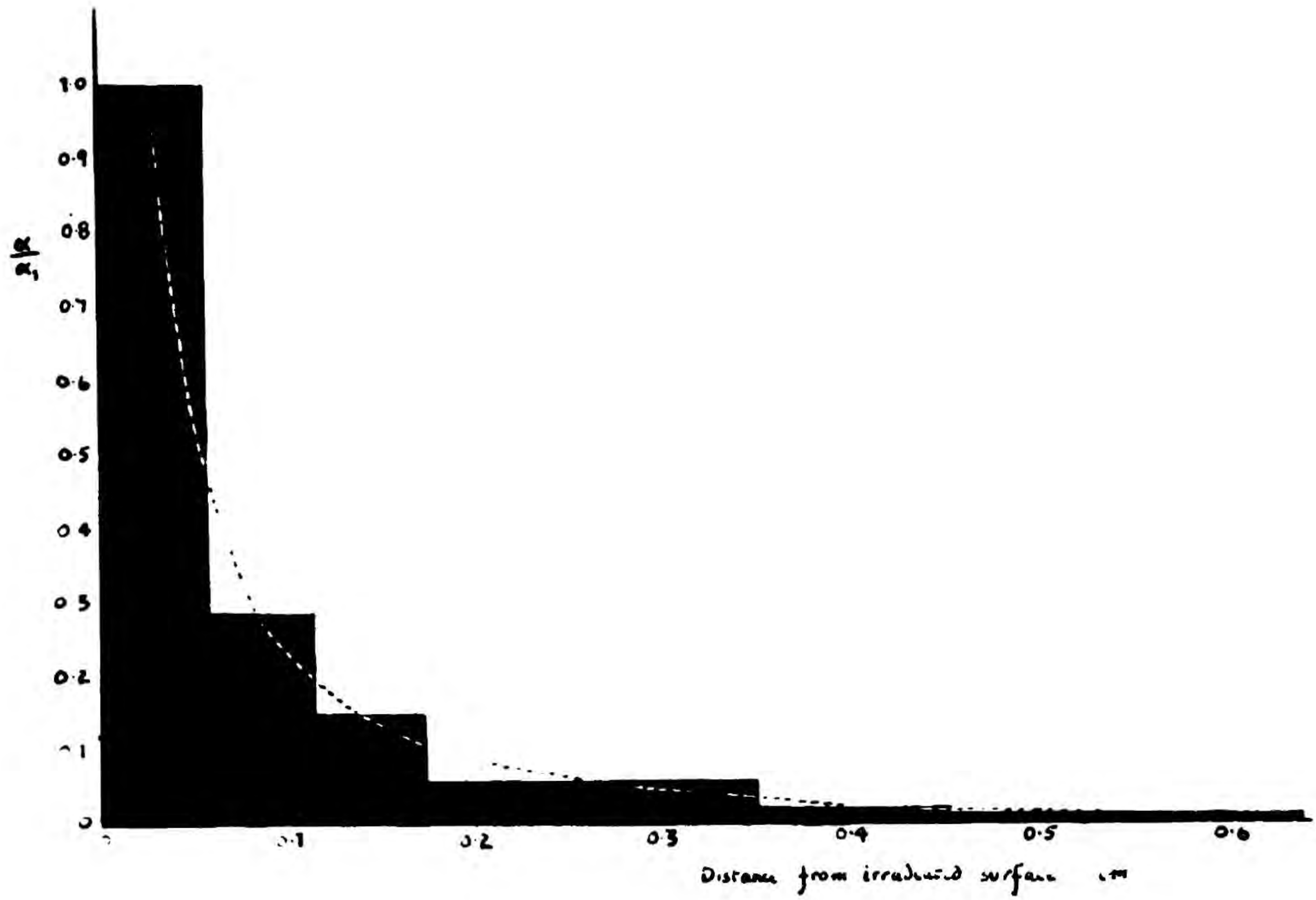

Fig 17. RELATIVE DISTRIBUTION OF F-CENTRES PRODUCED BY X-IRRADIATION.

to achieve more nearly uniform colouration in thicker specimens by reversing the specimen half way through the colouring process, it was thought more desirable in colouribility experiments to do this by using specimens of thickness less than 0.05 cm. The effect of non-uniformity is discussed in section 8.9.

4.6 Colouration by γ-Rays.

At the beginning of this work colouration of crystals was obtained by leaving the specimens near a radium capsule (1 m Curie). The specimens were placed in light-tight aluminium containers, one above and one below the radium in the manner shown in figure 15. The α-rays and most of the β-rays were absorbed by the aluminium so that the bulk of the colouring was due to γ-rays. The advantage of this method was the high degree of uniformity of colouration obtained, but this was outweighed by the length of time necessary to arrive at even a moderate darkening: three days near the source gave densities equivalent to one hour of X-irradiation. Unfortunately, a stronger radio-active source was not available and only a few crystals, notably some containing manganese (see Schneider and Caffyn, 1955), were coloured by this method.

4.7 Additive Colouration.

A high-temperature chamber, shown diagrammatically in figure 18 was constructed so that crystals could be additively coloured. It consisted of a cylinder of brass, closed at one end and carrying a flange on the other where the cylinder ends in a knife-edge, clearing the flange by 1/8 inch. A brass lid fitted closely on to the flange and was secured by eight brass bolts, so that the knife-edge cut into a copper annulus, making a moderately air-tight seal. A long brass tube was screwed into the centre of the lid and hard soldered, and its other end was joined to a vacuum tap and B19 cone by a metal-to-glass seal, effected with the thermally setting plastic, araldite. The chamber could thus be partially evacuated.

The technique, briefly, was to drop a fragment of sodium into the chamber, cover with a brass gauze, and place on top the crystal to be coloured. The lid was then bolted down tightly, but uniformly, and the enclosure was evacuated as far as possible. The chamber was then heated in the furnace for an hour, or longer if heavier colouring was desired, at a temperature of about 700°C. The chamber was withdrawn while hot and quenched in water. The crystals were then removed and cleaved (those, that is, which were not hopelessly shattered in quenching) to obtain a specimen with good surfaces (see section 4.3).

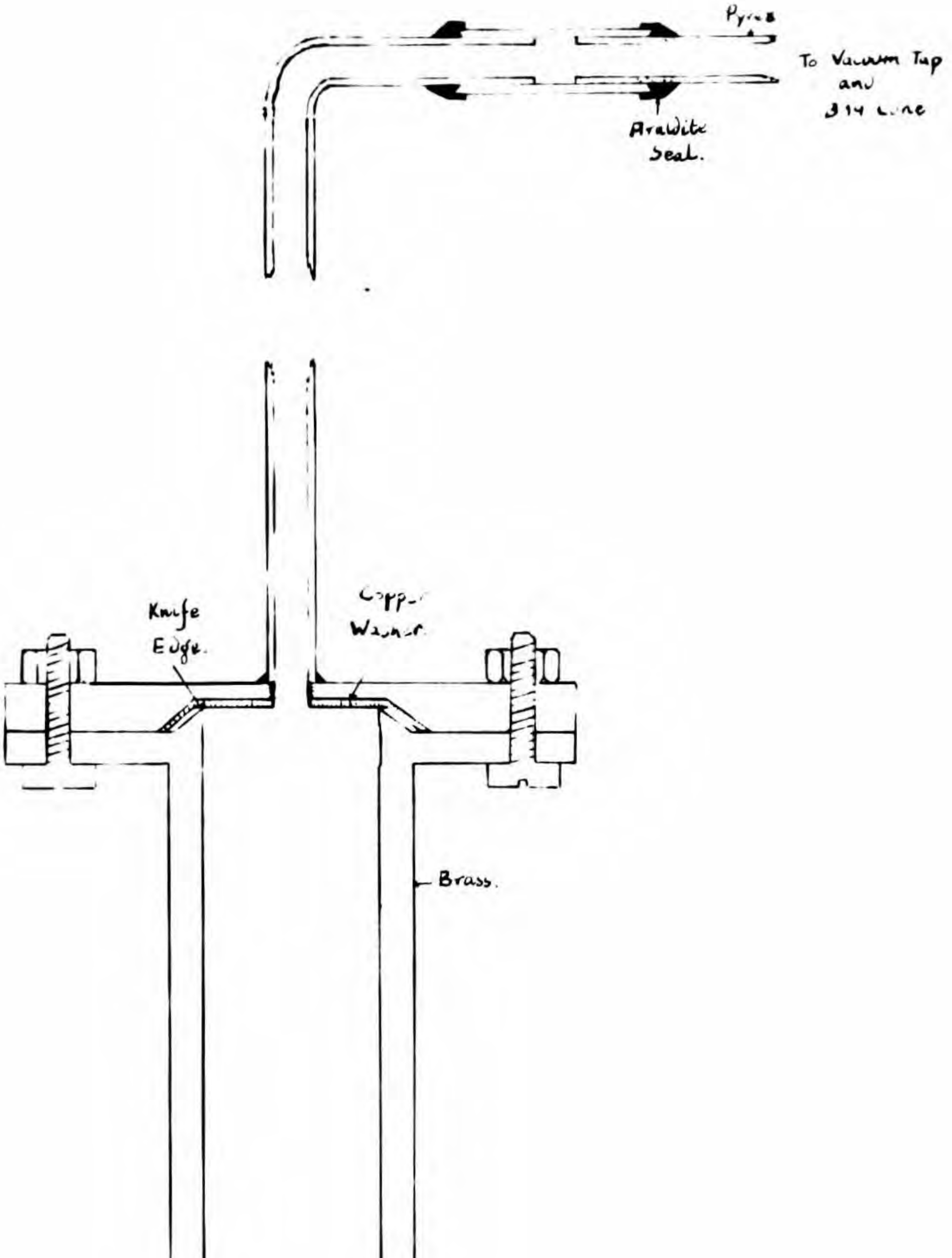

Fig. 18. APPARATUS FOR ADDITIVE COLOURATION

Several attempts were made to additively colour in an evacuated Pyrex container at a temperature just below the softening point of the glass (about 500°C). All attempts failed; prolonged heating was also ineffective. Although the specimen remained colourless, it was interesting to notice that the Pyrex apparently became coloured a deep brown. Closer examination showed the colour to be that of a thin layer on the inner surface of the tube, a layer which could be scratched off but resistant to concentrated acids, water and alcohol. Absorption measurements showed the colour to be due to a broad band peaking at 310 mμ. To assess the nature of the layer three containers were prepared, one containing a NaCl crystal plus sodium, one containing $CaCl_2$ powder plus sodium, and the third containing merely a piece of sodium. The $CaCl_2$ was included since it was known that all the crystals on which colouring attempts had been made contained calcium. It was found that only the tube containing NaCl plus sodium became coloured, which suggests that the layer was sublimed NaCl additively coloured in some way by the sodium. It was noted that the colour bleached very slowly in daylight, which supports the view that some type of colour centre was involved (see section 1.2). No further investigation was attempted.

4.8 Bleaching Procedures.

Optical bleaching of coloured specimens was carried out with light from either an ordinary 100 watt tungsten lamp or a cadmium vapour lamp (see figures 19 and 20). In both cases an Ilford filter was used to confine the light reaching the specimen to a band encompassing the wavelength of the F-band peak. To bleach the NaCl F-band, filter No. 602 was used. This passed a spectral band between 455 mμ and 470 mμ, which therefore confined the light from the cadmium lamp to the lines at 467 mμ and 480 mμ. The Ilford filter, No. 605, passing a band between 530 mμ and 575 mμ, was used for bleaching the KCl F-band. Bleaching was carried out in a dark-room to eliminate the effect of stray light,

The cadmium apparatus was designed so that the crystal could be bleached at a reproducible distance from the source, thereby allowing a comparison between crystals to be made easily. The tungsten lamp was mainly used for purely 'qualitative bleaching', that is, to find out what new bands were produced by bleaching without attempting to compare their intensities with those found in other crystals. The two methods gave similar results, i.e. in a bleaching time of 1 hour, roughly the same degree of bleaching was attained in a particular specimen, by each method.

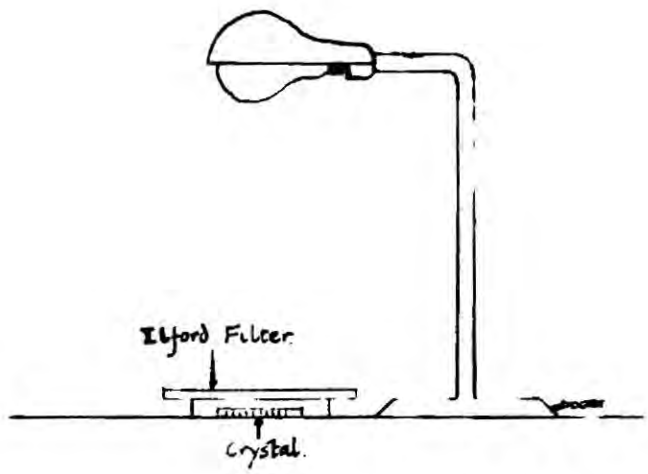

Fig. 19. THE TUNGSTEN LAMP BLEACHING UNIT.

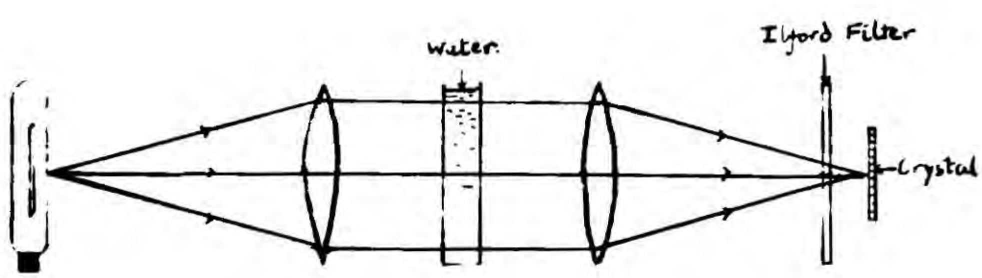

Fig. 20. THE CADMIUM LAMP BLEACHING UNIT.

4.9 Determination of Impurities.

Since the bulk of this work was done on crystals containing manganese and calcium as impurities it was important that the concentration of these metals in crystals be known. Analytical methods were considered in the light of the fact that only small quantities of impurity, a matter of micrograms in 1 gm of the crystal, had to be estimated. In view of this the general macro-analytical method of precipitating the substance to be determined, and weighing, was unsuitable, unless the substance could be precipitated as a compound of high molecular weight thus amplifying the effect of the small quantity. A much more convenient and sensitive amplification is to allow the impurity to form a coloured complex, or to change the colour of an existing complex, and to measure the effect with an absorption spectrophotometer. Colourimetric methods for estimating manganese and calcium were therefore used.

To determine manganese the method of Willard and Greathouse, (1917) was used. In principle the method consists of a conversion of the manganese to potassium permanganate, and a comparison of the intensity of the colour obtained with that of a standard solution of permanganate. A calibration curve was first obtained by measuring the optical density, at a wavelength of 525 mμ, of a solution having a known concentration of permanganate, and repeating this over a range of concentrations. The amount of manganese in each standard solution was calculated, and a graph was drawn plotting optical density against mass of manganese.

The procedure was then as follows. About 1 gm of the crystal was weighed and dissolved in 5 ml of concentrated H_2SO_4 in a boiling tube. The solution was placed in a fume cupboard, and boiled until all the chlorine had been driven off. 1 ml of concentrated phosphoric acid was then added and the solution was diluted to about 10 ml with distilled water. Excess KIO_4 (about 0.2 gm) was added while the solution was still warm, to form the permanganate. When cool the solution was made up to 25 ml in a graduated flask. Optical density measurements were then performed using standard absorption cells to hold the solution in the spectrophotometer. The instrument used for all analyses was a Unicam S.P.600. From the calibration curve, the amount of manganese in the original crystal was calculated and the result expressed as a mole fraction of NaCl.

From time to time the calibration was checked with known amounts of manganese. Errors found were of the order of 1% for mole fractions of about 10^{-4}, showing the method to be a very satisfactory one.

The concentration of calcium was determined by the spectrophotometric micro-titration method developed by Chalmers, (1954), which depends on the fact that calcium forms a coloured complex with murexide in alkaline solution. Thus, when murexide was added to the solution containing calcium, and the solution made alkaline, a strong pink colour was obtained. The complex was destroyed by the addition of disodium-ethylenediamine-tetra-acetate (E.D.T.A.), and murexide was reformed, giving the solution its characteristic purple colour. The reaction was therefore attended by a colour change from pink to purple, and this was used to determine the end-point when the calcium-murexide complex was micro-titrated against E.D.T.A. Since the colour change was a subtle one, the end-point was determined accurately by using the spectrophotometer to follow the change of absorption at 610 mμ as the complex was destroyed by the dropwise addition of E.D.T.A.

The method worked very satisfactorily so long as the mole fraction of calcium was 20×10^{-6} or greater, for with these concentrations it was possible to obtain solutions containing between 10 μgm and 150 μgm of calcium per cc, which were optimum concentrations for the method. With lower mole fractions, it was impossible to achieve optimum concentrations of calcium, since a limit was imposed by the solubility of the NaCl. Consequently, the error in measurements of mole fractions in the region 10×10^{-6} and below was about 25%. For mole fractions around 20×10^{-6} the error was about 10%, but above 100×10^{-6} the error became constant at about 2%.

5 WORK ON $NaCl.Mn^{++}$

5.1 Introduction

The optical investigation of crystals containing manganese began as part of a wider programme, designed to investigate the state of the manganese ions in the lattice by measurements of paramagnetic resonance absorption, optical absorption and ionic conductivity (see Schneider and Caffyn, 1955), and it was carried out on crystals coloured by γ-rays. Since the results of the programme have been published only the main points made will be discussed in this chapter. More recently, the optical work has been repeated and extended by the author, using X-ray coloured crystals, and also the distribution of manganese in single crystals has been investigated, and it is this work which will be described in this chapter.

The purpose of the investigation was to go some way towards answering the questions: how is the manganese built into the crystal, and what imperfections does it introduce into the lattice? It is known that some divalent impurities in NaCl and KCl give rise to Z-bands (see section 1.5) and it was of particular interest to see if manganese was similar in this respect, since only the alkaline earths are known to exhibit this phenomena. Also of interest was the effect of manganese on the crystal's colouribility to X-rays, since it is known that this is enhanced by the presence of some divalent impurities. Many solids containing manganese are luminescent (Kröger, 1939; Randall, 1939; Larasch, 1953; et al.), and it is thought that this is due to electronic transitions inside Mn^{++} ions built into the lattice. If this occurs in NaCl it will indicate how the manganese is built in.

5.2 The Growth of Crystals Containing Mn^{++}.

Crystals were grown from a melt containing Analar NaCl and Analar $MnCl_2$, present in the ratio of about 100:1. Since considerable decomposition of $MnCl_2$ occurred, with the formation of black MnO_2, when it was mixed with the initial charge of NaCl and melted, the impurity salt was added directly to the melt. It was found that when the melt contained a high proportion of $MnCl_2$ growth was difficult, and the crystals obtained were small, and far from clear. The manganese in the melt was gradually removed to form MnO_2 in a slow decomposition process, and this meant that the second crystal to be grown from the melt was usually large and clear, and easier to grow.

Crystals have been grown in which the mole fraction of manganese was as high as 3×10^{-3}. At this concentration the manganese is largely present in the crystal as colloidal aggregates, making the crystals almost opaque. Crystals having a mole fraction of about 1×10^{-3} were cloudy, but clear crystals were obtained with mole fractions of 500×10^{-6} and less. The investigations to be described were carried out using these clear crystals.

5.3 The Distribution of Mn^{++} in the Crystal.

The distribution of manganese in crystals of $NaCl.Mn^{++}$ has been investigated by Goodfellow (1955). His experiments showed that the concentration of manganese increased with distance away from the seed. His results were similar to those of Kelting and Witt (1949), who investigated the distribution of calcium in crystals of $NaCl.Ca^{++}$. In the course of determining the manganese concentration of several specimens the author became increasingly doubtful of the general validity of Goodfellow's result, and accordingly, he investigated the manganese distribution in three crystals.

The results of these experiments along with life-size drawings of cross-sections of the crystals are shown in figure 21. The shaded portions indicate the sections of the crystals which were used in the manganese determinations. The results show that there is no general increase of manganese concentration with distance from the seed, but rather, that the concentration depends

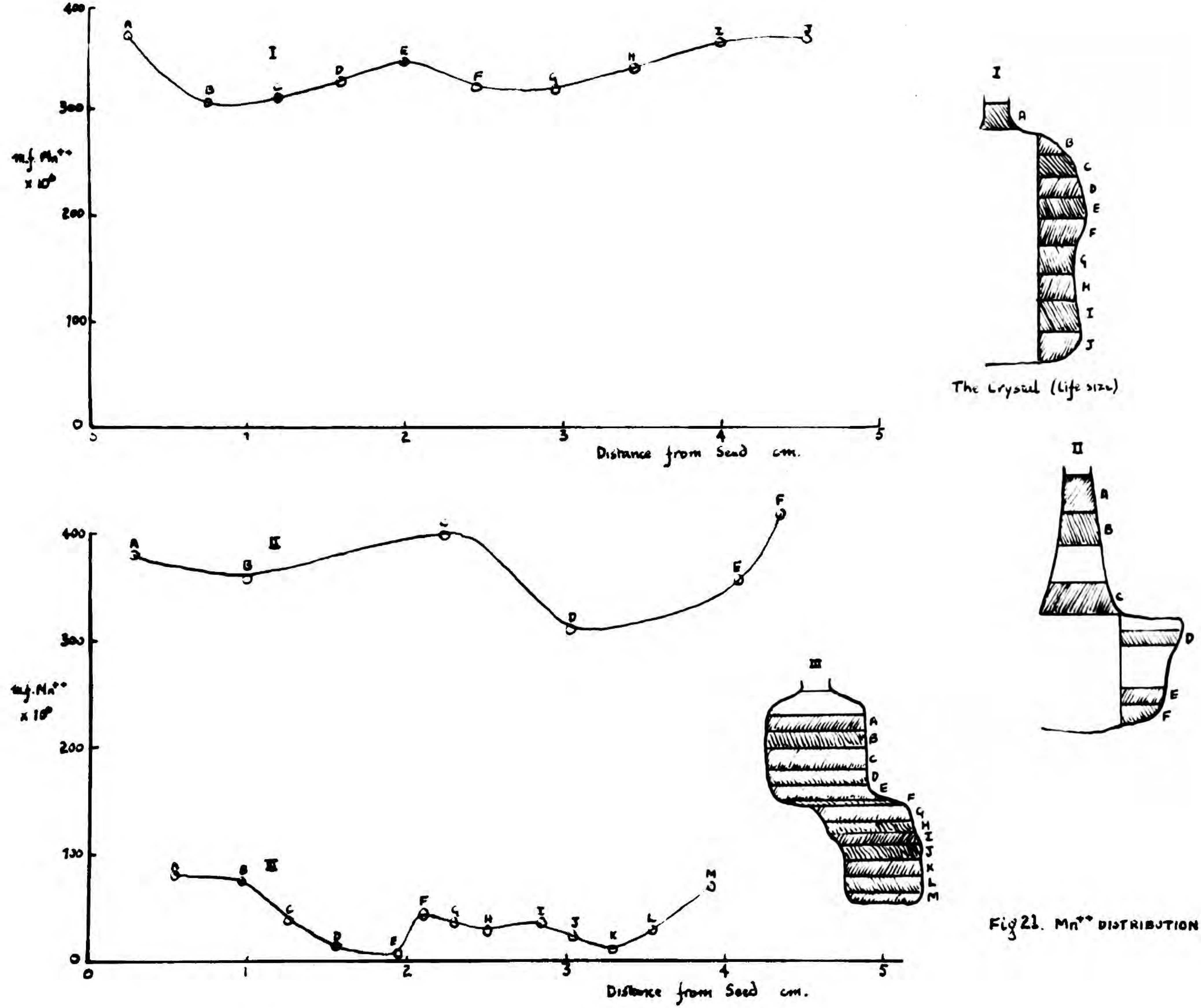

Fig 21. Mn++ DISTRIBUTION

upon the rate of growth, increasing when the rate rises and decreasing when the rate falls. Thus, concentrations were found to be higher where the crystal widened, and lower where it narrowed, and this suggested a dependence on growth rate, since when this is high the crystal grows outwards, and vice versa. Crystal 1 shows the dependence of concentration on shape particularly well. It is unfortunate that the section between C and D in Crystal 2 was not successfully analysed, for on the above theory it should have a higher manganese content than section C. Crystal 3 was grown at too high a temperature, which accounts for its thinness. When it had grown 2 cm from the seed, growth almost stopped. Growth began at an increased rate when the furnace temperature was lowered and the crystal raised almost out of contact with the melt. Section F reflects this in a relatively high concentration of manganese. It should be noted that the absolute values of the manganese concentrations have no significance in this discussion since the crystals were grown from different melts.

Goodfellow's result would suggest that there is a simple dependence of the concentration of manganese in the crystal to the concentration of manganese in the melt; as the crystal grows the melt becomes progressively richer in manganese, hence the rise in concentration in the crystal in the crystal during growth. A relationship of this sort is almost certainly true in the case of impurities which do not suffer decomposition in the melt, e.g. calcium; but as it has already been stated there is some decomposition of the manganese, and this will tend to counteract the enriching of the melt. Thus, a more uniform distribution may be expected in the crystal, and in fact, the results shown in figure 21 confirm this. A dependence upon the rate of growth is to be anticipated, since this, together with the rate of decomposition, determines the concentration of manganese in the melt. (For a theory of impurity distribution in crystals grown from the melt see, for example, Hulme (1955)).

5.4 Crystals Coloured with X-rays.

The crystals to be discussed in this section and the next are crystals which have been well-annealed.

The absorption spectrum at room temperature of the uncoloured crystal was measured. This was found to be identical with the spectrum of uncoloured NaCl in the visible and near infra red, but in the ultra violet region the presence of manganese gave rise to a weak band at 275 mμ and a general increase in absorption towards 200 mμ. The effect of increasing the concentration of manganese was to accentuate the rise towards 200 mμ without intensifying the band at 275 mμ notably. A very weak band at 275 mμ was also found in uncoloured $KCl.Mn^{++}$, which suggests that it is due to absorption by the manganese ion alone. The general rise towards shorter wavelengths has been noted before in the case of alkali halides containing other divalent impurities (see section 1.4).

A typical spectrum of the colouration due to irradiation with X-rays is shown in figure 22, in which the V-band at 220 mμ, the F-band, and the M-band at 725 mμ, are prominent. The colouration obtained in this way was compared with that obtained in crystals grown from Analar NaCl. It was found that the presence of manganese was responsible for:

(1) Increasing the general level of absorption in the ultra violet.

(2) Enhancing both the F-band and the V-band.

A propos to the first of these effects, it was found that in several specimens, irradiation with X-rays slightly enhanced the 275 mμ band. In the case of $KCl.Mn^{++}$ the ultra violet rise of absorption was not as marked, but the F- and V-bands were enhanced. This can be seen from figures 23 and 24 which are spectra of coloured specimens of about equal thickness, one of which

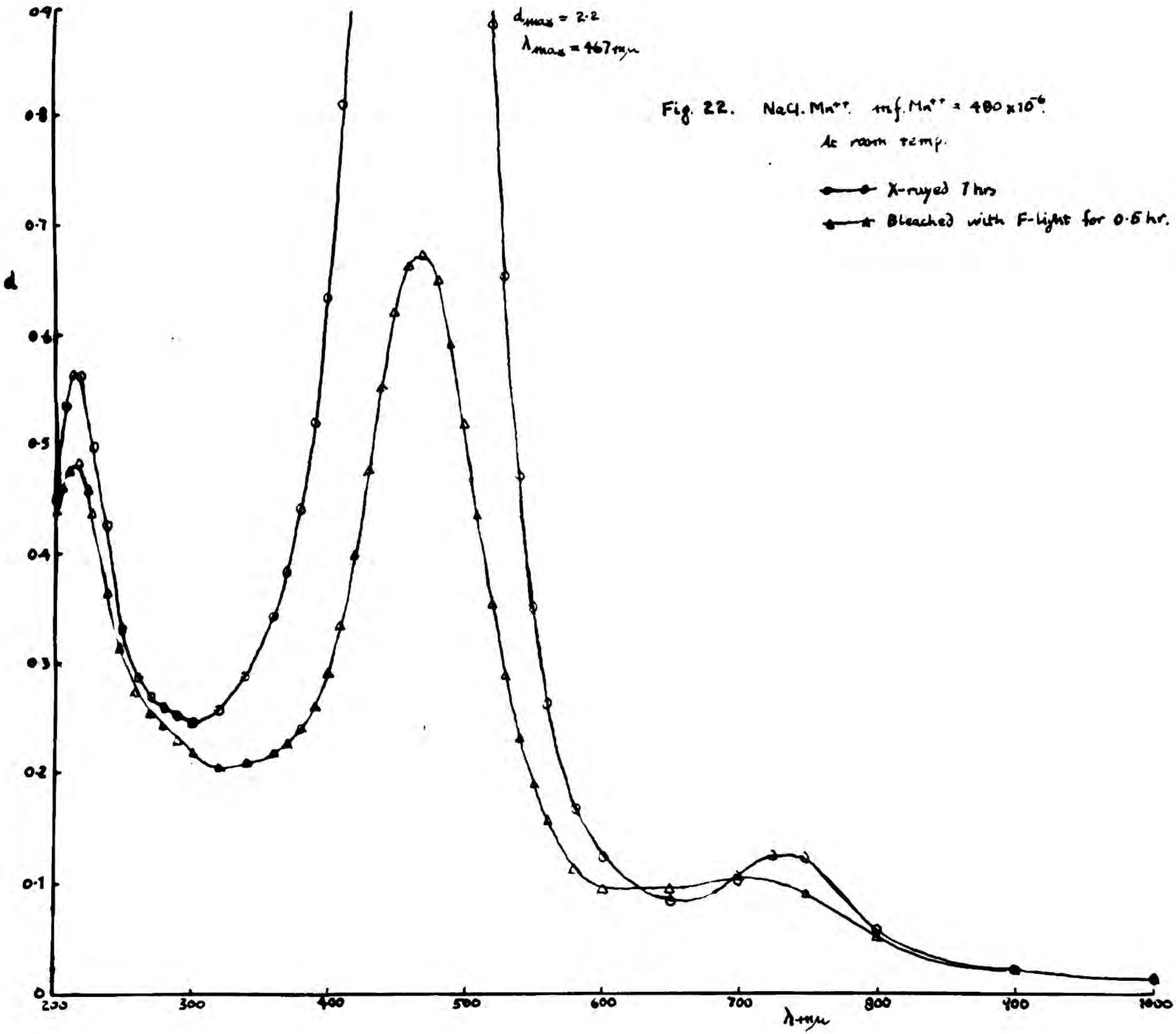

Fig. 22. NaCl. Mn^{++}. m.f. $Mn^{++} = 480 \times 10^{-6}$.
At room temp.

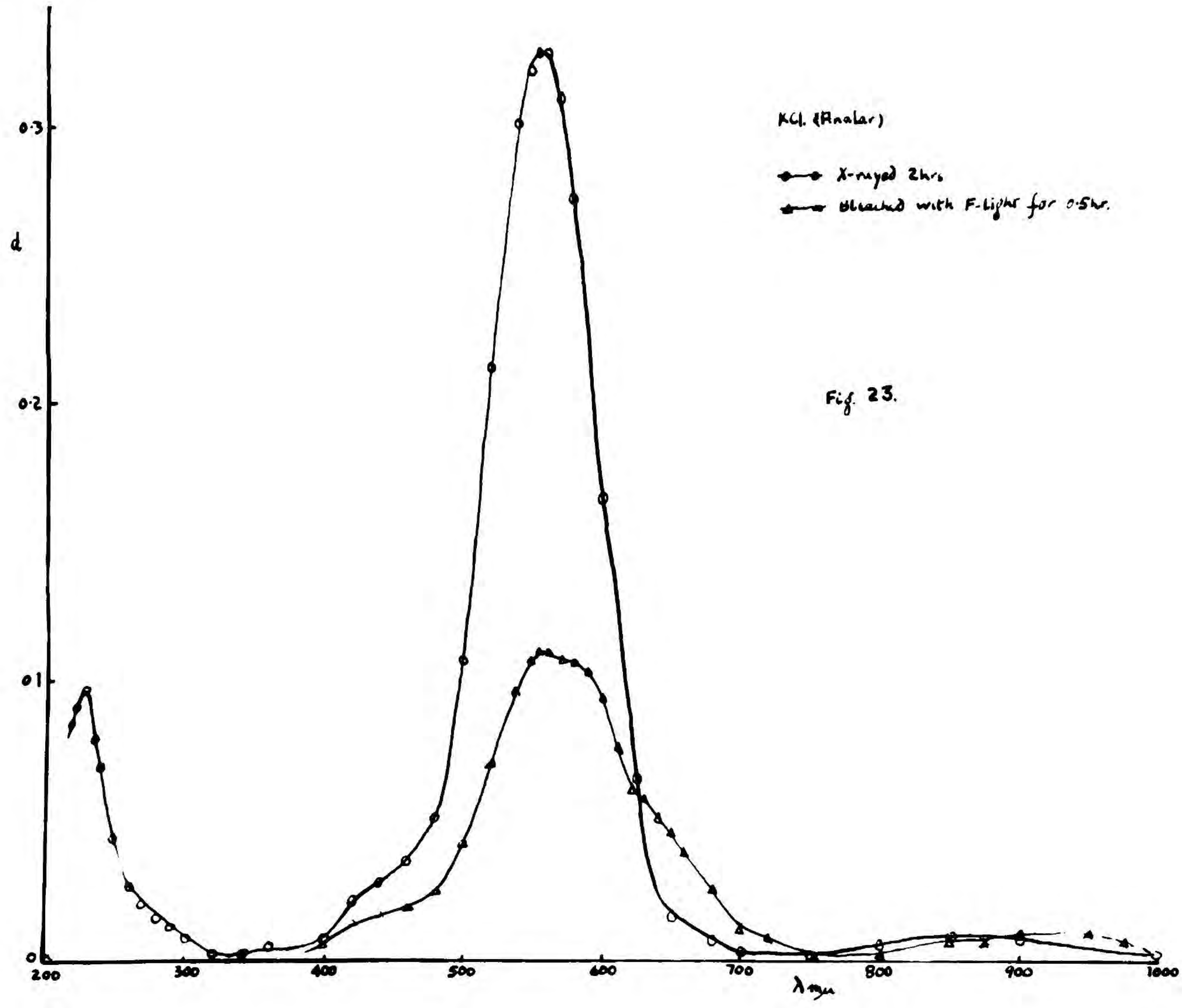
KCl. (Analar)
X-rayed 2hrs
Bleached with F-light for 0·5hr.
0·3
0·2
0·1
0
d
200
300
400
500
600
700
800
900
1000
λ mμ

Fig. 23.

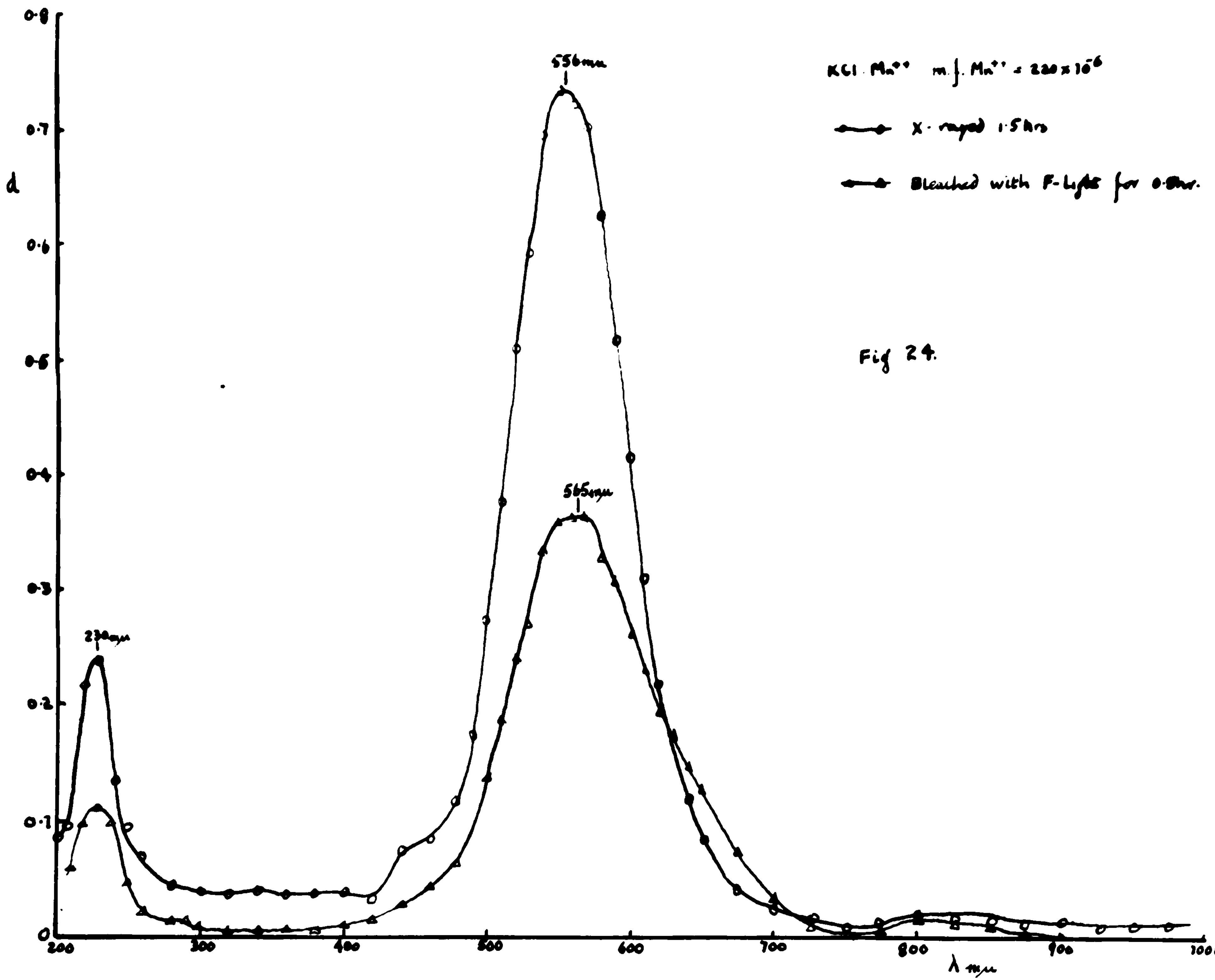

KCl. Mn⁺⁺ m.f. Mn⁺⁺ = 220 x 10⁻⁶
X-rayed 1.5 hrs
Bleached with F-light for 0.5 hr.
556 mμ
565 mμ
230 mμ
d
λ mμ
0·8
0·7
0·6
0·5
0·4
0·3
0·2
0·1
0
200
300
400
500
600
700
800
900
1000

Fig 24.

contains manganese while the other does not. The intensity of the F-band in the manganese bearing crystal is more than twice that of the other, after a shorter irradiation time, and the same is true of the V-band intensity.

5.5 The Effect of Bleaching.

The effect of exposing the crystal to F-light is shown in figures 22, 23 and 24. It can be seen that the decrease in the F-band is accompanied by the usual decrease in the V-band. There is also a fall in the general ultra violet absorption, but this occurs comparatively slowly in $NaCl.Mn^{++}$.

In all cases a broadening of the F-band on bleaching was observed. $KCl.Mn^{++}$ showed this particularly well. However, this broadening was found to occur in NaCl and KCl crystals which contained no manganese. This effect is discussed further in section 5.7.

A comparison of the bleaching rates of the F-bands in $NaCl.Mn^{++}$ and NaCl was made. A specimen of Analar NaCl was wrapped in black paper to eliminate any bleaching which might have occurred with stray light, and X-rayed for 2½ hours. The F-band intensity was measured. The crystal was irradiated with F-light for 5 minutes and the F-band peak absorption was again measured. By repeating this process a plot of the density, d, of the F-band peak against bleaching time was obtained. Exactly the same method was used to obtain a similar plot for the crystal of $NaCl.Mn^{++}$. For purposes of comparison the ratio d/d_o $(=\alpha/\alpha_o)$, where d_o was the density before bleaching, was used. The bleaching curves are shown in figure 25. It can be seen that the presence of manganese increases the bleaching rate quite substantially at the beginning of the bleaching.

5.6 The Effect of Quenching.

A crystal was quenched by heating it in the furnace for about 2 hours at $600^{o}C$ and then allowing it to cool rapidly in air. The crystal cooled to room temperature within 5 minutes. Some crystals were also quenched from $300^{o}C$. It was observed that some of the manganese was driven to the surface during the heating process, and this had to be wiped off before absorption measurements could be taken.

Typical spectra of a quenched crystal which has been coloured by X-rays, taken before and after bleaching, are shown in figure 26. It was generally found that quenching the crystal not only enhanced the 275 mμ band, but was responsible for the appearance of an equally strong band at 320 mμ

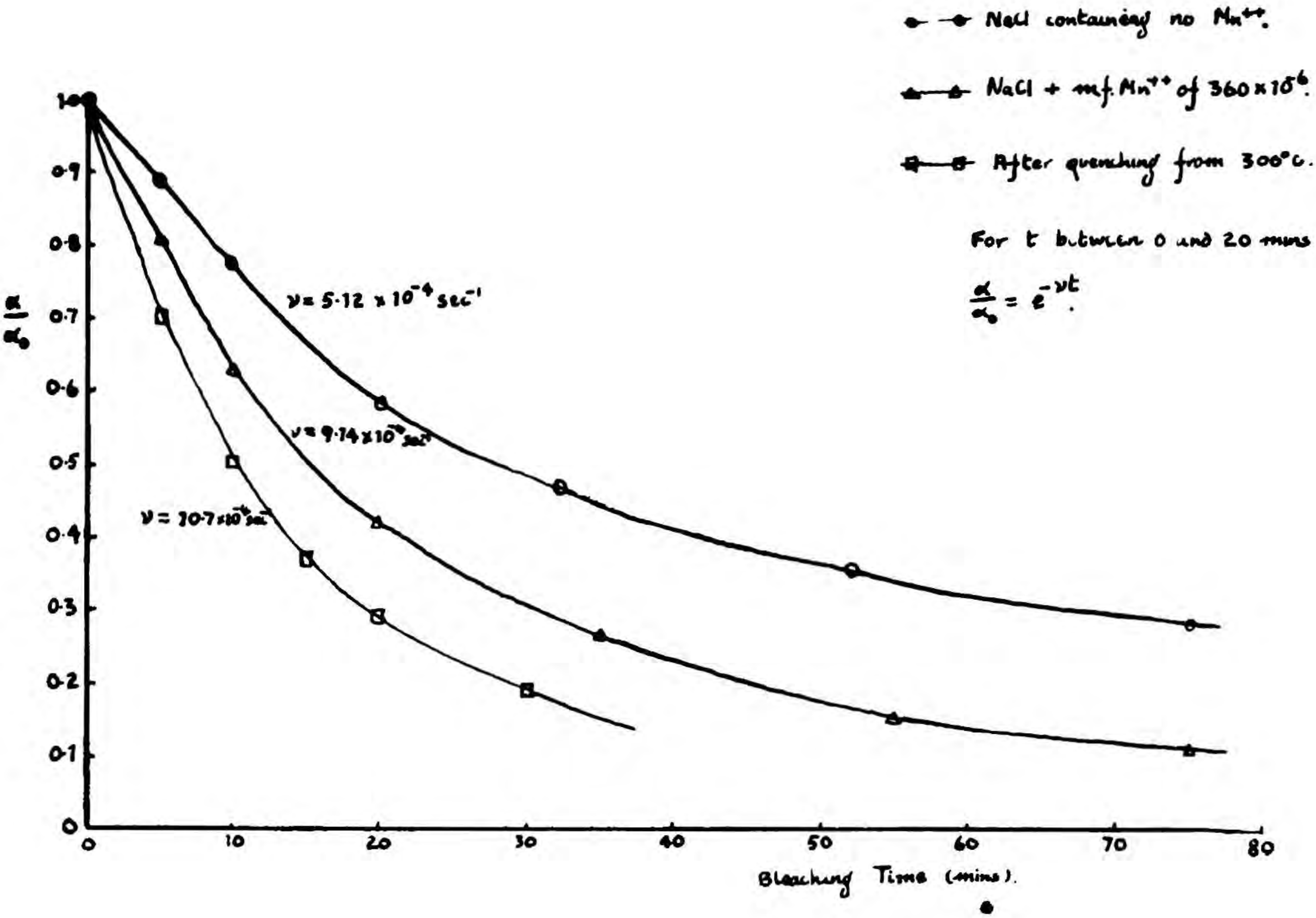

Fig. 25. THE EFFECT OF Mn^{++} ON THE F-BAND OPTICAL BLEACHING RATE.

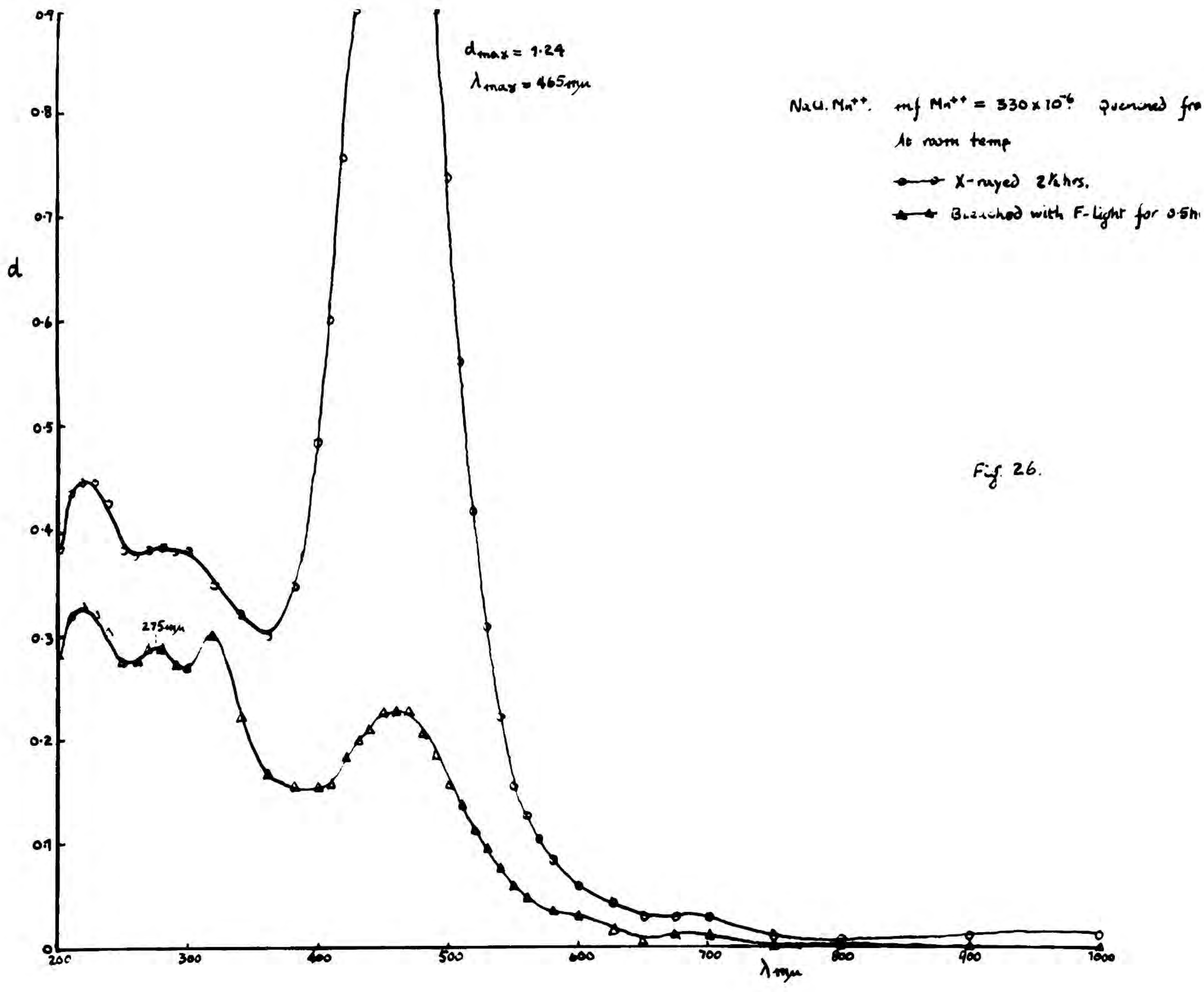

$d_{max} = 1.24$
$\lambda_{max} = 465 m\mu$
NaCl. Mn⁺⁺. mf Mn⁺⁺ = 330 x 10⁻⁶. Quenched fro
At room temp
X-rayed 2½ hrs.
Bleached with F-light for 0.5h
275 mμ
d
λ mμ
0.9
0.8
0.7
0.6
0.5
0.4
0.3
0.2
0.1
0
200
300
400
500
600
700
800
900
1000

Fig. 26.

and for very weak bands, at 440 mμ, 520 mμ and 240 mμ. It is interesting to notice that these bands appear in the absorption spectrum of $MnCl_2$. The bands appeared in the absorption spectrum of the uncoloured crystal and were slightly enhanced by the colouring treatment.

Quenched specimens were found to colour more rapidly than well-annealed specimens. An experiment to measure the bleaching rate of the F-band, carried out in the manner described in section 5.5, showed that they also bleached more rapidly, (see figure 25).

It is interesting to note that quenched specimens were luminescent when exposed to X-rays, and that this luminescence persisted for about 3 hours after irradiation. The luminescence was strong during irradiation, becoming weak immediately the X-rays were cut off. Observation of the crystal through a direct-vision spectroscope showed that the emission appeared to consist of white light, but the intensity of light emitted was too low for this to be more accurately ascertained. An attempt was made to induce luminescence by exposing the freshly quenched crystal to ultra violet light emitted by the hydrogen lamp but this failed. Whether this was due to the luminescence being too weak to be detected by the eye, or to the insufficient energy of the ultra violet light, cannot be told. Although photoluminescence as a property cannot be ruled out, the quenched crystal of $NaCl.Mn^{++}$ certainly exhibits radioluminescence. Examination of thick, and therefore non-uniformly coloured, luminescent crystals showed that the luminescence was confined to the more heavily coloured region, as was to be expected. It was also discovered that exposure to light destroyed the luminescence. Specimens were still radioluminescent, though weakly so, 1 month after being quenched, but after 3 months the property had entirely disappeared.

A further effect of quenching was to increase the thermal instability of the F-band. Thus, F-bands of coloured crystals left for a day in the dark suffered a higher degree of thermal bleaching, compared with their well-annealed counterparts.

5.7 Discussion

Any model which tries to explain how manganese is built into NaCl must lead to an explanation of the following:

(1) The general increase in ultra violet absorption.

(2) The enhancement of the F- and V-bands.

(3) The increase of the initial bleaching rate of the F-band.

(4) The increase of the rates of colouration, initial bleaching, and thermal bleaching, on quenching.

(5) The phenomenon of radioluminescence appearing on quenching.

Schneider and Caffyn (1955), on the basis of results obtained from measurements of electrical conductivity, paramagnetic resonance absorption, and, to a lesser extent, optical absorption, have proposed two models. These will now be described, and afterwards discussed in the light of the above criterion.

In model A, the manganese in the well-annealed crystal has formed aggregates during the slow cooling of the crystal. The manganese in these aggregates is held in solid solution in spite of the relatively high concentration of manganese in the locality, and has associated with it some of the povacs produced by the divalent impurity. Alternatively, in model B, the manganese ions are deposited at or near internal boundaries together with some of the povacs which, although associated with the divalent ions, are free to take part in ionic conduction. In both models heating the crystal to 300°C and above disperses the manganese, and therefore in the quenched crystal a more uniform distribution is frozen in, and the manganese finds itself in complexes of the type, Mn^{++} + povac. The proposal that the manganese congregates at internal boundaries, such as dislocations, where there exists to begin with a strain on the lattice, seems reasonable. The local degree of mismatch introduced into the lattice would in this case be relatively insignificant.

The high ultra violet absorption has been noticedin X-rayed crystals of NaCl containing lead and thallium by Arsenjewa (1929) and others, and Schulman (1950) has suggested that it is due to the formation of the neutral metal. Electrons freed by the X-rays are trapped by the divalent ions and colloidal specks of metal are formed, somewhat in the manner of the formation of the photographic latent image in silver halides (see Mott and Gurney, (1940)). It is reasonable to suppose that this process takes place in the case of manganese. The formation of colloidal specks would be made easier if the manganese ions were already in clusters, as proposed by the above models. Bleaching the F-band should have little effect on the general ultra violet absorption, and this is found to be the case.

The enhancement of the V-band shows that many of the povacs introduced into the lattice by the manganese are not associated with the Mn^{++} ion. Etzel (1952) has suggested that the introduction of disassociated povacs is responsible for enhancing the F-band, since this increases the probability of hole capture and hence decreases the frequency of electron-hole recombination. Although this will affect the rate of production of F-centres it is not as easy to see, with the intensity of the X-ray beam normally used to colour the crystal as high as it is, how it can increase the number of F-centres at saturation. More probably, negvacs are created by the impurity accentuating mis-match in the lattice near dislocations, themselves sources of vacancies. As Seitz (1954) points out, the disassociated povacs will assist migration of the negvacs by pairing. The increase in the initial rate of bleaching is probably due to the greater profusion of V-centres in the immediate vicinity of an F-centre increasing the rate of electron-hole recombination; the rate will decrease after the local V-centres have been destroyed.

According to model B the quenching process has the effect of liberating manganese ions from internal boundaries and also the povacs associated with these ions. If these povacs are loosely bound to the manganese ions an increase in the number of V-centres may be expected. The absorption in the V-band region relative to the F-peak absorption is certainly increased in the quenched crystal, as a comparison of figures 22 and 26 shows. The existence of a greater number of povacs in the quenched crystal would explain the increased rate of colouration by carrying out the function suggested by Etzel. The increase in the number of V-centres would account for the increased rates of optical and thermal bleaching, although another factor here is the bleaching effect of the light arising from luminescence, which, though negligible during optical bleaching, will be important during thermal bleaching experiments.

The luminescence itself is probably due to an internal process within the manganese ion when this is in solid solution in the crystal, as it is in the quenched state. In this case the manganese ion is surrounded by six chlorine ions, and this complex is probably responsible for the 275 mμ band and the other weak $MnCl_2$ bands. The fact that these bands are enhanced by X-rays may indicate a quenching action due to local heating during irradiation. There is strong support for the suggestion that the luminescence arises from the divalent manganese ion (see Brauer, 1952; Klick, 1952; Kroger, 1939; Jahoda, 1927; Randall, 1939; Rothschild, 1937; and Spencer, 1952). Consequently, the appearance of luminescence in the quenched crystal strongly supports the models proposed by Schneider and Caffyn.

No evidence for the formation of Z-centres by manganese ions was found. The investigation, however, was complicated by the fact that besides containing manganese the crystals contained calcium, derived from Analar NaCl, to a concentration of about 20 parts per million. The calcium gave rise to Z-bands whose position and shape was the same whether the crystal contained manganese or not. Further, measurements of the ratio d_z/d_f, where d_z was the peak density of the Z-bands and d_f that of the F-band, gave a value between 0.04 and 0.06 for manganese bearing crystals, compared with a value of about 0.10 when manganese was absent, indicating a suppression and not an enhancement. The ratio was also found to be lower in bleached specimens containing manganese than those without. Figure 27 shows the absorption of $NaCl.Mn^{++}$ measured at 90°K where the Z-bands are resolved more clearly.

Although these Z-bands are due to calcium it does not mean that manganese does not form Z-type centres. The band at 320 mμ which appears in quenched crystals may be due to such a colour centre, and it may be analogous to the band at 345 mμ found in $NaCl.Ca^{++}$, (see section 7.2). But there is no evidence to suggest that manganese forms Z-centres of the type produced by the alkaline earths.

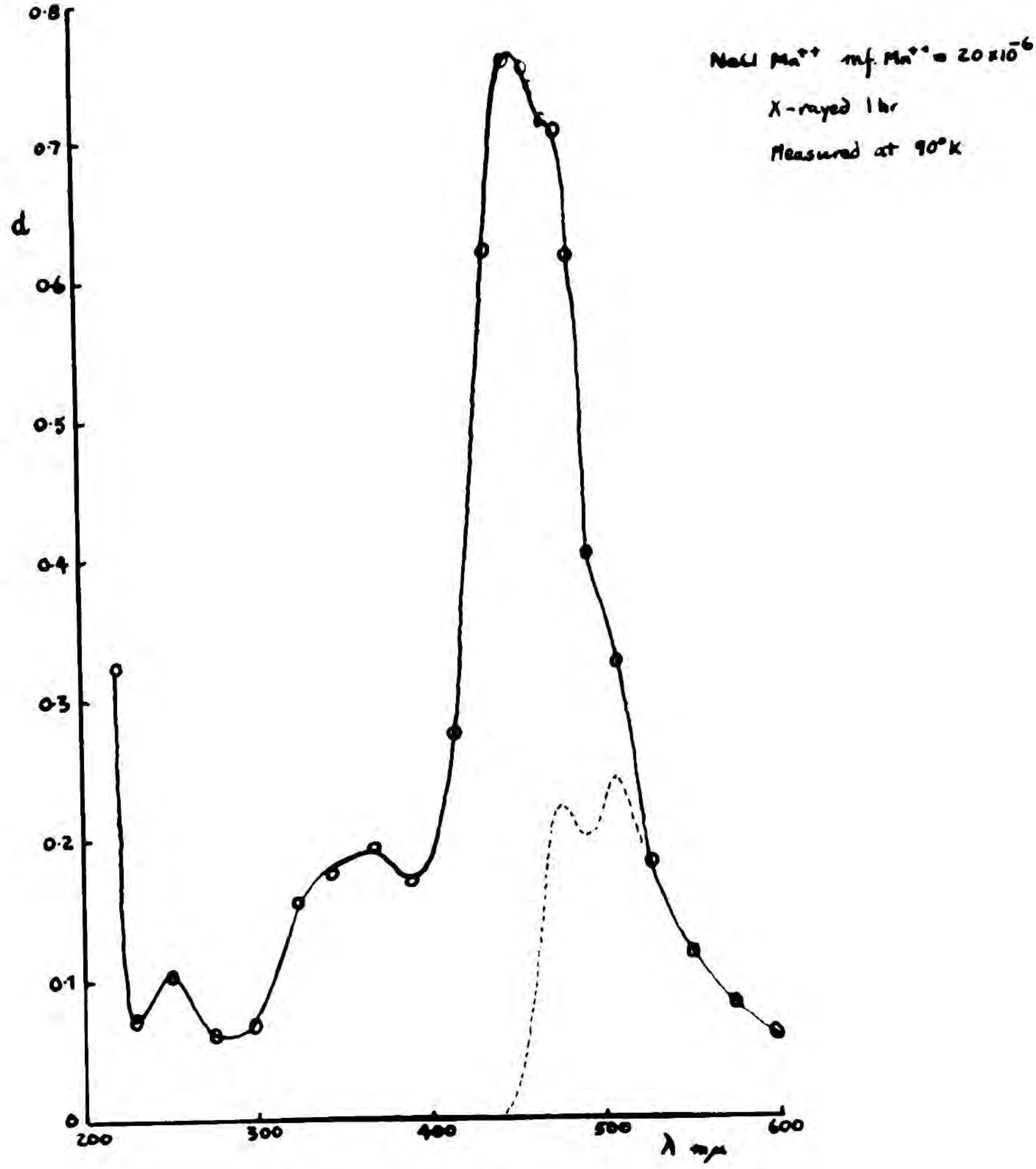

Fig 27.

6 WORK ON NaCl.Ni^{++} AND NaCl.Cu^{++}.

6.1 Introduction

Some preliminary studies were made on crystals of NaCl containing nickel and copper as impurities, mainly to find out if these impurity ions gave rise to Z-bands. A description of the results of this brief investigation is given in this chapter. The work was performed on crystals grown from the melt which contained the appropriate chloride of the impurity. It was found that no particular precautions were necessary to grow crystals containing these impurities, unlike the case of manganese (see section 5.2).

6.2 Coloured Crystals.

The uncoloured crystals were found to exhibit a characteristic band in the ultra violet, at 255 mμ for Cu^{++} and 247 mμ for Ni^{++}. The copper band has been observed by Smakula (1927) and Kats[b] (1952), but NaCl.Ni^{++} does not appear to have been investigated before. These bands are probably due to transitions of electrons within the divalent ion, (see F. Seitz (1938)).

X-raying the crystals produced the usual F-band and well pronounced V-bands. The curves denoting the effect of irradiation shown in figures 28 and 29 were obtained in the usual way by subtracting the uncoloured contribution from the measured absorption. This procedure is valid only if the uncoloured absorption remains unchanged during the colouring process, and the appearance of valleys in the curve at the wavelengths of the characteristic bands cast strong doubts that this is so here. In fact, the curves suggest that part of the characteristic band in each case is destroyed by the X-raying, some of the impurity ions having captured electrons to form atomic centres. Kats[a] (1952) has noted a similar effect with $NaCl.Ag^{+}$, and also with $NaCl.Cu^{+}$. The absorption curves also show a poorly resolved band at about 350 mμ. This band is particularly noticeable in quenched $NaCl.Cu^{++}$ after bleaching the F-band (figure 29). It may be due to the presence of Ca^{++} (see section 7.2) but its prominence makes this doubtful, since only 20 parts per million of Ca^{++} are present.

An analysis of the F-band showed no evidence of the formation of Z-bands in the case of either impurity. A suppression of the Ca^{++} Z-bands similar to that observed in the case of Mn^{++} was found (see section 5.7).

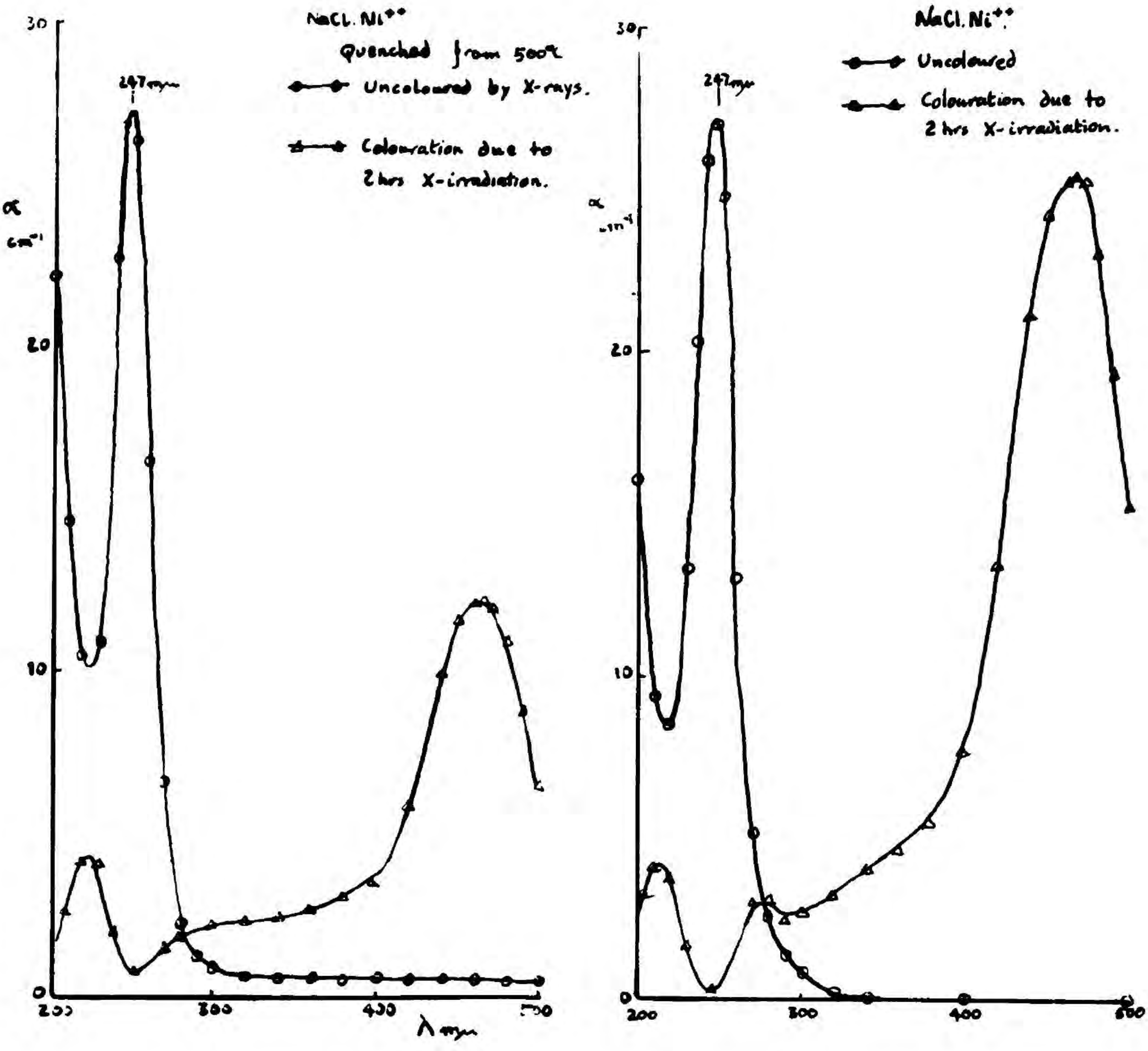

Fig 28. ABSORPTION OF NaCl. Ni⁺⁺

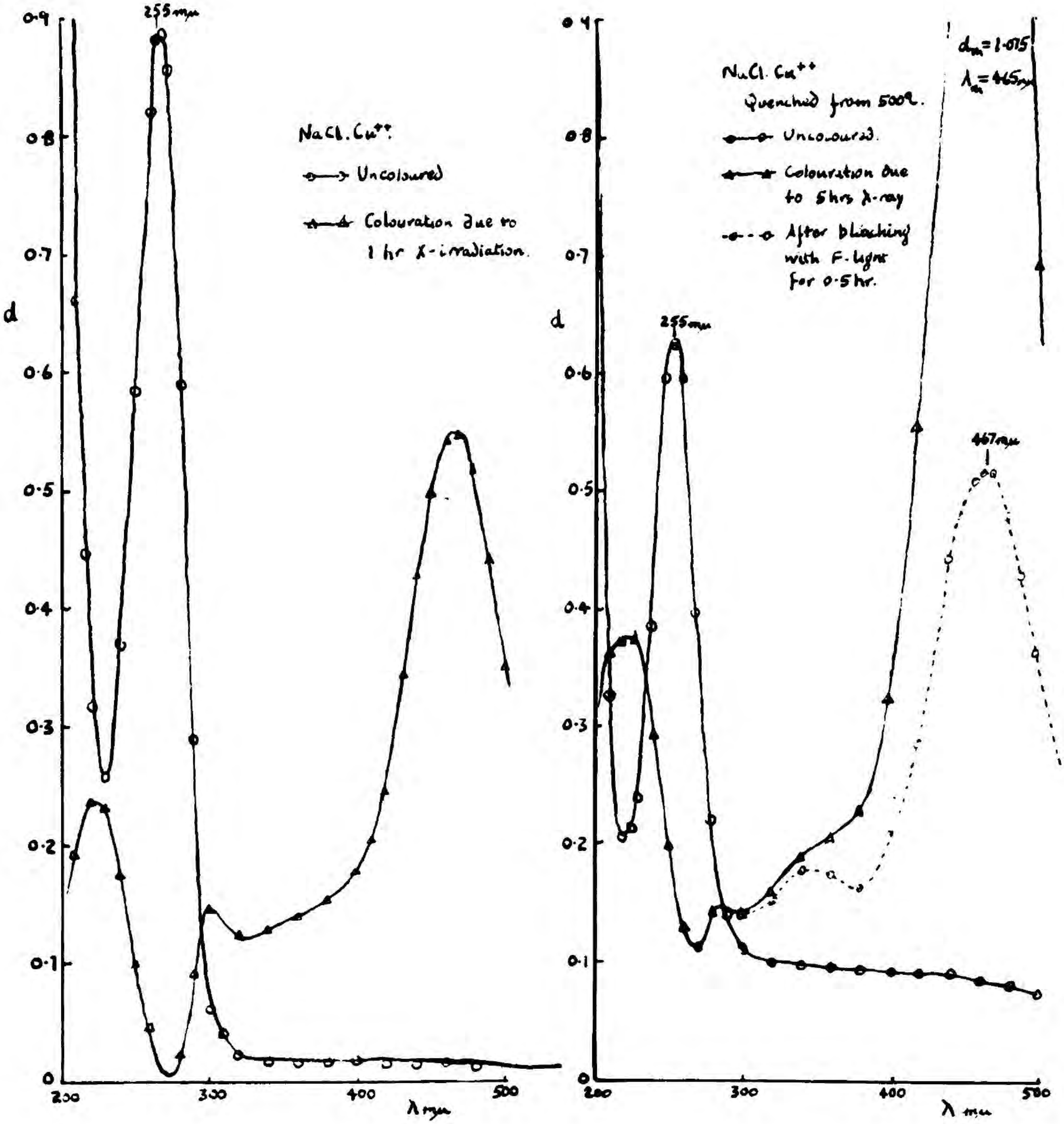

Fig 29. ABSORPTION OF NaCl.Cu++

6.3 The Effect of Bleaching.

The F-band in both types of crystal was found to be very unstable, decreasing in intensity rapidly when the crystal was exposed to F-light. In particular, the bleaching rate of the Cu^{++} bearing crystal was very high, a bleaching time of some thirty minutes being sufficient to destroy the F-band completely (compare $NaCl.Mn^{++}$, section 5.5, and $NaCl.Ca^{++}$, section 7.3). It was significant that the characteristic band at 255 mμ was reduced by the bleaching process - only a small decrease was found in the Ni^{++} 247 mμ band. The ratio d_z/d_f for the calcium Z-bands was measured and found to be 0.18, as compared with the value 0.30 (approx.) found in crystals not containing Cu^{++} or Ni^{++}, thus indicating once more a suppression. There was no evidence that any new bands were formed by bleaching.

6.4 The Effect of Quenching.

A specimen of $NaCl.Ni^{++}$ was cleaved to obtain two thin plates. One was heated to about 500°C and quenched by allowing it to cool in air, after which it was X-rayed for 2 hours. The other, without any further heat treatment, was also X-rayed for 2 hours. The absorption curves are those of figures 28b and 29b. The quenching treatment had no effect on the intensity of the characteristic band, supporting the view that the band arises from transitions within the nickel ion. Quenching did, however, have a marked effect on the rate of growth of the F-band, which was reduced by a factor of 2. A possible explanation of this effect is given in section 7.5.

It was interesting to notice that quenched crystals of $NaCl.Ni^{++}$, like $NaCl.Mn^{++}$, were luminescent under X-irradiation.

A similar experiment was not performed with $NaCl.Cu^{++}$.

6.5 Summary

The results of this preliminary investigation may be summarised as follows:

(1) Ni^{++} and Cu^{++} give rise to bands in the ultra violet which are probably due to electronic transitions within the ion.

(2) The reduction in intensity of these bands on X-raying suggests that these ions act as electron traps. Monovalent and/or atomic centres should therefore be formed, and the band near 350 mμ may be due to such centres. If the Seitz model for Z-centres is correct the non-appearance of Z-bands would indicate that stable monovalent centres are not formed.

(3) The V-bands are enhanced, indicating free povacs.

(4) The F-band stability is decreased.

(5) In $NaCl.Ni^{++}$ the rate of growth of the F-band is considerably reduced by quenching. (Compare $NaCl.Mn^{++}$, section 5.6, where quenching was found to increase the rate).

(6) $NaCl.Ni^{++}$ became radioluminescent after quenching.

6.6 $NaCl.Pb^{++}$.

An attempt to grow crystals containing Pb^{++} was made. Specimens which were obtained from a melt consisting of NaCl and $PbCl_2$ were almost opaque, containing precipitated $PbCl_2$. The absorption curves for a specimen uncoloured, coloured and bleached are given in figure 30.

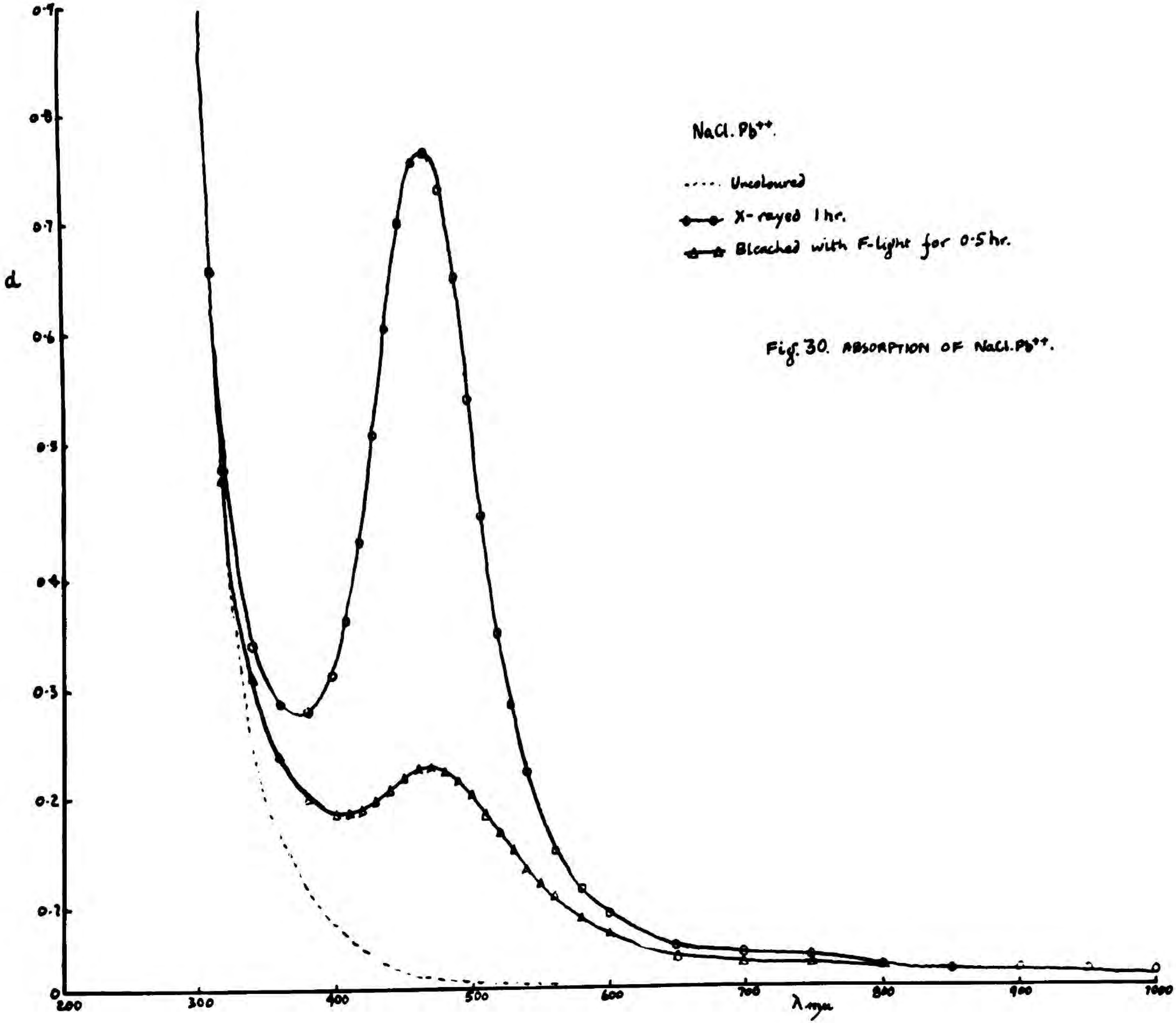

Fig. 30. ABSORPTION OF NaCl. Pb^{++}.

7 WORK ON $NaCl.Ca^{++}$.

7.1 Introduction

In this chapter the absorption spectra of coloured crystals of $NaCl.Ca^{++}$ will be described, and the effect of quenching, and of thermal and optical bleaching, will be discussed. Inferences will be drawn on the probable state of the calcium ions in the crystal at the end of the chapter.

Since Analar NaCl contains about 20×10^{-6} parts of calcium to 1 of NaCl (manufacturer's figure) it was to be expected that all crystals grown from this material would contain calcium. Kelting and Witt (1949) had shown that only 0.1 of the calcium concentration in the melt would be built into the crystal, approximately, so it was expected that Analar crystals would contain roughly 2×10^{-6} parts of calcium. However, during an attempt to purify NaCl by fractional crystallization, analyses of the crystals, by Johnson and Matthey, spectrographically, and also by the author, using the E.D.T.A. method (see section 4.9), showed that the crystals contained anything up to 40×10^{-6} parts of calcium; other impurities were present to the extent of 5×10^{-6} parts only. Thus, in this investigation of $NaCl.Ca^{++}$ crystals having comparatively low concentrations of calcium were readily available.

Concentrations up to 6,000 x 10^{-6} were obtained by straightforward addition of $CaCl_2$ (anhydrous) to the melt.

7.2 Coloured Crystals.

The absorption spectrum of the uncoloured crystals was measured at room temperature and at liquid nitrogen temperatures for various concentrations of calcium. The usual rise in the absorption curve towards 200 mμ was present, but to a much lesser extent than was found in the case of manganese. Even with mole fractions of the order of 6 x 10^{-3} the effect was comparatively small, and it was not until the concentration of calcium became such that precipitation of $CaCl_2$ occurred that the rise became large. Apart from this rise the spectrum was otherwise uneventful. It is reasonable to suppose that the smaller effect on the ultra violet spectrum is coupled with the greater solubility of calcium.

Crystals coloured by X-rays showed in general the F-band and an increase in ultra violet absorption. At low concentrations of calcium the unresolved V-bands at 210 mμ were evident but with increasing concentration these became obscured by the general rise in absorption in the ultra violet. In no case were the V-bands as prominent as those found in crystals containing Mn, Ni, or Cu.

The spectra of low calcium content crystals (or low content crystals, as they will be called in future) was prima facie uneventful (but see section 8.3). The effect of adding calcium appeared to be an enhancement of the general ultra violet absorption and an increase in the rate of colouration under X-irradiation, confirming the work done by Etzel (1952). High content crystals, containing mole fractions of calcium of about 5×10^{-3}, however, gave exceedingly interesting absorption curves. A new band poorly resolved was found at 345 mμ, whose intensity was about 20% that of the F-band. Further, after prolonged irradiation of the crystal, i.e. from 5 to 7 hours X-raying, the resulting F-band was found to have broadened on the long wavelength side, suggesting the formation of unresolved bands in the range 500 mμ to 600 mμ. A typical result is shown in figure 31, obtained at room temperature. Figure 32 shows the spectrum at 90°K. Additively coloured crystals also showed the band at 345 mμ (see figure 34 - the background absorption in this figure is due to precipitated sodium). The long wavelength broadening was particularly interesting, since it pointed to the production of Z-bands during the X-raying. Hitherto, Z-bands have only been observed after bleaching the coloured crystal with F-light. The suggestion that Z-centres are formed during X-raying is discussed in section 8.3.

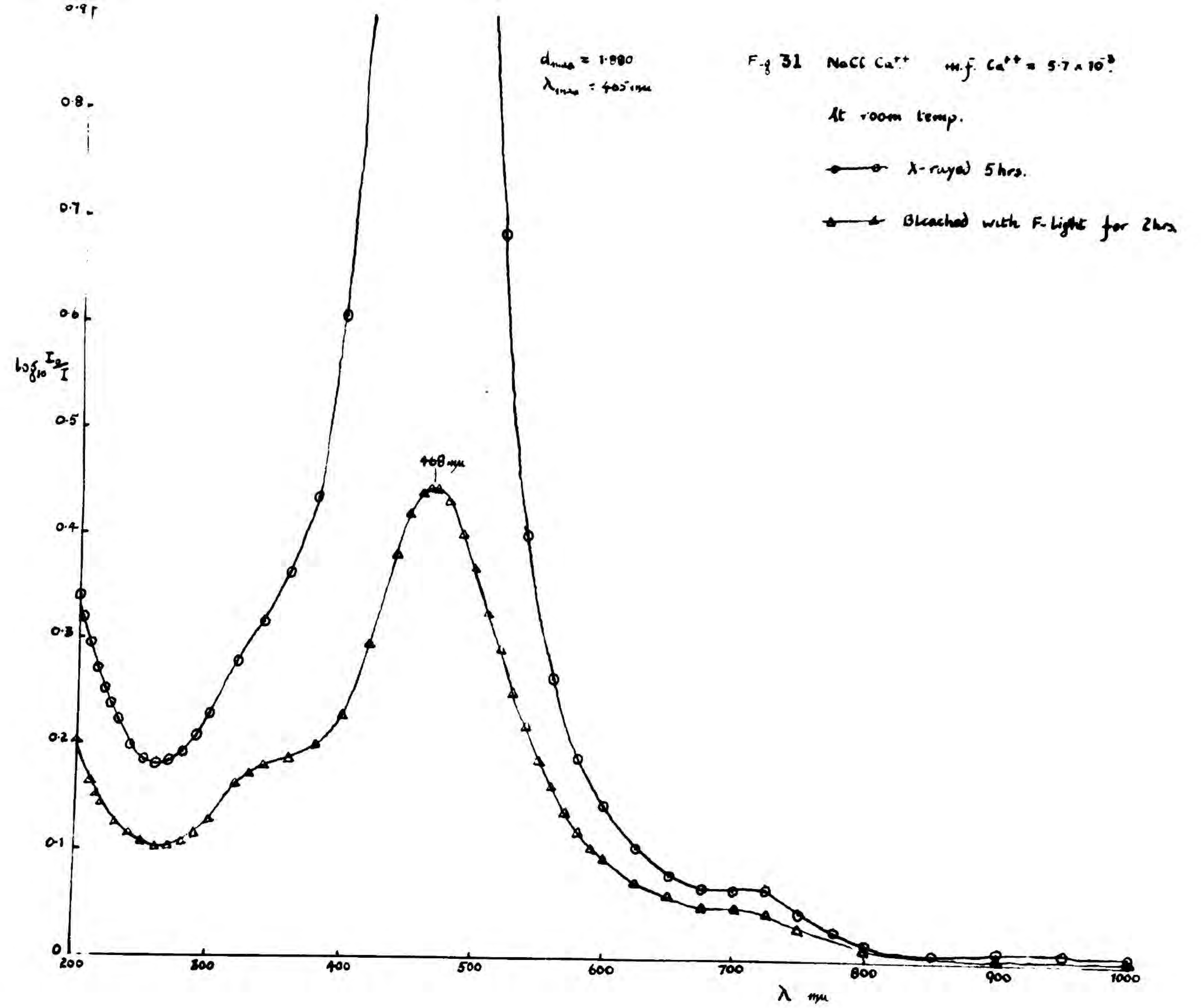

Fig 31 NaCl Ca++ m.f. Ca++ = 5.7 x 10-3
At room temp.
X-rayed 5 hrs.
Bleached with F-light for 2 hrs
d max = 1.880
λ max = 465 mμ
468 mμ
log10 I0/I
λ mμ
0
0.1
0.2
0.3
0.4
0.5
0.6
0.7
0.8
0.9
200
300
400
500
600
700
800
900
1000

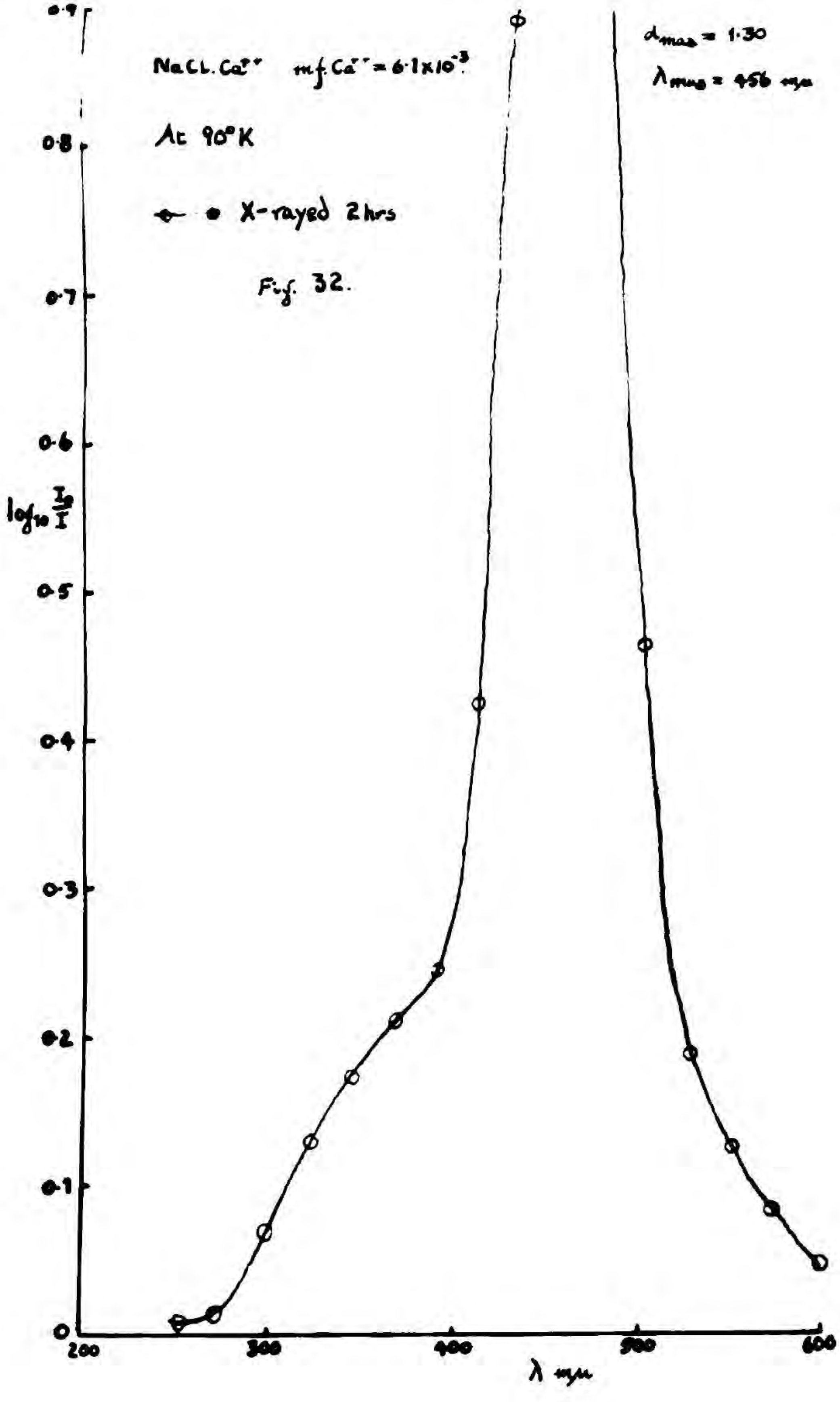
NaCl.Ca++ m.f. Ca++ = 6.1 x 10^-3
At 90°K
X-rayed 2 hrs
Fig. 32.
d max = 1.30
λ max = 456 mμ
log10 I0/I
λ mμ
0
0.1
0.2
0.3
0.4
0.5
0.6
0.7
0.8
0.9
200
300
400
500
600

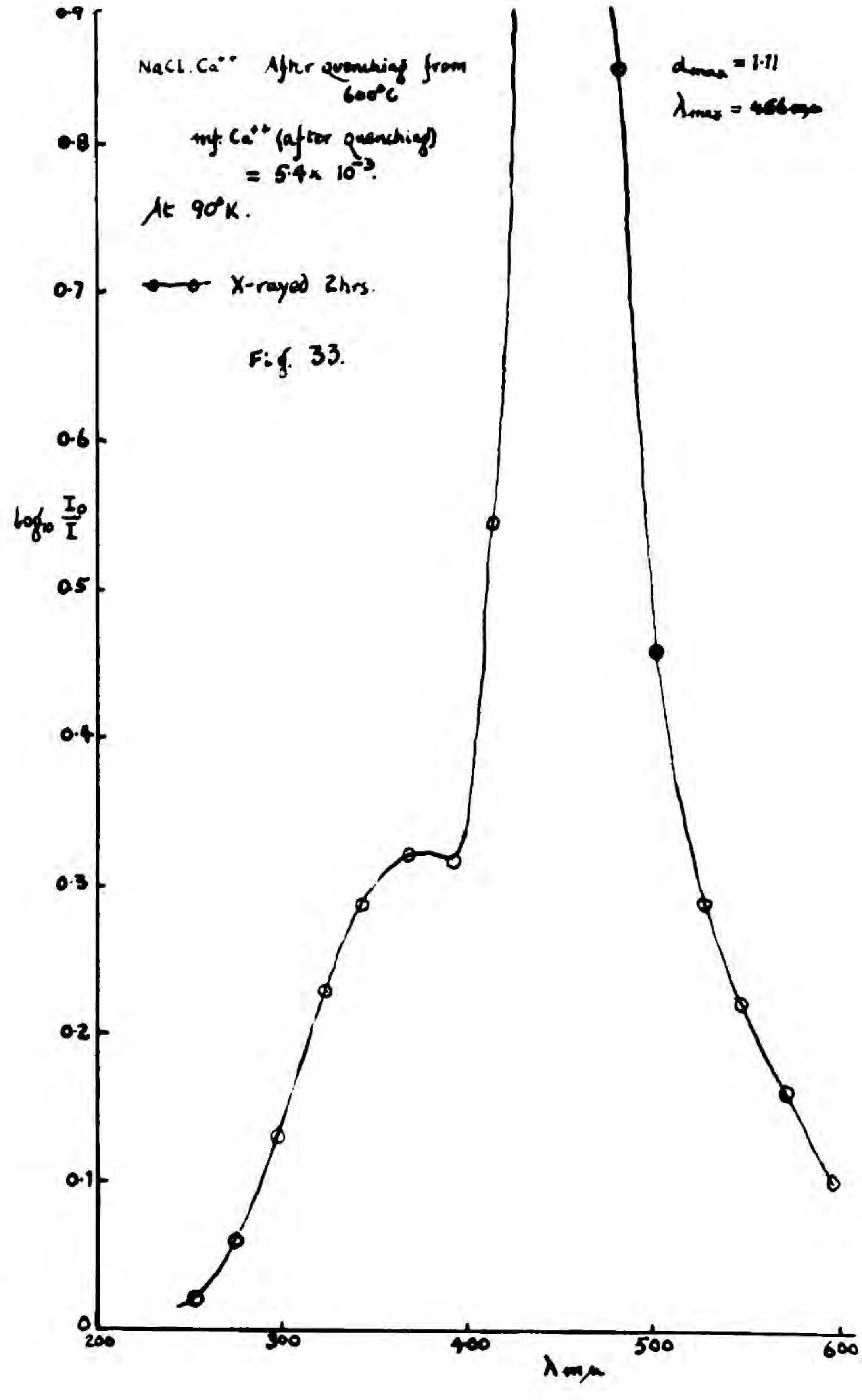
NaCl.Ca++ After quenching from 600°C
m.f. Ca++ (after quenching) = 5.4 x 10^-3.
At 90°K.
X-rayed 2 hrs.
Fig. 33.
d max = 1.11
λ max = 466 mμ
log10 I0/I
λ mμ
0
0.1
0.2
0.3
0.4
0.5
0.6
0.7
0.8
0.9
200
300
400
500
600

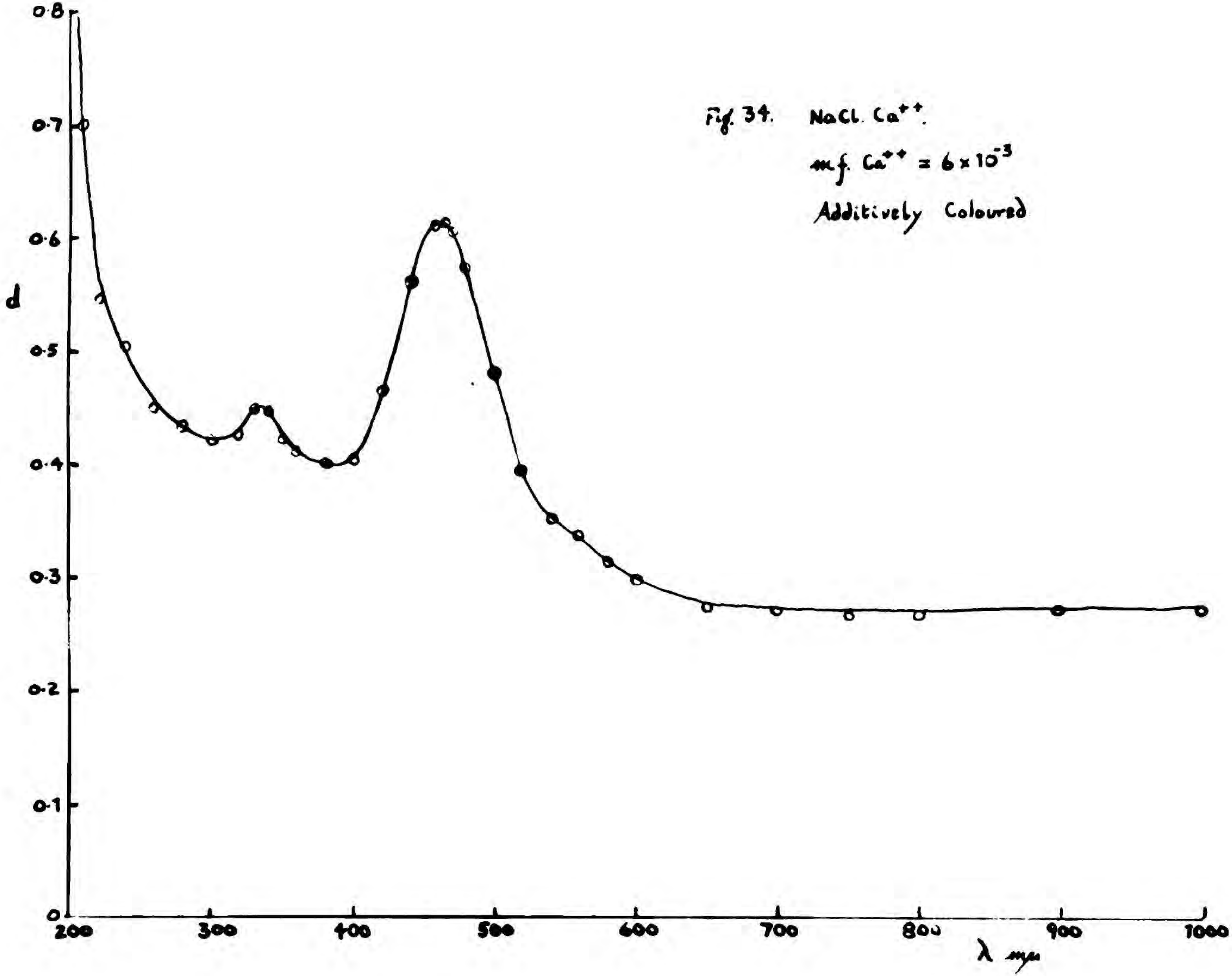

Fig. 34. NaCl. Ca^{++}.
m.f. $Ca^{++} = 6 \times 10^{-3}$
Additively Coloured

7.3 The Effect of Optical Bleaching.

When a coloured crystal was bleached with F-light it was found that the F-band, besides decreasing in intensity, broadened on the long wavelength side. This effect has been observed by Pick (1939), and Camagni et al (1954), and is attributed to the formation of the Z_1-band. At room temperature this band was unresolved (see figure 31) but at $90^{\circ}K$ some resolution was obtained (see figure 35) and it was seen that the Z_1-band, peaking at about 490 mμ, was present in fact. The curves showed a slight bump at about 500 mμ which indicated that Z_2-centres, peaking at about 510 mμ, were also present. Hitherto these centres have only been observed after heating the bleached additively coloured crystal to $100^{\circ}C$, but it is reasonable to suppose they exist in high content crystals, from which the evidence was obtained. By reducing the F-band, bleaching also made the band at 345 mμ more evident. It also reduced the general ultra violet absorption.

7.4 The Effect of Thermal Treatment.

High content crystals were heated for 1 to 2 hours at $600^{\circ}C$ and it was observed that they became cloudy due to the deposition of a layer of $CaCl_2$ on the surface. The crystals were quenched by removing them from the furnace and letting them cool in air, after which the surface layer was wiped off. Analysis of the calcium content before and after heating showed that the mole fraction (m.f.) had decreased by about 3×10^{-4}. To see what effect this had on the rate of colouration two specimens, of about equal thickness, viz. 0.045 cm and 0.043 cm, were cleaved from the same crystal. One was coloured and the other was quenched from 600°C and then coloured, both colouring treatments being identical. The absorption constant α_f at 465 mμ was determined for each, and the specimens were then analysed for calcium by the E.D.T.A. method. The results are shown in Table 1. It was observed that the net effect

TABLE 1

Crystal	m.f. $Ca^{++} \times 10^3$	$\alpha_f (cm^{-1})$
Well-annealed	7.17	64.8
Quenched	6.84	52.5

of the quenching process was to reduce the rate of colouration. This is discussed more fully in section 7.5, but at this stage the result may be compared with that obtained with nickel, and contrasted with the effect obtained with manganese.

Quenching was found to have little effect on the absorption spectra of low content crystals, but with high content crystals the result was to enhance both the 345 mμ band and the Z-bands. These bands became particularly noticeable on optically bleaching, (see figures 33, 36, 37, 38 and 40). The effect on the Z-bands at room temperature may be seen by comparing the peak wavelengths of the bleached band in figures 31 and 37. The F-bands before and after bleaching are of nearly equal intensity, but the peak of the bleached band is at 468 mμ in the well annealed specimen and at 476 mμ in the quenched specimen, showing that in the latter case the Z-band intensity is stronger. An estimation of the intensities of the 345 mμ and Z-bands, made by subtracting from the experimental curves a Gaussian, peaking at 465 mμ and of width 0.414 eV, showed that the quenching process increased these bands by the same factor - about 1.4.

To see if any conversion from Z_1 to Z_2-centres was possible the quenched crystal was coloured and bleached, and then heated for 15 minutes at 110°C. All bands were found to have been reduced, but the 345 mμ and Z-bands suffered much more than the F-band (see typical case in figure 38). Further heating virtually destroyed the Z-bands.

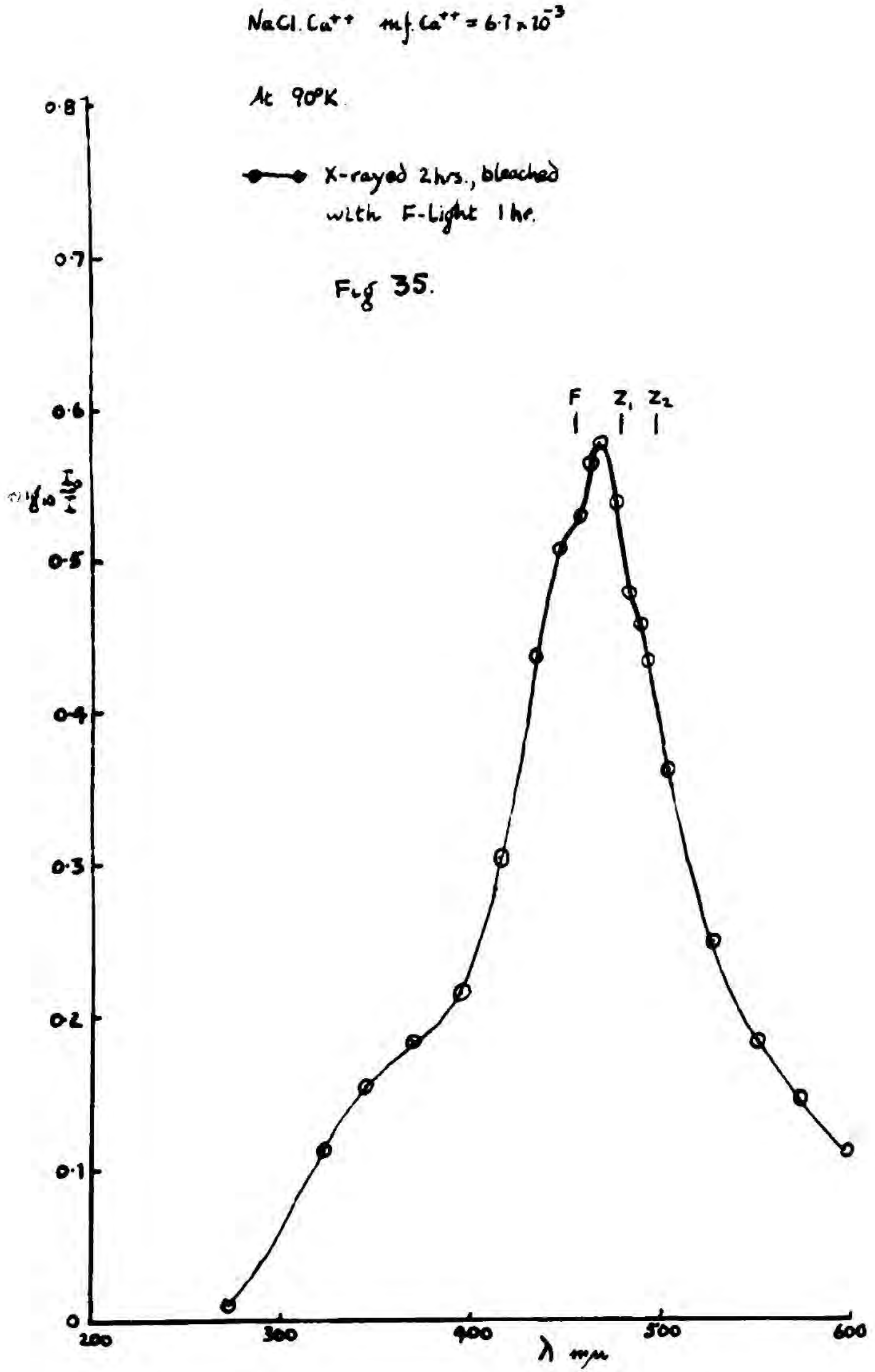

NaCl. Ca++ m.f. Ca++ = 6·7 x 10-3
At 90°K.
X-rayed 2hrs., bleached with F-Light 1hr.
F
Z1
Z2
$\log_{10}\frac{I_0}{I}$
λ mμ

Fig 35.

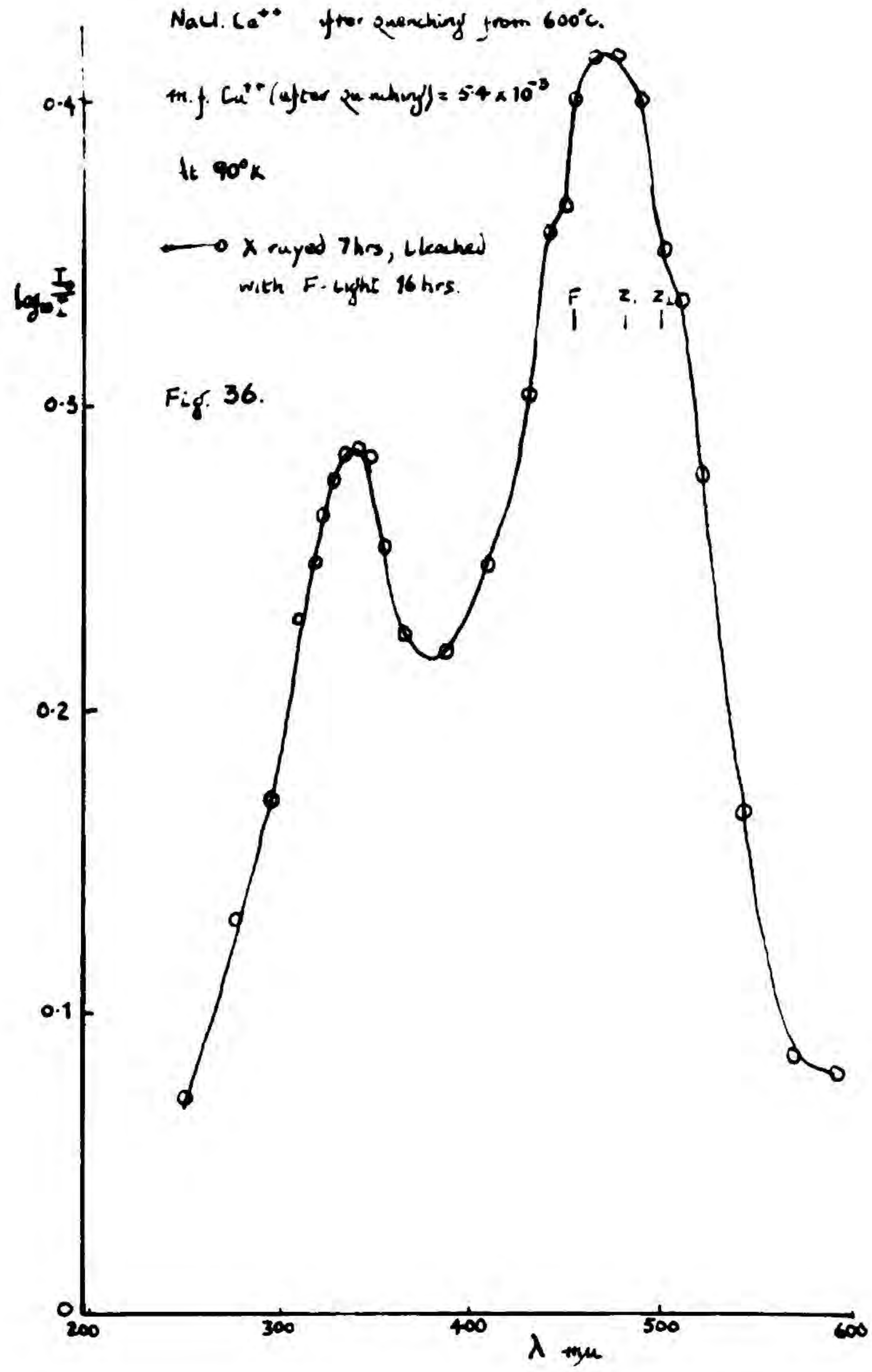

NaCl. Ca++ after quenching from 600°C.
m.f. Ca++ (after quenching) = 5·4 x 10-3
At 90°K
X rayed 7hrs, bleached with F-light 16hrs.
F
Z1
Z2
$\log_{10}\frac{I_0}{I}$
λ mμ

Fig. 36.

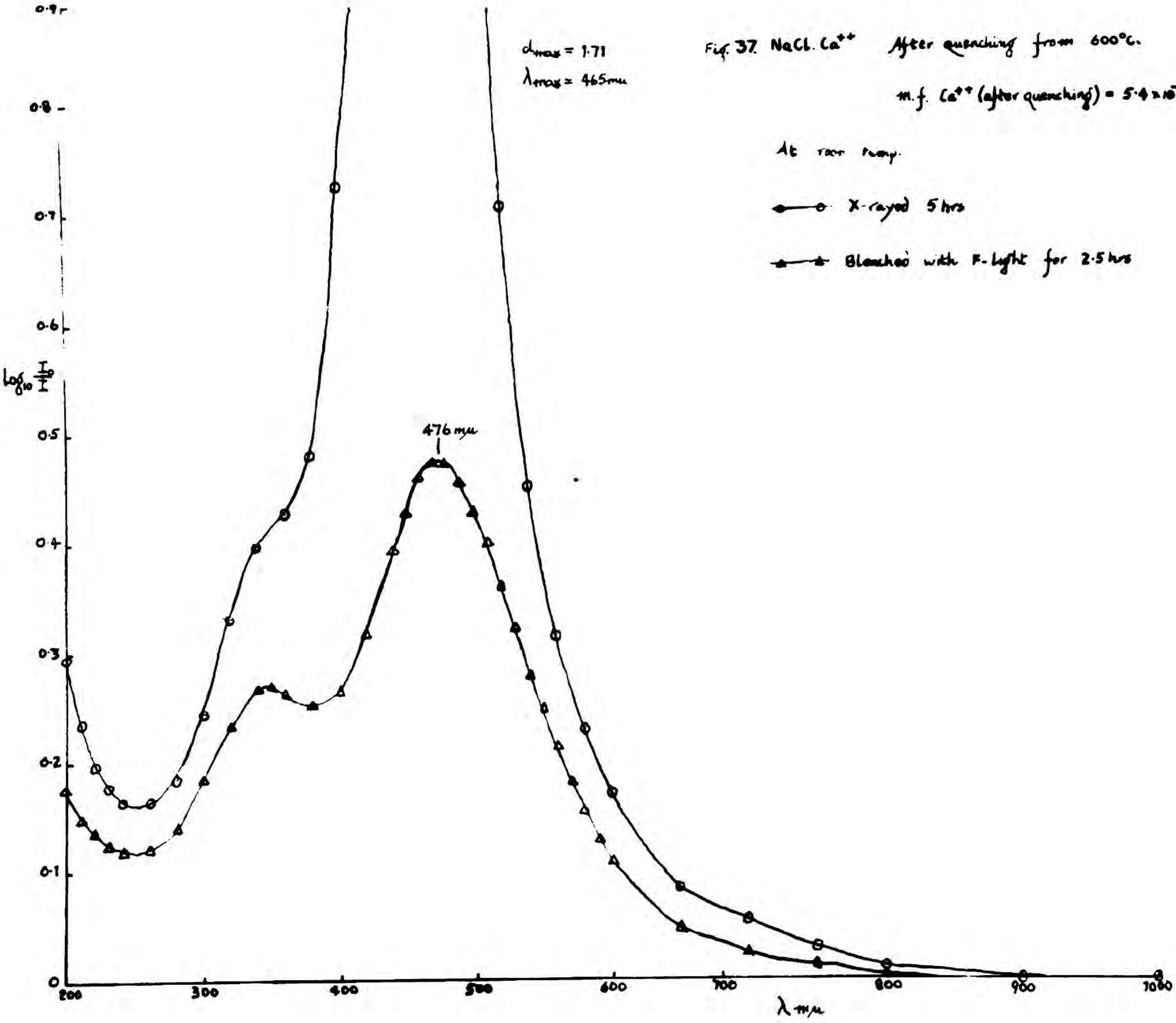

Fig. 37 NaCl. Ca^{++} After quenching from 600°C.

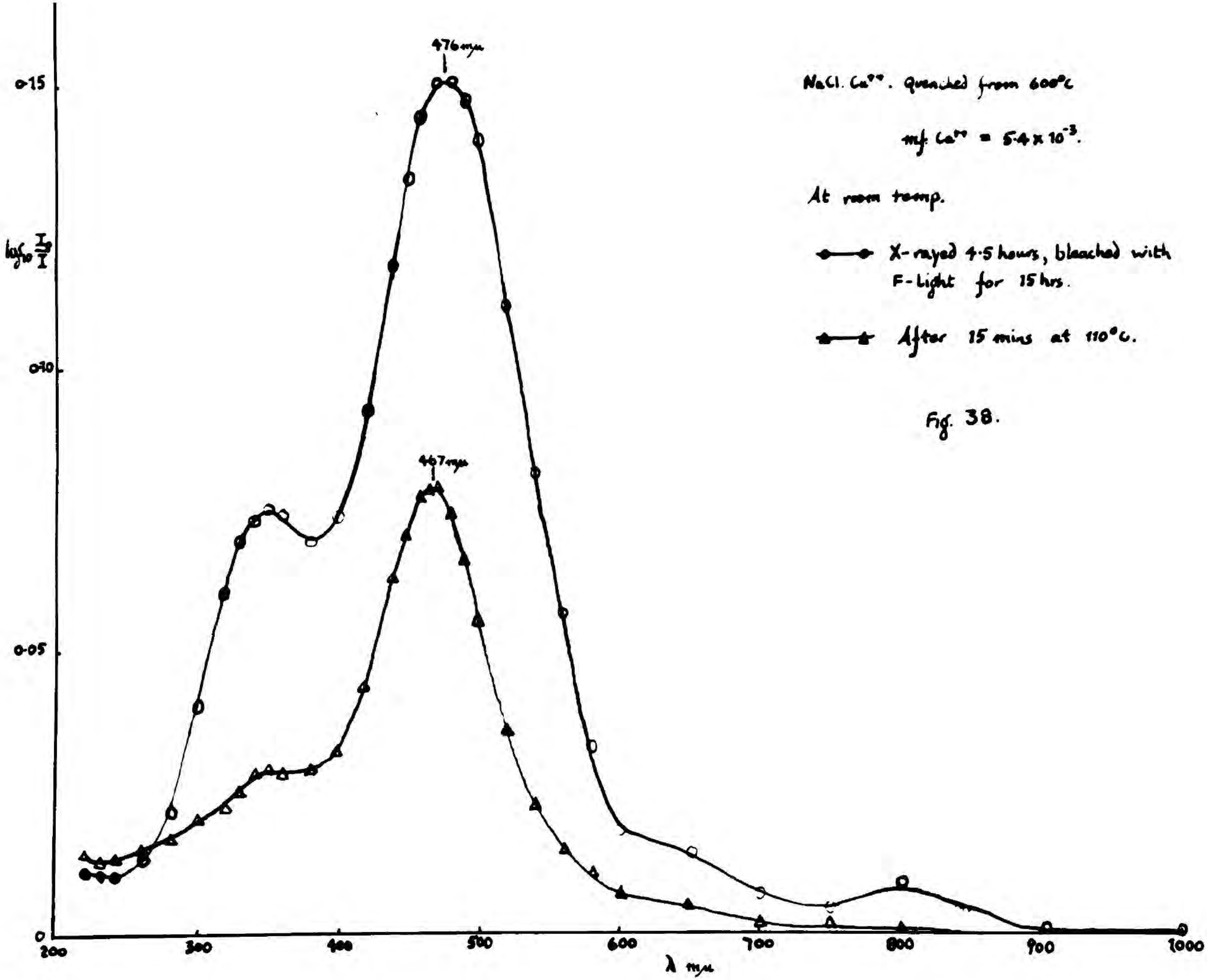
476 mμ
467 mμ
0·15
0·10
0·05
0
$\log_{10} \frac{I_0}{I}$
200
300
400
500
600
700
800
900
1000
λ mμ
NaCl. Ca^{++}. Quenched from 600°C
mf. Ca^{++} = $5·4 \times 10^{-3}$.
At room temp.
X-rayed 4·5 hours, bleached with F-Light for 15 hrs.
After 15 mins at 110°C.

Fig. 38.

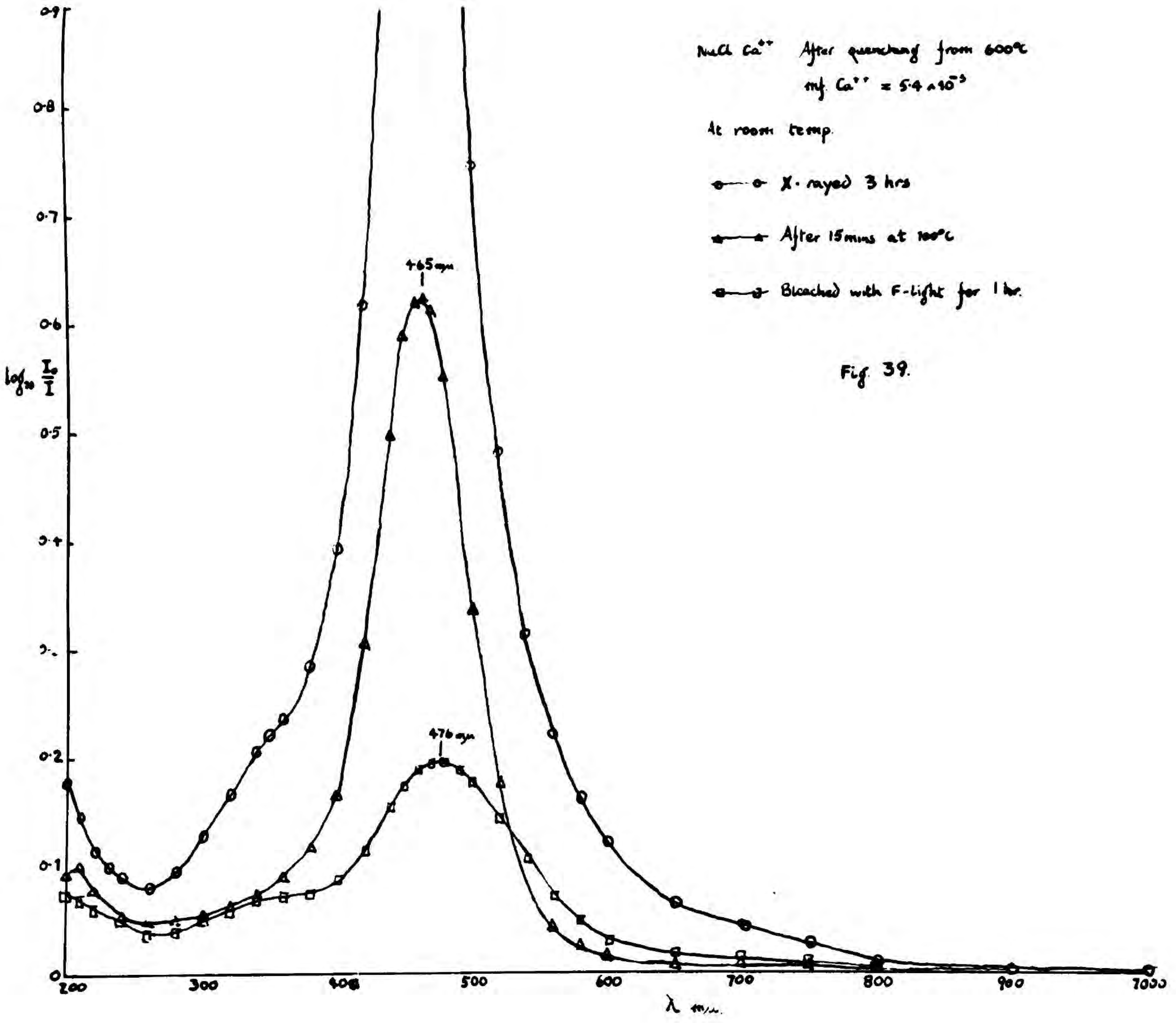

NaCl Ca⁺⁺ After quenching from 600°C
m.f. Ca⁺⁺ = 5·4 × 10⁻⁵
At room temp.
X-rayed 3 hrs
After 15 mins at 100°C
Bleached with F-light for 1 hr.
465 mμ
476 mμ
$\log_{10} \frac{I_0}{I}$
0
0·1
0·2
0·4
0·5
0·6
0·7
0·8
0·9
200
300
400
500
600
700
800
900
1000
λ mμ

Fig. 39.

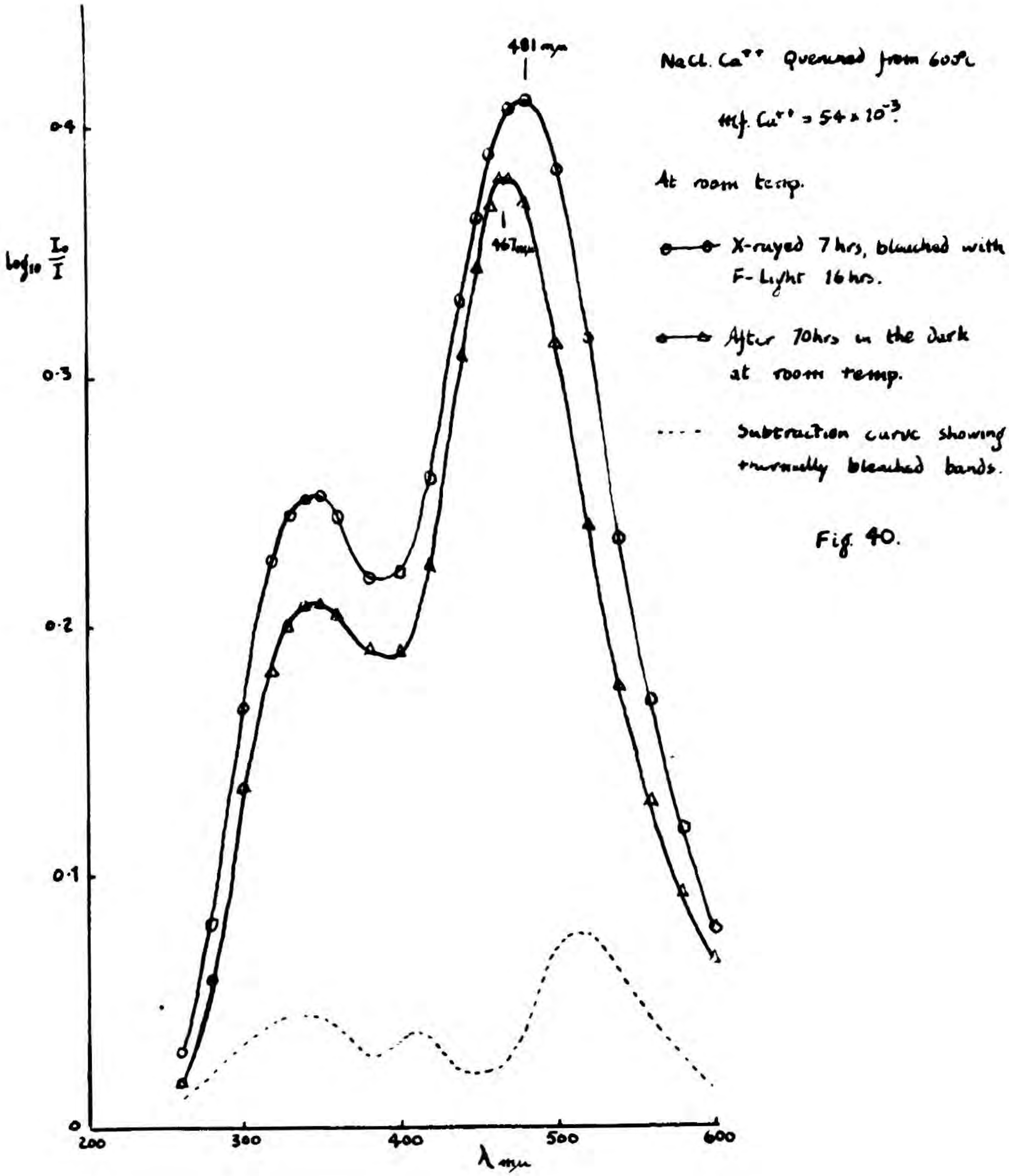
481 mμ
467 mμ
0·4
0·3
0·2
0·1
0
$\log_{10} \frac{I_0}{I}$
200
300
400
500
600
λ mμ
NaCl. Ca⁺⁺ Quenched from 605°C
M.f. Ca⁺⁺ = 54 × 10⁻³.
At room temp.
X-rayed 7 hrs, bleached with F-Light 16 hrs.
After 70 hrs in the dark at room temp.
Subtraction curve showing thermally bleached bands.

Fig. 40.

The destruction of the Z-band by the heat treatment meant that either the impurity centres themselves were undergoing some change or the rate of thermal ionization of the trapped electron had been increased. A crystal which had been coloured and heated for 15 minutes at 100°C was therefore bleached with F-light at room temperature. It was found that the Z-band was re-formed (see figure 39) indicating that the effect was due to thermal ionization.

The fact that the F-band and the Z-bands thermally bleach at different rates offered a method of obtaining the shape of the latter at room temperature fairly unambiguously. A crystal was coloured and bleached with F-light and left in the dark for about three days. Absorption curves were obtained before and after dark-bleaching (see figure 40). Since the F-band bleaches in the dark comparitively slowly the difference between the two curves was mainly due to the more rapid bleaching of the Z-bands and the 345 mμ band. This was seen clearly when the curve taken after dark-bleaching was subtracted from the other, showing the thermally bleached bands at 515 mμ (Z) and 345 mμ. It was observed that the Z-bands bleached more rapidly than the 345 mμ band. A third band was discovered at 410 mμ by this method. The origin of this band is obscure.

To obtain an approximate value for the decay constant, θ_f, associated with the dark-bleaching of the F-band, the peak density of the band before (d_o) and after (d) a period t seconds of dark-bleaching was measured in several cases. d_o and d were also measured for the Z-band by the method of subtracting a 0.414 eV-wide Gaussian, and an estimate was obtained for θ_z. θ was calculated assuming an exponential decay process,

$$\text{i.e.} \quad d = d_o \exp(-\theta t).$$

The results are shown in Table 2.

All the specimens had been previously bleached by F-light to enhance the Z-bands except for specimen 1. It was realised that owing to the presence of several centres, all taking part in the bleaching process, the assumption that the mechanism was monomolecular in nature could only lead to approximate results. If the process was monomolecular θ would be constant for all t in the case of a particular specimen, but as specimens 1 and 2 show, there is a variation in θ_f of some 25%. Since there were fewer Z-centres than F-centres in the crystals it was expected that the monomolecular approximation would fit more closely in their case. θ_z in the case of specimen 2 still showed an appreciable variation however. A considerable variation from specimen to specimen was also observed.

TABLE 2

Approximate thermal bleaching rates for various specimens.

A The F-band

	Specimen	m.f. of Ca^{++} $\times 10^{+6}$	Time in dark (hours)	d_o	d	θ_f $sec^{-1} \times 10^{+7}$
At 20°C	1 (Korth)	5	264.0	0.312	0.196	4.8
			600.0	0.312	0.142	3.6
			336.0	0.196	0.142	2.7
	2 (Analar)	20	84.0	0.215	0.197	1.3
			144.0	0.215	0.187	1.2
			60.0	0.197	0.187	1.1
	3	5,700	72.0	0.345	0.295	2.6
	4 (quenched)	5,400	70.0	0.390	0.370	0.9
	5 (quenched)	5,400	48.0	0.245	0.230	1.6
At 100°C	6	220	3.0	0.108	0.028	540.0
	7 (quenched)	5,400	0.25	0.145	0.126	670.0

TABLE 2 (Cont'd).

B The Z-band

	Specimen	m.f. of Ca^{++} $\times 10^{+6}$	Time in dark (hours)	d_o	d	θ_f $sec^{-1} \times 10^{+7}$
At 20°C	2	5	84.0	0.065	0.030	110
			144.0	0.065	0.021	95
			60.0	0.030	0.021	72
	3	5,700	72.0	0.100	0.060	88
	4	5,400	70.0	0.190	0.115	88
	5	5,400	48.0	0.105	0.060	140
At 100°C	7	5,400	0.25	0.064	0.011	8,500

θ_f (mean) = $\underline{2 \times 10^{-7}\ sec^{-1}}$. θ_z (mean) = $\underline{1 \times 10^{-5}\ sec^{-1}}$.

These measurements only served, therefore, to give the orders of magnitude of the bleaching constants. The mean values

$$\theta_f = 2 \times 10^{-7} \text{ sec}^{-1},$$

$$\theta_z = 1 \times 10^{-5} \text{ sec}^{-1},$$

were then regarded as lower limits to the respective probabilities of ionization of the centres in unit time. These values will be referred to in section 8.6.

7.5 Discussion

The results just described may be summarized as follows:

(1) The usual increase in ultra violet absorption with increasing impurity content was observed, but the effect was not as marked as in the case of manganese, nickel or copper. Colouring the crystals was found to enhance the general ultra violet absorption, but again the effect was comparitively small.

(2) The F-band was enhanced but not as efficiently as in crystals containing manganese: a m.f. of manganese of 4×10^{-4} gave roughly the effect of a m.f. of calcium of 60×10^{-4}.

(3) The F-band was broader on the long wavelength side in high content crystals due to the formation of Z_1-centres, and Z_2-centres.

(4) A band at 345 mμ was found in high content crystals. Its intensity was about 20% that of the F-band.

(5) Bleaching the F-band reduced the ultra violet absorption but appeared to have little effect on either the 345 mμ band or the Z-bands apart from making them more obvious by reducing the F-band.

(6) Quenching had little effect on low content crystals, but in high content crystals it enhanced the Z-bands and the 345 mμ band in the same proportion, and slightly reduced the rate of colouration. The latter was in contrast to the effect found with manganese, but was similar to that found with nickel, though much smaller.

(7) All bands were found to bleach in the dark, the rate of thermal bleaching of the Z-bands being by far the highest.

The results in the ultra violet range differ from those obtained with manganese significantly, for they show that the effect of bleaching the F-band is to reduce the ultra violet absorption. This means that the absorption is not due to the presence of colloidal specks of calcium (see section 5.7), but must be due to hole traps, probably complexes of calcium ions and povacs. Compared with manganese and copper, calcium enhances the V-bands only slightly, indicating that many of the povacs produced by the doubly charged calcium ion are associated with the calcium in some way, and cannot form V-centres. The presence of both the Z-bands confirms that calcium can exist with and without an associated povac. Etzel (1952) came to the conclusion that the povacs were all disassociated from the calcium ions by comparing $NaCl.Ca^{++}$ and $NaCl.Cd^{++}$ and noting the enhancement of the V-bands in the former (which was of the same order as found by the present author). From which he drew the conclusion that the enhancement of the F-band by calcium was due to the reduction of lifetime of the free hole caused by the increased concentration of unassociated povacs, thereby reducing the chance of hole-electron recombination: the probability of forming an F-centre was then correspondingly greater. The evidence obtained here does not fit this theory, although evidence that only a small proportion of associated Ca^{++} ions occurred was found (see section 8.8).

The fact that Z-centres are formed on X-irradiation is particularly interesting, since, as it has been mentioned before, their non-appearance under this treatment has been difficult to explain. The evidence here suggests that they are in fact formed but their absorption bands are usually hidden by the F-band, even at low temperatures, and only become observable when the F-band is reduced by bleaching. This is discussed further in section 8.3.

The evidence from the quenching experiments suggests that the calcium, like manganese, can be placed along dislocations or other internal boundaries, from which it can be freed by heating the crystal. Quenching therefore increases the concentration of calcium ions in the body of the crystal, thus enhancing the Z-band and the 345 mμ band. Since the V-bands are not enhanced by the quenching process it seems likely that the calcium at, or near, internal boundaries is unassociated with povacs (unlike manganese). Although the theory due to Etzel is insufficient to explain the enhancing of the F-band it is relevant to the problem of colouration rate. Thus, the slight reduction of colouration rate observed can be explained by the removal of povacs due to associations formed with calcium ions liberated from internal boundaries, to form, for example, Z_2-centres.

The origin of the band at 345 mμ is not clear, although, since it occurs in additively coloured crystals it must be an electron trap. Since it only appears strongly in high content crystals it is probably associated with a centre consisting of more than one calcium ion, or, since the concentration of negvacs is high, a calcium ion near a vacant negative ion site. The latter model, or one involving a pair of calcium ions, would be equivalent to singly ionized helium and may be expected to give a band in the near ultra violet. An electron in the ground state would have a much lower energy than one trapped in a F-centre and will therefore thermally ionize much less readily. This can be reconciled to the observation that the 345 mμ band bleaches in the dark faster, in fact, than the F-band by assuming the two components of the centre to have a binding energy lower than the thermal ionization energy. However, the centre may well be more complex.

The lower efficiency of calcium, compared with manganese, in enhancing the F-band reflects its greater solubility in NaCl. That calcium is very soluble indicates that the degree of mis-match in the lattice introduced by it is small; and, consequently, the production of vacancies at regions of strain is low. A rough comparison of calcium and manganese is shown in Table 3.

TABLE 3

Impurity	Ionic Radii (Å)	S	C	S_1/S_2	C_1/C_2
1. Calcium	1.06	1×10^{-2}	6×10^{-3}		
2. Manganese	0.91	7×10^{-4}	4×10^{-4}	14	15
(Sodium)	0.98	-	-	-	-

S = max. m.f. giving clear NaCl crystal.

C = m.f. to give comparable enhancing of the F-band.

S_1/S_2 and C_1/C_2 are approximately equal and in the region of 15. This means that a manganese ion finds it 15 times more difficult to be built in than a calcium ion and produces about 15 times more F-centres than a calcium ion, when it is built in. The equality of these two ratios indicate a strong relationship between the formation of F-centres and the mis-match introduced into the lattice by the impurity.

8 THE FORMATION OF Z-CENTRES IN $NaCl.Ca^{++}$.

8.1 Introduction

The results of the work on $NaCl.Ca^{++}$ described in the previous chapter suggested that Z-centres were formed when the crystal was X-rayed. If this were true it would mean that the width of the F-band, on the long wavelength side, would be greater in crystals containing calcium than in those free of Z-centre forming impurities. Furthermore, the latter, pure, crystals would furnish the true width of the F-band and this could be used to calculate the intensity of the Z-band formed in a calcium-bearing crystal. Thus the growth of the Z-band under X-irradiation could be observed quantitatively, and this might lead to interesting correlations between Z- and F-band intensities and calcium concentration.

This chapter contains a description of the work undertaken along the lines of this argument. The results of the work are given and discussed, and deductions made from them are theoretically justified. The statistical mechanics of a model which describes the formation of incipient Z-centres is given, and the energy of formation of the latter is estimated.

8.2 Analysis of the F-band.

It is well known that the absorption bands associated with electrons trapped in solids have a form which is Gaussian rather than Lorentzian, the shape to be expected if the electron behaved as a damped simple harmonic oscillator. This is due to interactions with the thermal vibration of the atoms or ions surrounding the trap, and this effect has been taken into account in the theory of absorption by O'Rourke (1953), Lax (1952), and, more recently, Dexter (1956). Hesketh and Schneider (1954) have shown that, in particular, the F-band in X-rayed KCl is Gaussian at least over 75% of its range, and I.L. Mador et al (1953) have reported that the F-band in KBr is an asymmetric Gaussian, being broader on the short wavelength side. The present work of the author confirmed that the NaCl F-band was Gaussian in nature, but showed that it was asymmetrical, as in the case of KBr.

The method used to obtain the bandwidth was as follows. The experimental curve of d, the optical density, against wavelength was converted to one of d against E, the photon energy in electron-volts. Since the F-band is Gaussian

$$d = d_o \exp(-k(E-E_o))^2,$$

where d_o = peak density, E_o = energy at the band maximum, and k is related to the half bandwidth σ at half-maximum. Taking logarithms we have

$$u \log_{10} d/d_o = -k^2(E-E_o)^2$$

where

$$u = \log_e 10 = 2.303.$$

When $d = d_o/2$, $E-E_o = \sigma$, hence

$$k^2 = \frac{u \log_{10} 2}{\sigma^2} .$$

A plot of $(\log_{10} d/d_o)^{\frac{1}{2}}$ against E should then give two straight lines, one for E less than E_o, and these should intersect at $E = E_o$. If the Gaussian is symmetrical they will have the same slope, $ku^{-\frac{1}{2}}$.

In practise, $(\log_{10} d_o/d)^{\frac{1}{2}}$ was plotted against E so that positive axes could be used. The slope was still

$$ku^{-\frac{1}{2}} = \frac{(\log_{10} 2)^{\frac{1}{2}}}{\sigma} .$$

The plot shown in figure 41 was obtained from a Harshaw specimen of NaCl. Qualitatively, it is typical of all specimens investigated. The straight lines showed that the band was, in fact, Gaussian, but the difference in slopes indicated asymmetry. The bandwidth, w, as calculated from the lower energies line, and the bandwidth, w', as calculated

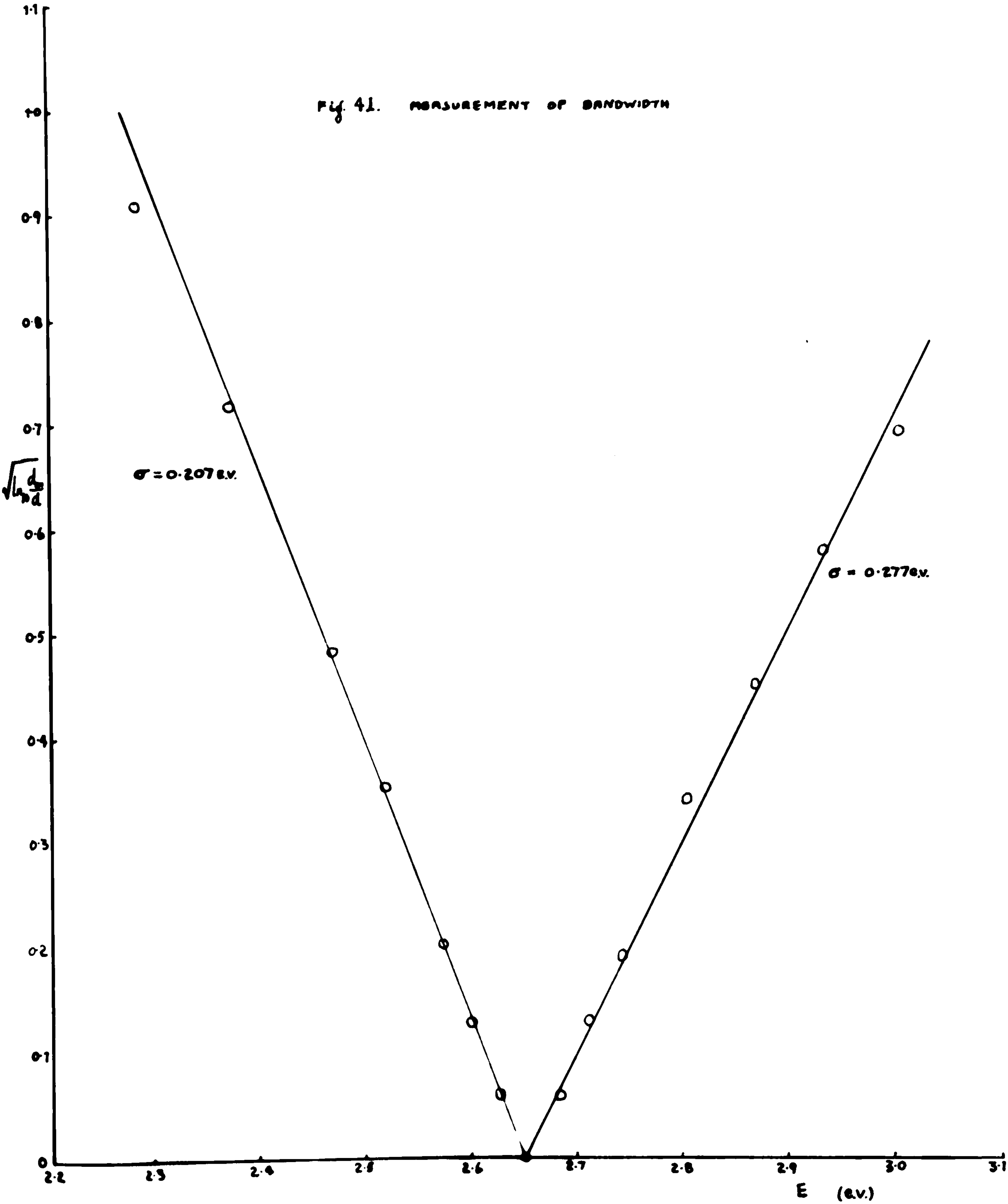
Fig. 41. MEASUREMENT OF BANDWIDTH
σ = 0·207 e.v.
σ = 0·277 e.v.
1·1
1·0
0·9
0·8
0·7
0·6
0·5
0·4
0·3
0·2
0·1
0
2·2
2·3
2·4
2·5
2·6
2·7
2·8
2·9
3·0
3·1
E (e.v.)

from the higher energies line, were found in a number of cases (see Table 4). The values were accurate to within 0.005 eV.

TABLE 4

Specimen	m.f. of $Ca^{++} \times 10^6$	w (eV)	w' (eV)
Harshaw	less than 1	0.414	0.554
Korth (a)	5	0.440	-
(b)		0.464	0.620
Manchester	19	0.436	-
Durham (a)	15	0.428	-
(b)	15	0.434	-
(c)	20 (approx.)	0.482	0.582
(d)	20 (approx.)	0.470	0.540

The Manchester and Durham specimens were grown from Analar NaCl without addition of $CaCl_2$. It was seen that there was a considerable variation in bandwidths and that in all cases w was less than w'. These results are similar to those obtained by Mador et al (1953) for KBr. It was also noted that the smallest bandwidth occurred in Harshaw specimens, which contained undetectable amounts of calcium.

8.3 Discussion of Bandwidth Data.

Kleinschrod (1936) observed that the F-band is not a simple bell-shaped band, since if examined under sufficient resolution it possesses a shoulder and tail on the short wavelength side. The shoulder is known as the K-band, and Mott and Gurney (1940) have suggested that it is associated with transitions to discrete levels above the first excited state of the F-band; the ratio of the K- and F-band intensities should therefore be constant. Geiger (1955), however, has shown that the ratio does not remain constant when the F-band is bleached, a result which casts doubt on the validity of this explanation. The K-band in KCl can be seen clearly in figures 23 and 24. Although the K-band would not seem to be associated with transitions to discrete levels in the F-centre the latter probably occur, and consequently they, as well as the K-band, will broaden the F-band on the short wavelength side. Also, experiments have shown a band at 410 mμ in $NaCl.Ca^{++}$ (see section 7.4). The Gaussian nature of the band in this region is therefore somewhat fortuitous, and the bandwidth, w', has no direct significance. Short wavelength broadening of similar origin~~s~~ is probably responsible for the asymmetry of the F-band in KBr.

It is suggested that, in general, broadening by unresolved bands occurs on the long wavelength side of the F-band, though to a lesser extent than that on the short wavelength side, and this accounts for the variation in bandwidth from specimen to specimen observed by the author, and by Mador et al in KBr. Since the F-band is Gaussian from 465 mμ (the peak wavelength) to 540 mμ, the region over which the bandwidth is found, the bands causing the broadening are of comparitively low intensity and do not destroy the Gaussian nature. The only bands which are known to occur in this range are the Z-bands, and it is suggested that these are formed along with the F-band when the crystal is X-rayed, if the crystal contains alkaline earth metals as impurity. Pure specimens may therefore be expected to show the smallest bandwidths, and this is observed with the Harshaw specimens. Variations in bandwidth with time of irradiation may also be expected, and this has been investigated and verified (see figure 46). The increase of bandwidth on prolonged irradiation mentioned in section 7.2 (see also figure 31) also lends the theory support. Further, measurements of bandwidth in crystals containing a high percentage of calcium before and after quenching, showed that the quenching process increased the width of the F-band, corresponding to an enhancement of the Z-band caused by the liberation of Ca^{++} from dislocations etc. It was also found that heating coloured high content crystals at 100°C reduced the bandwidth, indicating a destruction of Z-centres.

Apart from the evidence accumulated from observation, there is every reason, theoretically, to suppose that Z-centres are formed during X-irradiation. At least one of the centres, the unassociated divalent ion, is positively charged, and its capture cross section should not differ from that of the F-centre by more than an order of magnitude. Given a sufficiently high impurity concentration in the crystal Z-bands of observable intensities should be formed. The evidence presented here indicates that in fact they are formed. The hitherto unaccountable absence of the bands reported by workers in this field, may be explained by the low intensity of the bands causing them to remain hidden by the F-band.

8.4 Measurement of Z-band Intensities.

The bandwidth obtained in the Harshaw specimens (0.414 eV) was assumed to be the true width of the F-band, and it was used to calculate the appropriate Gaussian for the peak intensity given by the experimental curve. It seemed reasonable to assume that the Z-bands, located about 520 mμ, contributed little to the absorption at 465 mμ, therefore the peak intensity of the experimental curve was very nearly that of the true F-band.

Subtraction of the calculated F-band then gave the Z-bands, which appeared in general as an unresolved band peaking at 520 mμ (at room temperature), with a plateau from 520 mμ to about 550 mμ. The high absorption in the region of 550 mμ suggests that R-bands were also formed during X-irradiation.

Figure 42 shows the results of such subtractions for several specimens. The intensity of the Z-band, d_z, was taken to be the density at 520 mμ, and the relative intensity, d_z/d_f, where d_f was the density at 465 mμ, was calculated in all specimens investigated. The following points brought out by figure 42 are worthy of note.

(1) The relative intensity of the Z-band is independent of calcium concentration to a remarkable degree, remaining at about 0.1 while the calcium concentration increases a thousandfold. This indicates that the calcium introduces negative ion vacancies into the crystal.

(2) The quenched crystal (figure 42b) shows a higher relative intensity.

(3) Heating at 100°C rapidly destroys the band (figure 42b).

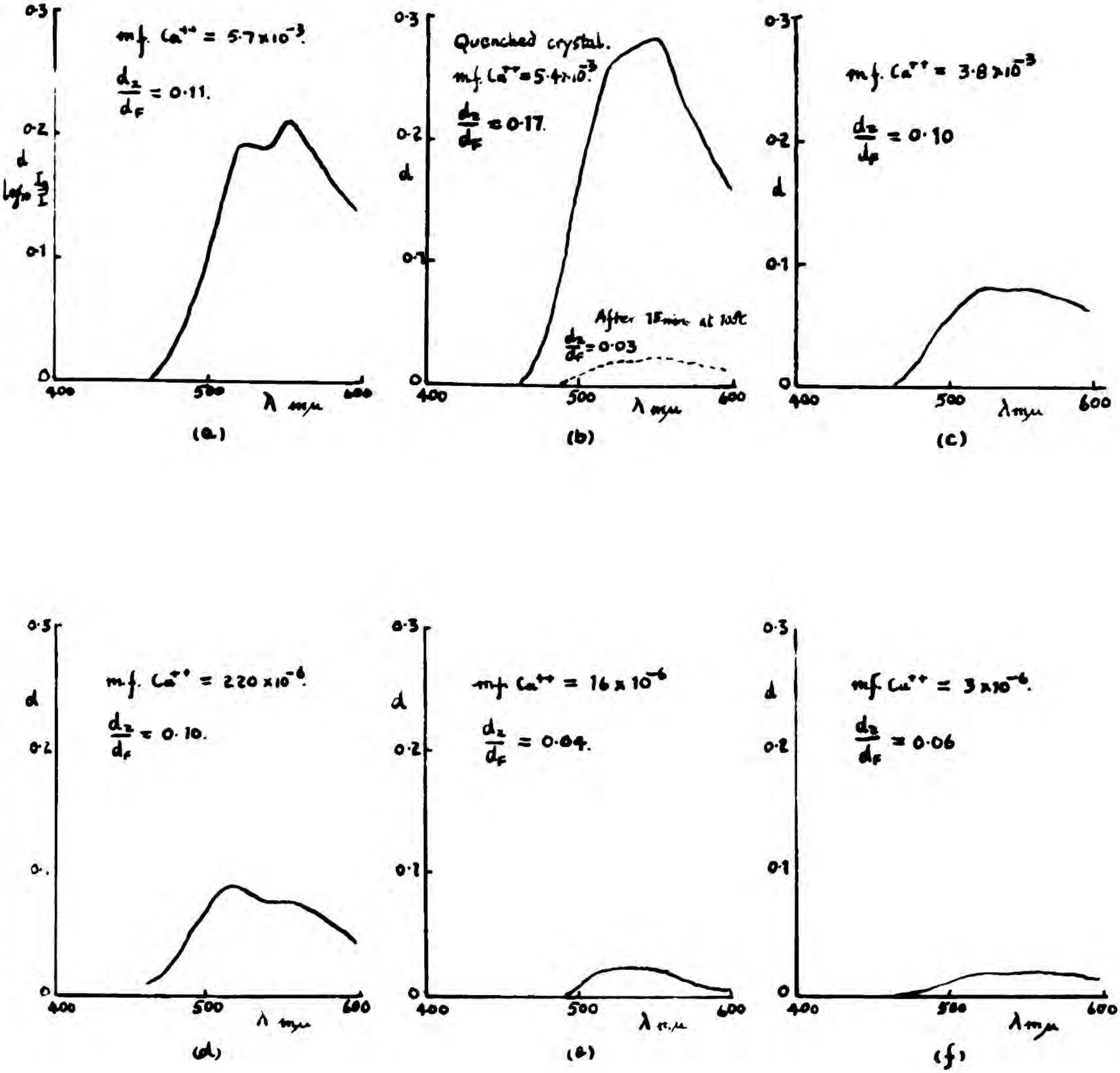

Fig. 42. Z- AND R-BANDS PRODUCED BY X-RAYS.

FROM ABSORPTION MEASUREMENTS AT 20°C.

Subtraction bands for optically bleached specimens are shown in figure 43. It can be seen that bleaching increases the relative intensity. This is due largely to the reduction of the F-band and only slightly to an increase in the Z-band. The increase in relative intensity accounts for the observation of Z-bands hitherto only in bleached crystals.

Figure 44 shows the bands at $90^{\circ}K$, obtained by subtracting a Gaussian of width 0.240 eV (the width of the F-band being proportional to the square root of the absolute temperature). At this temperature some resolution is obtained, and two bands may be seen, the Z_1-band at 490 mμ and the Z_2-band at 510 mμ. It would appear, therefore, that both types of centres are present in the crystal.

The relative intensity was measured in a large number of specimens. Table 5 shows the results for X-rayed crystals together with the time of irradiation and the calcium content of each specimen.

The constancy of the relative intensity with increasing calcium concentration in the higher content specimens indicated that for every Z-centre introduced into the crystal a definite number of F-centres were produced. The smaller relative intensities found in the lower content specimens is due to F-centres which are present at

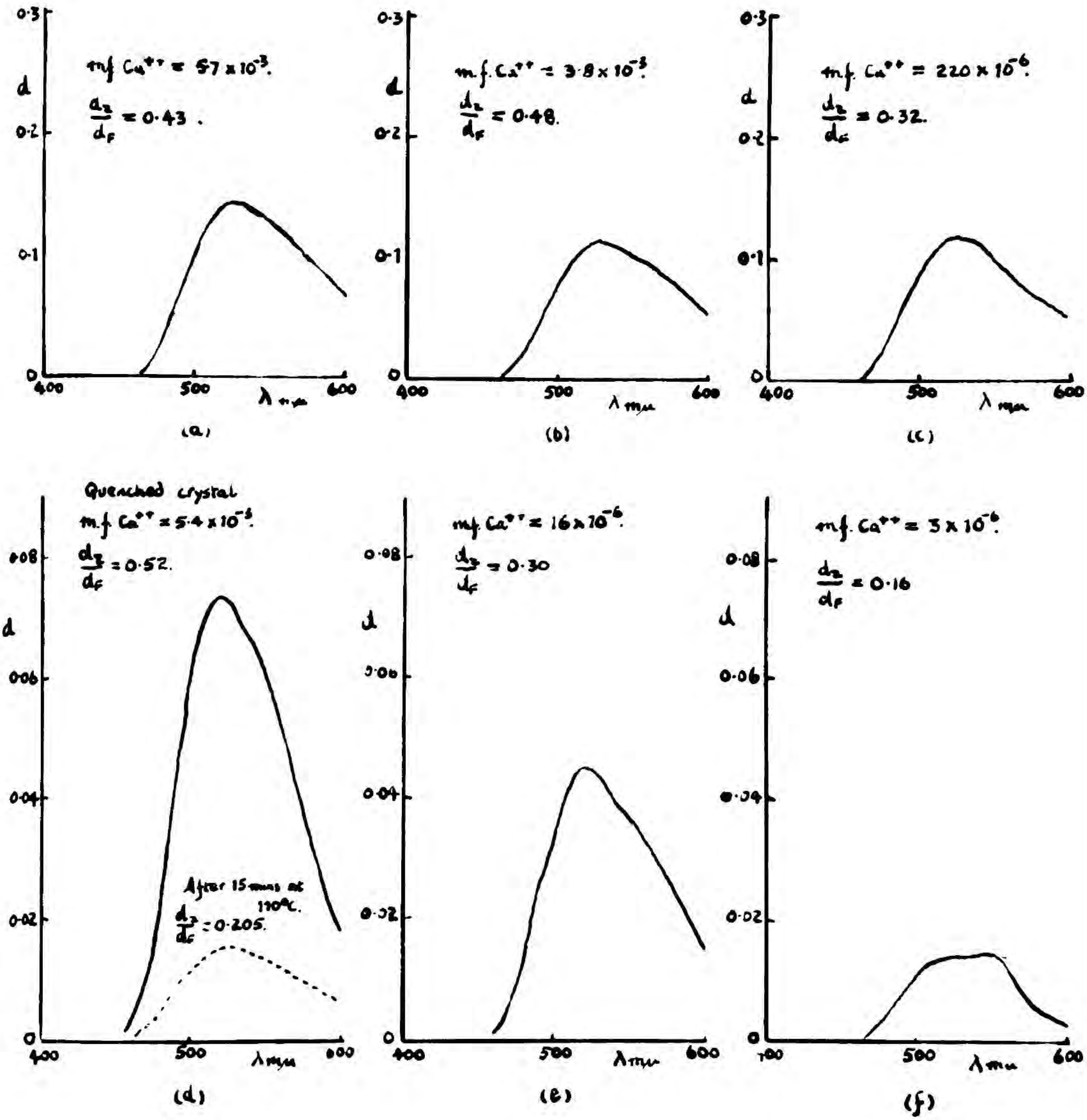

Fig 43. Z- AND R-BANDS PRODUCED BY F-LIGHT BLEACHING. FROM ABSORPTION MEASUREMENTS AT 20°C.

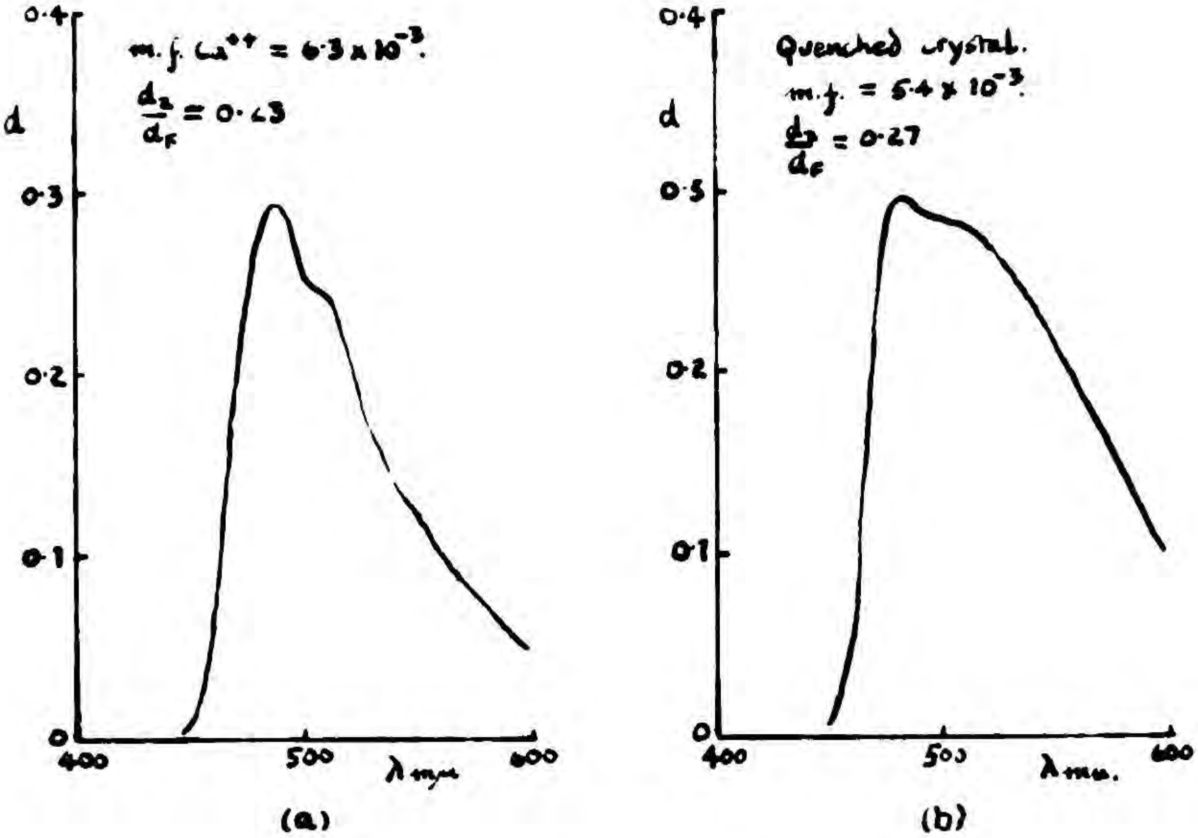

(i) Z-bands produced by X-rays.

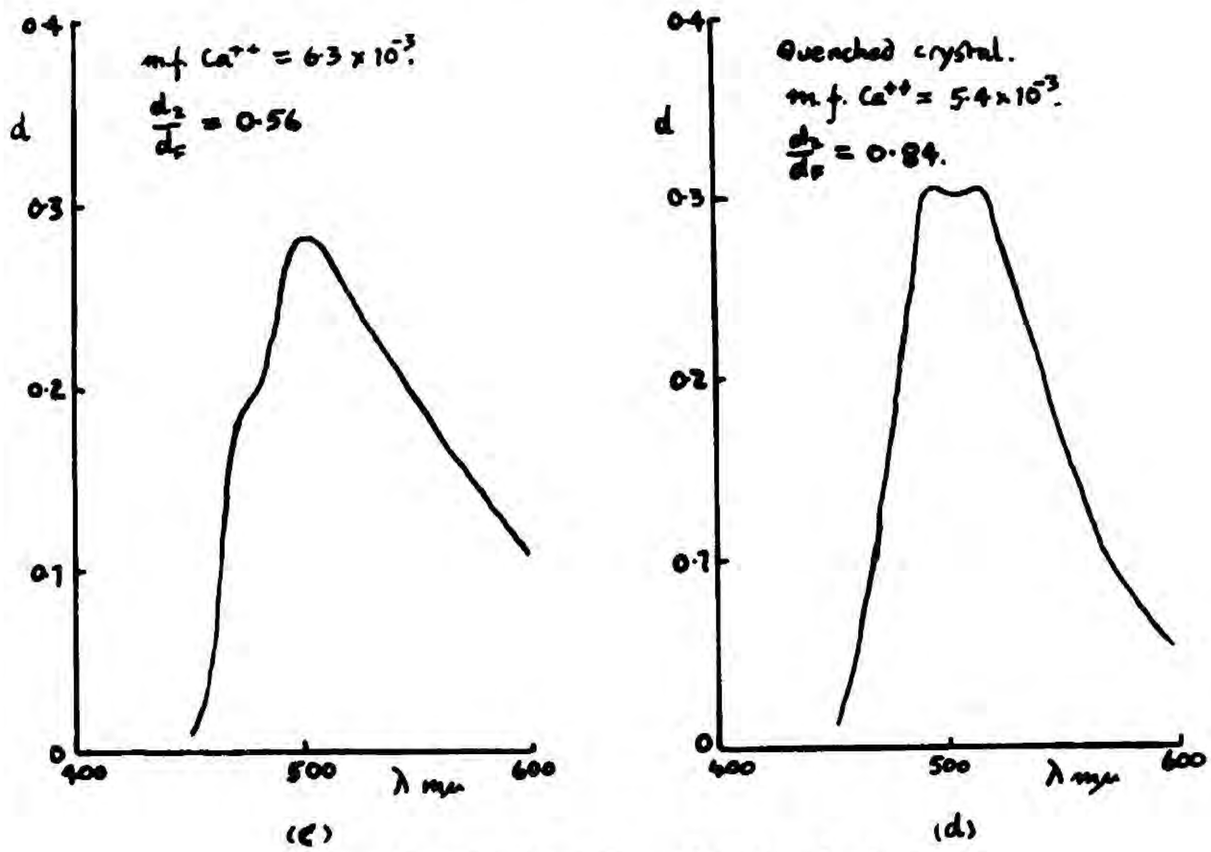

(ii) Z-bands after F-light bleaching.

Fig. 44. Z-BANDS FROM ABSORPTION MEASUREMENTS AT 90°K.

TABLE 5

Specimen	m.f. $Ca^{++} \times 10^6$	X-ray Time (hours)	Relative Intensity d_z/d_f
Korth (a)	3	3.0	0.07
(b)	5	2.0	0.05
(c)	5	5.0	0.06
Manchester	19	5.0	0.03
Durham (a)	15	0.5	0.05
		3.0	0.08
		4.0	0.04
(b)*	30	2.0	0.02
(c)	220	3.0	0.11
		5.0	0.10
(d)	3,800	2.5	0.09
(e)	5,700	2.0	0.10
		5.0	0.11
(f)*	5,400	3.3	0.18
		5.0	0.17

*Quenched specimens

zero calcium concentration due to other causes. These "intrinsic" F-centres probably vary in concentration from specimen to specimen and this would account for the spread of values found in the purer crystals. Another factor here is the increasing inaccuracy of measurement as the intensity of the band becomes low.

The relative intensity was also measured in specimens which had been exposed to F-light. The results obtained with the specimens of Table 5 are shown in Table 6.

TABLE 6

Specimen	m.f. $Ca^{++} \times 10^6$	Relative Intensity d_z/d_f
Korth (a)	3	-
(b)	5	0.161
(c)	5	0.156
Manchester	19	0.343
Durham (a)	15	0.440
		-
		0.320
(b)*	30	0.340
(c)	220	-
		0.323
(d)	3,800	0.477
(e)	5,700	0.400
		0.433
(f)*	5,400	0.510
		0.536

*Quenched specimens

In general, it was found that bleaching had the effect of increasing the relative intensity by a factor of 4 in the higher content crystals.

Measurements of the variation of relative intensity with bleaching time showed that the former eventually reached a saturation value, corresponding to the state when both the F- and the Z-band were bleaching at the same rate.

8.5 The Growth of the F- and Z-bands.

The growth of the F-band and of the Z-band, and the behaviour of the F-bandwidth, as functions of the time of X-irradiation of the crystal, were investigated. The procedure was to irradiate a thin specimen for 5 minutes, measure the absorption from 400 mμ to 540 mμ, irradiate for another 5 minutes, measure, and so on. After the initial growth was plotted the intervals of irradiation were increased first to 15, then to 30, and finally to 60 minutes, until the specimen had had 3 hours irradiation. It was found that when the X-ray machine was cold the tube current, a measure of the X-ray intensity, fell appreciably over the first half hour of running, and consequently the precautions were taken of (a) allowing the machine to warm up before exposing the specimen, and (b) checking, and, if necessary, adjusting the current frequently during irradiation periods. Each specimen investigated was therefore given precisely the same irradiation treatment. After the final measurement the width of the specimen was measured with a micrometer screw gauge at several places on the specimen, and a mean value was obtained and used to convert optical density to absorption coefficient.

Figure 45 shows the growth curves of the F-band for five specimens of widely varying calcium content. It illustrates strikingly the enhancement of the F-band by calcium. That calcium is not the sole cause of the F-centres is indicated by the results obtained with nearly pure crystals - the Harshaw specimen contains less calcium than the Korth specimen yet it shows a slightly higher colourability.

Analysis of these curves showed that they were closely exponential in nature, being of the form

$$\alpha = \alpha_{\infty} (1 - \exp(-vt)),$$

where α_{∞} was the absorption coefficient at saturation, and v was the growth constant. α_{∞} and v were calculated for each specimen investigated (see figure 45); v was found to be about 2×10^{-4} sec^{-1} and, unlike α_{∞}, appeared to be unrelated to calcium content.

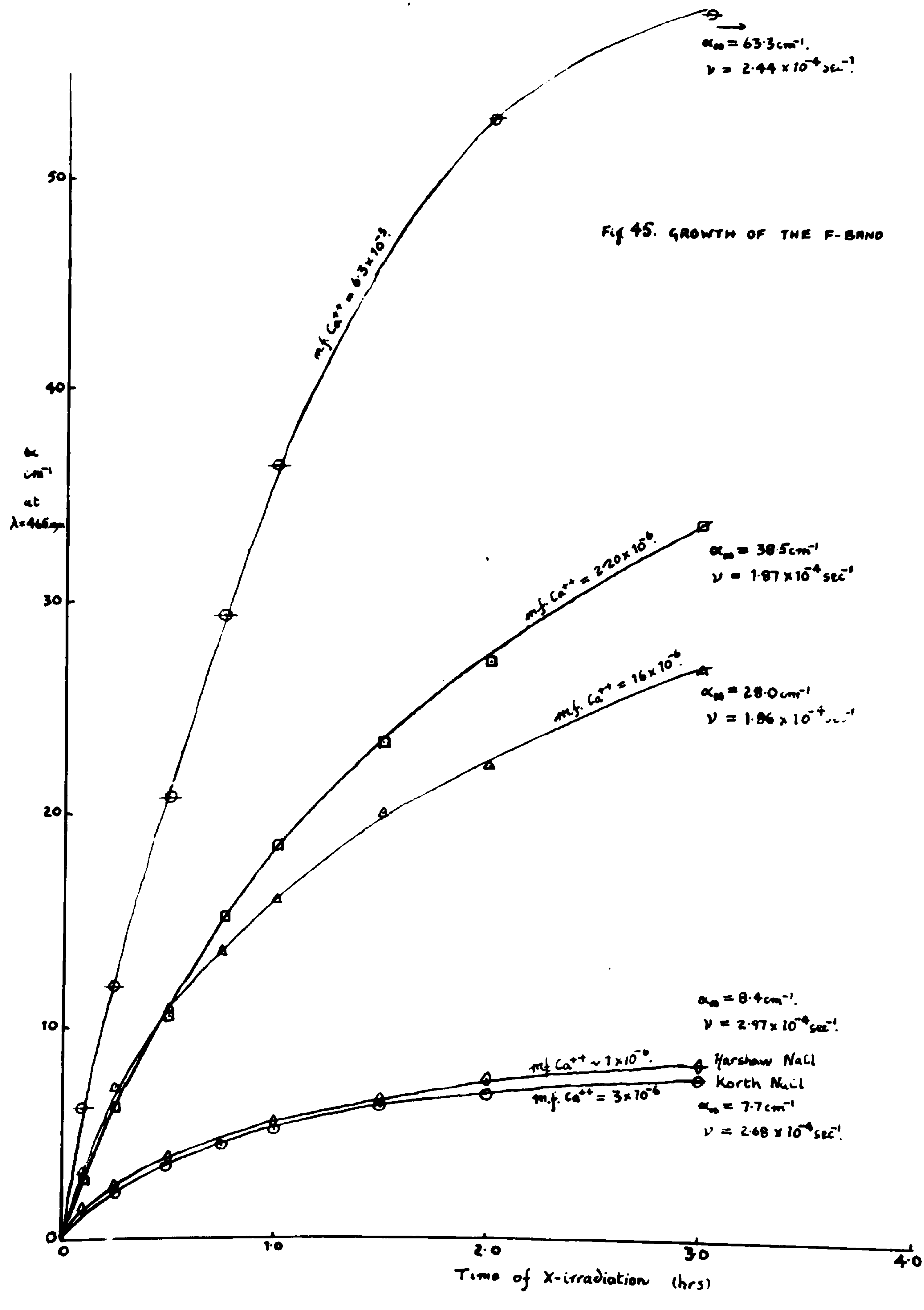

Fig 45. GROWTH OF THE F-BAND
α cm^{-1} at $\lambda = 466m\mu$
Time of X-irradiation (hrs)
0
10
20
30
40
50
1·0
2·0
3·0
4·0
$\alpha_\infty = 63·3 cm^{-1}$.
$\nu = 2·44 \times 10^{-4} sec^{-1}$.
m.f. $Ca^{++} = 6·3 \times 10^{-5}$.
$\alpha_\infty = 38·5 cm^{-1}$
$\nu = 1·87 \times 10^{-4} sec^{-1}$
m.f. $Ca^{++} = 220 \times 10^{-6}$.
$\alpha_\infty = 28·0 cm^{-1}$
$\nu = 1·86 \times 10^{-4}$
m.f. $Ca^{++} = 16 \times 10^{-6}$.
$\alpha_\infty = 8·4 cm^{-1}$.
$\nu = 2·97 \times 10^{-4} sec^{-1}$.
m.f. $Ca^{++} \sim 1 \times 10^{-6}$.
Harshaw NaCl
Korth NaCl
m.f. $Ca^{++} = 3 \times 10^{-6}$
$\alpha_\infty = 7·7 cm^{-1}$
$\nu = 2·68 \times 10^{-4} sec^{-1}$.

From the absorption measurements taken between 465 mμ and 540 mμ the bandwidth of the experimental absorption band was calculated after each irradiation interval, so that its variation with the degree of colouration (defined as the ratio α/α_{∞}) could be followed. The results for the five specimens investigated in this way are shown in figure 46, where the half-bandwidth, σ , is plotted against the degree of colouration. That a variation was observed at all in calcium bearing crystals indicated the influence of other bands besides the F-band in the wavelength region considered, and therefore these results support the theory that Z-centres are produced during X-irradiation. As expected on this theory, the calcium free Harshaw specimen showed a bandwidth which remained constant, within experimental error (less than 0.003 eV in these cases).

Assuming the Harshaw bandwidth 0.414 eV to be the F-bandwidth the growth curves for the Z-band were calculated, and are shown in figure 47. At least over the first 2 hours of irradiation they were found to be of the same form as that found for the F-band, i.e.

$$\alpha = \alpha_{\infty} (1 - \exp(-vt)).$$

Beyond $t = 2$ hours deviations occurred in the cases of the higher content crystals, suggesting some liberation of Ca^{++} from dislocations as a

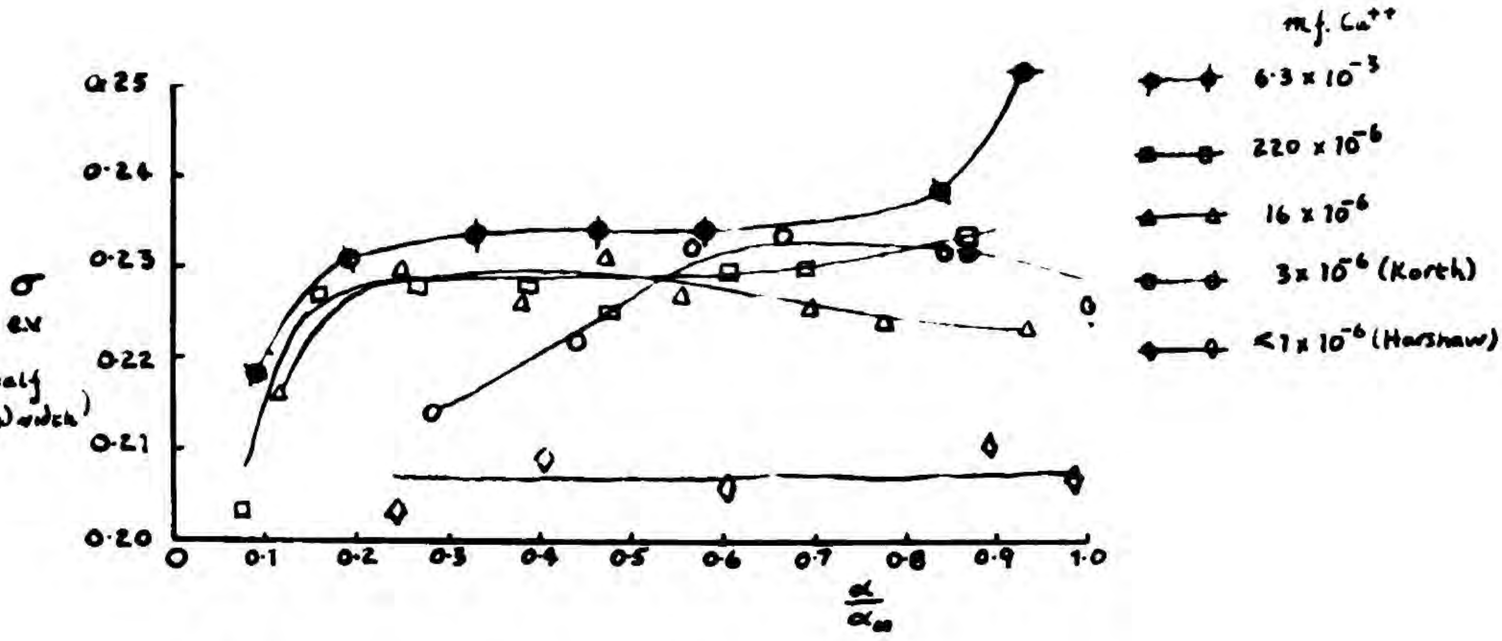

Fig 46. BANDWIDTH DEPENDANCE ON DEGREE OF COLOURATION.

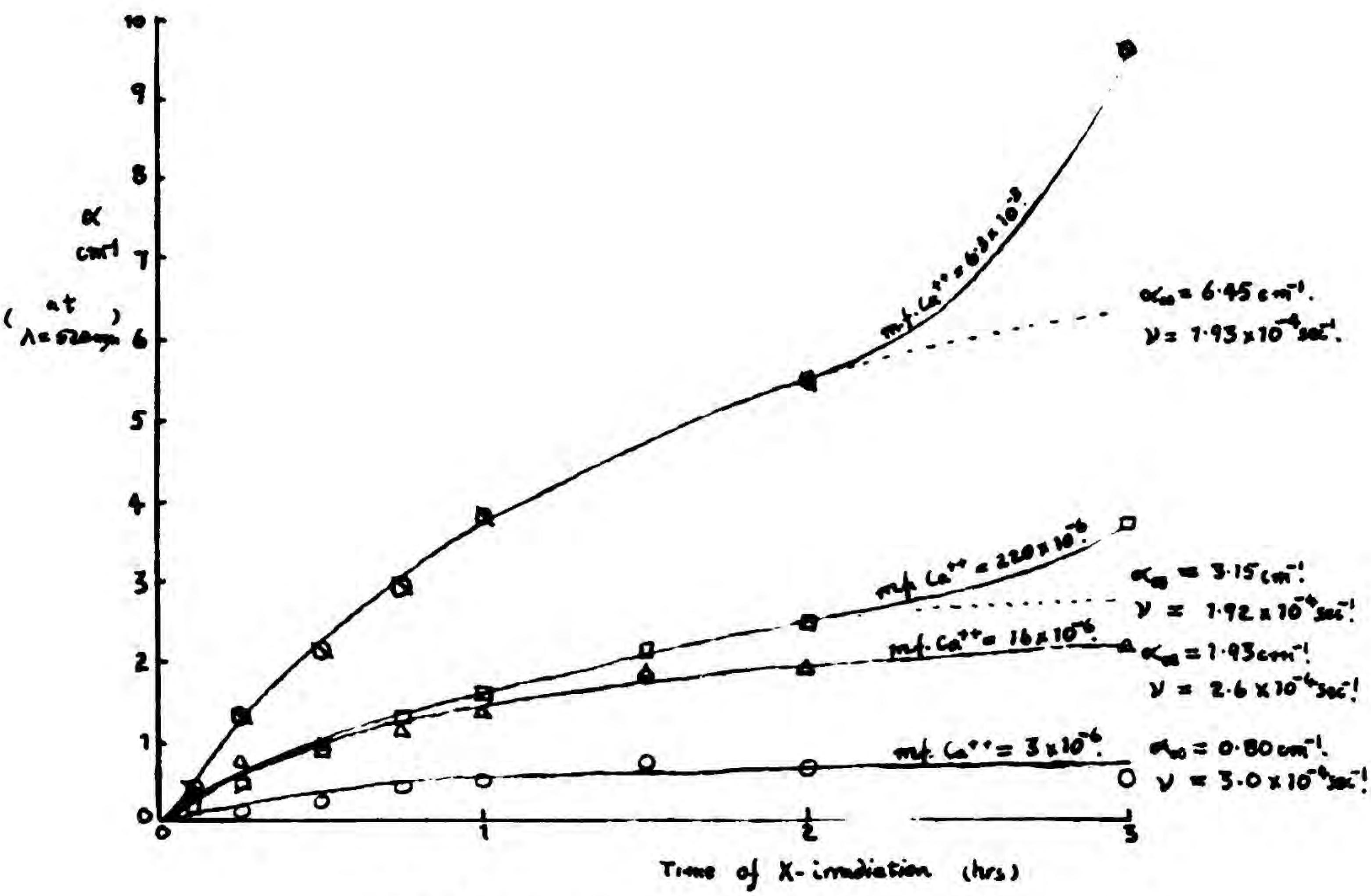

Fig 47. GROWTH OF 'Z'-BAND

result of the X-irradiation. (A similar effect was found in $NaCl.Mn^{++}$ (section 5.4). α_{∞} and v were measured from the exponential part of the curves, and $(\alpha_{\infty})_z/(\alpha_{\infty})_f$, or, dropping the subscript, simply α_z/α_f, and v_z/v_f were calculated for each specimen. The results appear in Table 7.

It may be noted from the values of the two ratios that (a) the growth rates of the two bands were approximately equal; and (b) the saturation intensity of the Z-band was approximately one-tenth that of the F-band; and (c) these properties were independent of calcium concentration.

8.6 Phenomenological Theory of Colouration.

To explain these results let us consider a crystal containing hole and electron traps undergoing X-irradiation. For simplicity we shall assume that the only electron traps which are present are negative ion vacancies and Ca^{++} ions, and the only hole traps are positive ion vacancy pairs. (It is possible to consider the complexes associated with Z_2-centres and R-centres if it is assumed that the capture probability of the individual traps in the complex remains unchanged by the complex, but for clarity this is not dealt with here).

TABLE 7

Specimen	α_f (cm^{-1})	α_z (cm^{-1})	v_f ($sec^{-1} \times 10^4$)	v_z ($sec^{-1} \times 10^4$)	α_z/α_f	v_z/v_f	m.f.$Ca^{++} \times 10^6$
Korth	7.7	0.80	2.68	3.0	0.10	1.1	3
Durham (a)	28.0	1.93	1.86	2.6	0.070	1.4	16
(b)	38.5	3.15	1.87	1.92	0.082	1.03	220
(c)	63.3	6.45	2.44	1.93	0.102	0.79	6,300

Let

F = X-ray flux, (quanta/cm^2/sec)

N = density of ions,

S = ionization cross-section of ions,

n = density of electrons in the conduction band,

p = density of holes in the valence band,

k_o = probability of direct recombination of electrons and holes per unit time.

The following table gives the notation for the densities of the traps and colour centres at any time, t; the capture probabilities per unit time of the traps, k; and the probability per unit time of ionization of the colour centres, w.

	density	k	w
Negative ion vacancies	n_1	k_1	-
Ca^{++} ions	n_2	k_2	-
F-centres	n_f	-	w_f
Z_1-centres	n_z	-	w_z

Finally, let n_3 be the density of positive ion vacancies, n_v be the density of those which have captured a hole, and k_3 be the probability per unit time that an electron recombines with a trapped hole. Since the n_v centres are in pairs or associated with positive ion vacancies in NaCl, forming V_2 and V_3-centres respectively, we assume for simplicity that k_3 is unaltered by complex formation.

Although Leivo et al (1949) have found evidence that vacancies are created during X-irradiation we shall assume that this effect is negligible here, so that at all times

$$n_1 + n_f = \text{a constant} = N_f.$$

Similarly, we have

$$n_2 + n_z = N_z$$

$$n_3 + n_v = N_v.$$

The rate of increase of the density of electrons in the conduction band is given by

$$\frac{dn}{dt} = SFN - k_o pn - k_1 n_1 n - k_2 n_2 n - k_3 n_v n + w_f n_f + w_z n_z.$$

We can simplify this equation if we assume that:

(1) The terms involving w_f and w_z are negligible.

(2) $k_1 = k_2 = k_3 = k$.

(3) At all times electrical neutrality is preserved,

i.e. $n = p$

and $n_3 = n_1 + n_2$.

We obtain

$$\frac{dn}{dt} = SFN - k_o n^2 - kN_v n,$$

using the condition that $n_3 = N_v - n_v$.

Integration gives n as a function of t:

$$n = \frac{KK' \left(\exp\left(k_o(K + K')t\right) - 1\right)}{K' \exp\left(k_o(K + K')t\right) + K}$$

where

$$K = \frac{kN_v}{2k_o}\left(\left(1 + \frac{4SFNk_o}{k^2 N_v^2}\right)^{\frac{1}{2}} - 1\right)$$

and

$$K' = \frac{kN_v}{2k_o}\left(\left(1 + \frac{4SFNk_o}{k^2 N_v^2}\right)^{\frac{1}{2}} + 1\right).$$

Here we have used the boundary condition $n = 0$ when $t = 0$.

When t is large enough

$$n = K.$$

That is to say, the density of conduction electrons becomes constant as t increases.

It is of interest to estimate how quickly this state is reached. The time constant associated with the growth of n is $(k_o\ (K + K'))^{-1}$. Now k_o and k can each be written as the product of a capture cross-section and the arithmetic mean thermal velocity of the electrons, so that since the former will be about 10^{-16} cm^2, and the latter is about 10^7 cm/sec we can put $k_o = k = 10^{-9}$; and if we let $S = 10^{-16}$ cm^2, $F = 10^7$ quanta/cm^2/sec, $N = 10^{22}$, and $N_v = 10^{17}$, we find the time constant to be of the order of 10^{-8} sec. Thus, over the range of time which is of interest, we may consider n to be constant at about 10^5 electrons/cm^3; as estimated from

$$n = K \doteq \frac{SFN}{kN_v}.$$

We can now consider the growth of the number of F-centres.

The rate equation is

$$\frac{dn_f}{dt} = k_1 n_1 n - w_f n_f .$$

Putting $n_1 = N_f - n_f$ and integrating we obtain

$$n_f = \frac{k_1 n N_f}{v_f} \left(1 - \exp\left(-v_f t\right)\right),$$

where

$$v_f = k_1 n + w_f .$$

Since the absorption coefficient, α, is proportional to the number of F-centres, this is just the form of the growth curve of the F-band found experimentally, with $v_f \doteqdot 10^{-7}$ $\sec^{-1}$ (see section 7.4),

$$v_f \doteqdot k_1 n,$$

hence

$$\underline{n_f = N_f \left(1 - \exp\left(-v_f t\right)\right).}$$

In a similar manner we can derive the growth formula for the Z_1-centres and obtain, if w_z is neglected,

$$\underline{n_z = N_z \left(1 - \exp\left(-v_z t\right)\right).}$$

However, the estimation of w_z described in section 7.4 showed that w_z can be as large as 10^{-5} sec^{-1}; consequently, the expression for n_z is a somewhat poorer approximation than that for n_f.

We may note that

$$\frac{v_z}{v_f} = \frac{k_2}{k_1} .$$

From experiment this ratio was found to be approximately unity, hence this means that the capture cross-sections of a negative ion vacancy and a Ca^{++} ion are approximately equal. This also justifies putting $k_1 = k_2$ to calculate n.

8.7 Estimations of Vacancy and Ca^{++} Ion Densities.

The specimens used in the investigation of the growth of the F- and Z-bands were less than 0.05 cm thick, so that it was assumed, to a first approximation, that the colouration by the X-rays was produced uniformly. (The question of non-uniformity is discussed in section 8.9). The formula given by Smakula (1930), relating the number of absorbing centres per unit volume to the band peak absorption coefficient, was then applicable. For NaCl the formula becomes

$$n_i = 1.06 \times 10^{16} \frac{W\alpha_i}{f} ,$$

where n_i is the density of absorbing centres, W, the bandwidth at half maximum, f, the oscillator strength of the centre, and α_i is the peak absorption coefficient. Substituting f = 0.81 (Mott and Gurney, 1940), W = 0.414 eV, and $\alpha_i = \alpha_f$, the value at saturation as calculated from the growth curves, N_f, the density of negative ion vacancies, was calculated.

To estimate the density of Ca^{++} ions it was assumed that:

(1) The Z-band absorption was due to only Z_1-centres, so that the saturation absorption coefficient, α_z, referred to N_z, the density of Ca^{++} ions.

(2) W and f for the Z_1-band were the same as for the F-band. (The similarity between the two centres makes this a reasonable first approximation).

The density of Ca^{++} ions, N_c, determined chemically, was also calculated, from the mole fraction. The values of N_c, N_f and N_z for six specimens are shown in Table 8.

Since the specimens came from crystals slowly cooled from the growth temperature to room temperature, N_z and N_f were taken to be the thermal equilibrium values at 20°C. Particularly striking

TABLE 8

Specimen	$N_c(Ca^{++}/cc)$	$N_z(Ca^{++})Z_1/cc$	N_f Neg. ion vacs/cc
1	7×10^{16}	4.4×10^{15}	4.2×10^{16}
2	3.5×10^{17}	1.0×10^{16}	1.3×10^{17}
3	8.8×10^{17}	1.4×10^{16}	1.4×10^{17}
4	4.8×10^{18}	1.7×10^{16}	2.1×10^{17}
5	1.4×10^{20}	3.3×10^{16}	3.4×10^{17}
6	1.6×10^{20}	-	3.5×10^{17}

was the considerable disparity between the density of Ca^{++} ions determined chemically and the density of Ca^{++} ions giving rise to colour centres, indicating that a greater proportion of the calcium by far, existed in the crystal as agglomerates, probably at dislocations. It was also interesting to notice that, while neither N_z nor N_f were simply related to N_c, N_f was closely related to N_z, the ratio N_f/N_z being a constant with respect to N_c and approximately equal to 10. Therefore it appeared that for every Ca^{++} ion, in the lattice substitutionally and unassociated, there were ten negative ion vacancies.

8.8 Theory of Z-centre Concentration.

The following explanation is suggested to account for the disparity between the density of

Ca^{++} ions (N_c) as determined chemically and the Z-centre density N_z.

Consider the N_c $CaCl_2$ molecules per cc inside the crystal to be aggregated at dislocations, where their energy is much lower than it would be if they were distributed throughout the bulk. Since solute atoms and molecules can reduce the strain energy around an imperfection like a dislocation by virtue of their size, which is generally different to that of the host molecules (Cottrel, 1953; Kurtz and Kulin, 1954), this would seem to be reasonable. At a temperature above absolute zero, however, n of the N_c impurity molecules will find themselves built into the lattice, away from the aggregates, i.e. spread throughout the bulk, and this density, n, will be governed by an activation energy, E. If E is high enough n will be only a small fraction of N_c at room temperature, and since n will be related to N_z the disparity is explained.

We can take the model further by considering how a $CaCl_2$ molecule is built into the lattice. A reasonable mechanism for this is as follows:

(1) The Ca^{++} ion is placed at one of the N lattice site positions normally occupied by a Na^+ ion.

(2) Each of the Cl^- ions is placed at one of the N negative ion sites.

(3) To preserve electrical neutrality within the bulk of the crystal a vacancy is created at one of the N positive ion sites.

(4) If the positive ion vacancy is associated with the Ca^{++} ion, forming a complex, we can regard the complex as replacing one of the N NaCl molecules.

Suppose that a fraction f of the n Ca^{++} ions built into the lattice is associated with positive ion vacancies. Then, if the density of unassociated Ca^{++} ions (= density of unassociated positive ion vacancies) is p, and the density of complexes is q,

$$p = (1 - f)n, \text{ and } q = fn.$$

We may now proceed by well-known arguments of statistical mechanics to calculate the equilibrium density of $CaCl_2$ molecules built in at any temperature, T.

The contribution to the entropy change, S, from the distribution of the p Ca^{++} ions over N sites is given by

$$S_1 = k \log \frac{N!}{(N-p)!p!} ,$$

and this is equal to the contribution from the unassociated vacancies, S_2. Hence we have

$$S_1 + S_2 = 2k \log \frac{N!}{(N-p)!p!} .$$

The contribution from the complexes is

$$S_3 = k \log \frac{N!}{(N-q)!q!} ,$$

and that from the 2n Cl^- ions

$$S_4 = 2k \log \frac{N!}{(N-n)!n!} .$$

There is yet a further change in entropy which arises from the selection of n from the N_c $CaCl_2$ molecules, i.e.

$$S_5 = k \log \frac{N_c!}{(N_c-n)!n!} .$$

If E is the energy required to build in a $CaCl_2$ molecule, the change in free energy, F, is given by

$$F = nE - TS.$$

Since, at thermal equilibrium, F is a minimum, i.e. $dF/dn = 0$, we have

$$E = T\frac{dS}{dn} .$$

Adding the components of S and using Sterling's approximation, i.e.

$$\log N! = N \log N - N,$$

where N is large, we obtain an expression for S which, after substituting for p and q and differentiating, gives

$$\frac{E}{kT} = \log(N_c - n) - (5-f)\log n + (4-f)\log N - \log f^f(1-f)^{2(1-f)}.$$

In deriving this we have neglected n in comparison with N. The last term in the above equation may also be neglected, so that

$$\log(N_c - n) = (5-f)\log n - (4-f)\log N + E/kT.$$

The theory therefore predicts that a plot of $\log(N_c - n)$ against $\log n$ will give a straight line of slope $(5-f)$ and intercept $E/kT - (4-f)\log N$, and hence f and E may be found.

A comparison of theory and experiment was effected by associating n, the density of $CaCl_2$ molecules built in to the lattice in the manner proposed above, with N_z, the density of absorbing centres calculated using the assumptions of the previous section. Anticipating the result found here, N_z was associated in that section with the density of unassociated Ca^{++} ions. However, the results of absorption measurements indicated that both associated and unassociated Ca^{++} ions were present (see section 8.4), but in what proportions it was impossible to judge since there was insufficient resolution of the Z_1- and Z_2- bands. Therefore, in equating N_z and n the following assumptions were implicit;

(1) The saturation absorption coefficient, α_z, was the sum of the corresponding absorption coefficients of the two Z-bands. (Since the peak wavelengths of the bands were separated by only 20 mμ this was a reasonable first approximation).

(2) The bandwidths and oscillator strengths of the bands were those of the F-band.

A breakdown of either of these assumptions would affect the intercept, and hence the value of E, but would not appreciably affect the slope, since, in this case, $n = N_z$ could be replaced by $n = KN_z$, where K is a constant.

The result of plotting log $(N_c - n)$ against log $n(n = N_z)$ is shown in figure 48(a). The straight line was found to have a slope of 4.98 ± 0.10, so that $f = 0.02 \pm 0.10$, indicating that, at the most, only 2% of the Ca^{++} ions were associated at room temperature. This result confirms the work of Etzel (1952), with regard to the predominance of unassociated ions. Thus,

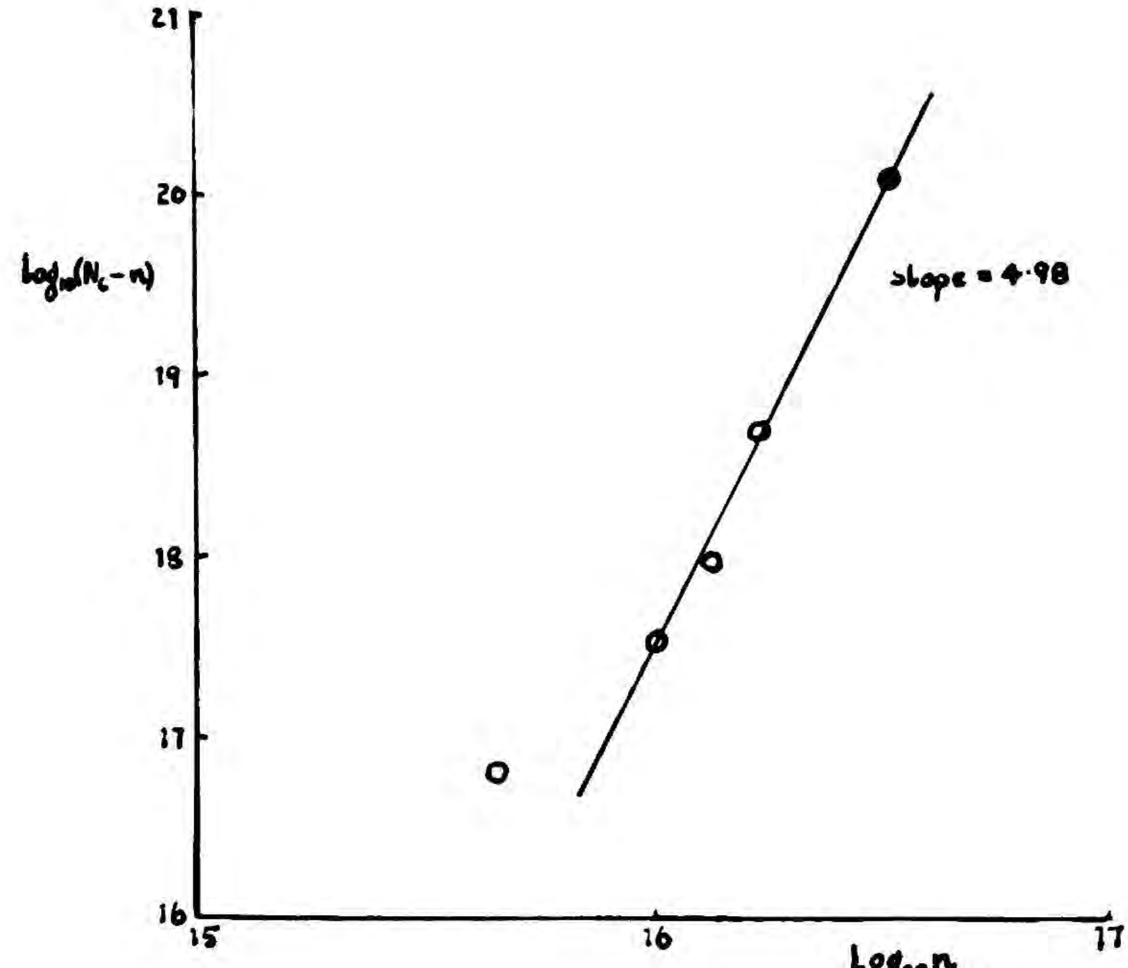
21
20
19
18
17
16
$\log_{10}(N_c - n)$
Slope = 4·98
15
16
17
$\log_{10} n$

(a)

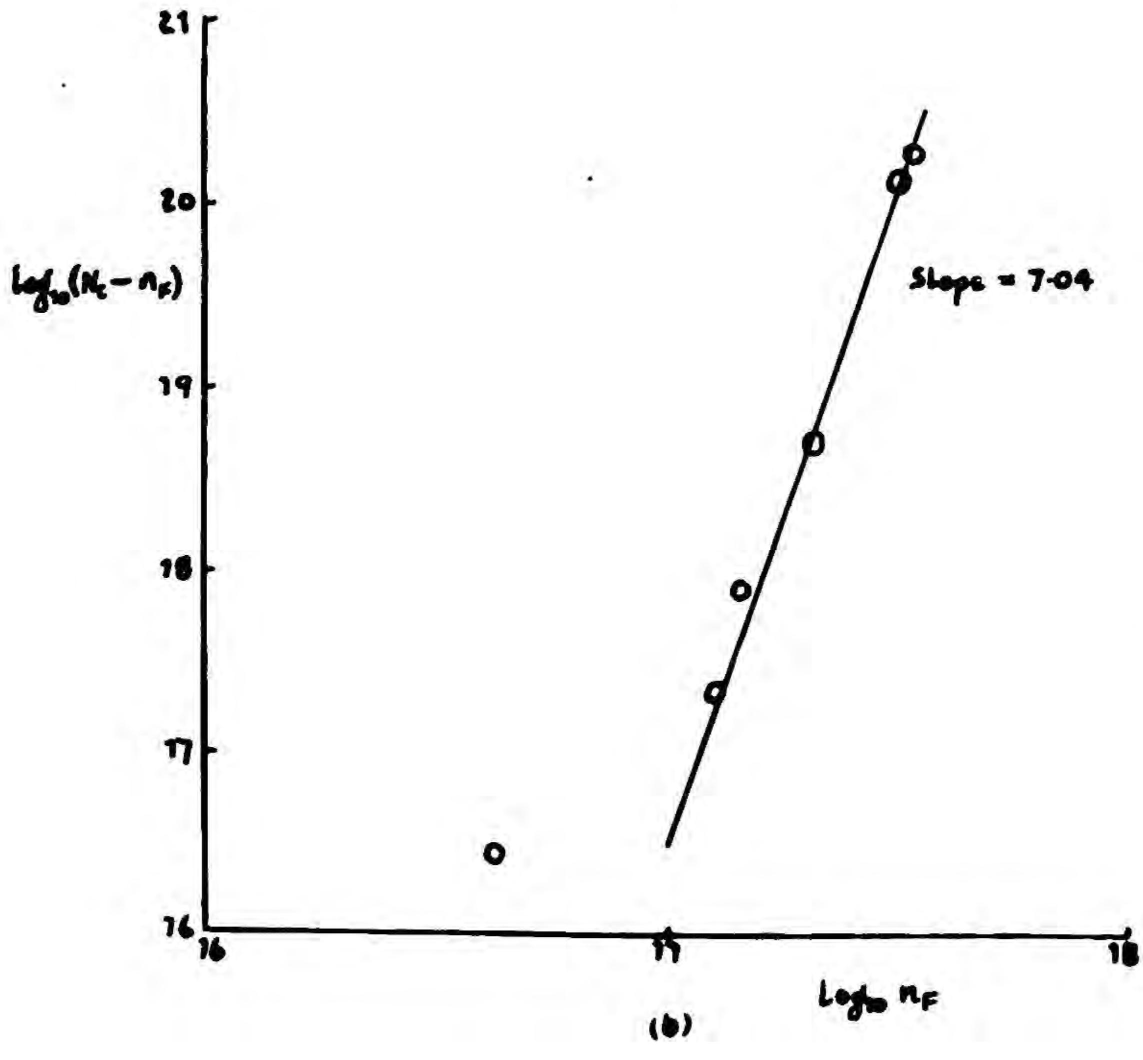
21
20
19
18
17
16
$\log_{10}(N_c - n_F)$
Slope = 7·04
16
17
18
$\log_{10} n_F$

(b)

Fig. 48.

n was, to a good approximation, the density of Z_1-centres at saturation, and hence assumption 1 above was largely unnecessary. The value of E obtained from the intercept was 1.78 eV, using $N = 2.21 \times 10^{23}$ for NaCl.

To summarize, the density of Ca^{++} ions giving rise to Z_1-centres was found from theory and experiment to be given by the relationship

$$\underline{N_z = (N_c N^4)^{1/5} \exp(-E/5kT),}$$

when N_z is small compared to N_c.

It was also found that a plot of $\log(N_c - n_f)$ against $\log n_f$, where n_f was the number of F-centres at saturation, gave a straight line whose slope was 7.04 (see figure 48(b)). By analogy with the above result this would suggest a relationship of the form

$$n_f = (N_c N^6)^{1/7} \exp(-E_f/7kT)$$

but, if this were true, the ratio n_f/N_z would depend upon N_c, and this is not in agreement with experiment. It would seem that the production of negative ion vacancies by the calcium, as might be expected, is a more complicated process than that of forming (incipient) Z-centres, and the detailed mechanism whereby they are produced is far from clear.

8.9 Accuracy of Results.

In order to assess the weight to be attached to these results, and in particular the accuracy of the activation energy, E, as determined above, it is necessary to consider the errors involved in the experimental results, and the validity of the assumptions made in the interpretation of them.

(a) Uniformity of Colouration.

It was assumed, in calculating an absorption coefficient from optical density measurements, that the crystals were uniformly coloured. Although the specimens were thin this condition was only approximately attained in practice because of the heterogeneous nature of the colouring X-ray beam and the high X-ray absorption of NaCl. Due to the latter, the colouration near the exposed surface deepens rapidly while that near the more distant surface deepens only slowly. The rate of growth of colouration obtained from the growth curves is therefore a mean value, and as such, depends upon the thickness of the specimen. It is important to note that lack of uniformity would not affect the result for the absorption coefficient at saturation, α_{∞}, provided the rate of growth was everywhere much greater than the rate of thermal decay, i.e. $kn \gg w$ (see section 8.6), but since this was not the case it was necessary to estimate t, the thickness of NaCl to reduce F, the flux of X-rays, low enough for kn to become comparable with w, i.e. about 10^{-6} sec^{-1}.

The emission from the copper target contained short wavelength lines situated on the wavelength scale around 1.4Å and these are responsible for the bulk colouration. The mass absorption coefficient for NaCl at 0.709Å is 7.89 cm^{-1}/gm per cc. Assuming the Bragg-Peirce Law to hold, viz. mass absorption coefficient proportional to the cube of the wavelength, the coefficient at 1.4Å is about 60 cm^{-1}/gm per cc. Since the density of NaCl is 2.2 gm per cc the absorption coefficient is about 130 cm^{-1}. Thus

$$F = F_o \exp(-130t),$$

where F_o is the X-ray flux falling on the surface of the crystal. From section 8.6

$$kn = \frac{SFN}{N_v} \doteqdot 10^{-10} F_o \exp(-130t),$$

putting $S = 10^{-16}$ cm^{-2}, $N = 10^{23}$ cm^{-3}, and $N_v = 10^{17}$ cm^{-3}. Letting F_o, as before, be 10^6 quanta/cm^2, the thickness, t, for which $kn = w \doteqdot 10^{-6}$ sec^{-1} is given by

$$t \doteqdot 130^{-1} \log_e 10^2$$

$$\doteqdot 0.03 \text{ cm}.$$

Thus the optical density at saturation as measured from the growth curves arises mainly from the colouration of the section of the crystal lying within 0.03 cm from the irradiated surface. The corresponding absorption coefficient, obtained by dividing the optical density by the total thickness of the crystal (about 0.05 cm), is therefore too small by a factor of 1.5 to 2.0. The N_z values are thus too low by the same amount.

The lack of uniformity explains why the points in the graphs of figure 48(a) and figure 48(b) at low concentration deviate markedly from the straight line, since these were obtained from the same specimen, which happened to be thicker than the rest (about 0.07 cm).

(b) Production of Vacancies.

It is known that X-rays produce vacancies (Leivo et al, 1949), but since it might be expected that the growth of colour centres in this way would be linear with time, whereas the actual growth tends exponentially towards a saturation value, this effect is probably negligible here. However, while the vacancies produced by the X-rays appear not to have a great effect on the colouration they may diffuse to dislocations and liberate Ca^{++} ions thus causing the deviation from exponential growth of the Z-band, noticed in high content crystals.

(c) Smakula's Formula.

The formula used to calculate the density of absorbing centres was derived by Smakula, who made the assumptions (a) that the electron was closely bound to the centre, and (b) that the shape of the absorption curve was Lorentzian. While the first of these assumptions is reasonable for the F- and Z-centres (see the calculations of J. H. Simpson, 1949, K. Lehovac, 1953, for example) the second is invalid since the absorption curve is Gaussian (see section 8.2, and C. Herring, 1956). When this is taken into account the formula for NaCl becomes

$$n = 7.24 \times 10^{15} \frac{\alpha W}{f},$$

instead of

$$n = 1.06 \times 10^{16} \frac{\alpha W}{f},$$

where n = the density of absorbing centres, α = the absorbtion coefficient at the peak, W = the bandwidth at half-maximum, and f = the oscillator strength, (see Dexter, 1956). This means that the n determined by Smakula's formula is too high by a factor of 1.48. However, as Herring points out, the oscillator strength as determined for the alkali halides by Pohl and his co-workers was estimated using Smakula's formula, and they obtained the value 0.81 for f. Using the formula given by Dexter they would have obtained the value 0.55, and this is presumably the correct value. Smakula's formula, therefore, gives the correct value for n, where the f of the formula is regarded as a factor arising from the Gaussian nature of the absorption curve and the oscillator strength, i.e. $f = 1.48 \times 0.55 = 0.81$.

(d) Vibrational Frequencies.

The formula

$$N_z = (N_c N^4)^{1/5} \exp(-E/5kT)$$

was derived neglecting the effect of changes brought about in the vibrational frequencies of the ions surrounding the calcium ion and the positive ion vacancy. If it is assumed that the effect on neighbouring ions is the same in each case, the formula becomes

$$N_z = (GN_c N^4)^{1/5} \exp(-E/5kT),$$

where

$$G = (v/v')^{2x},$$

v is the unchanged frequency of vibration of the x neighbours of an imperfection in the two directions perpendicular to the line joining the neighbour to the imperfection, and v' is the frequency along the line (see Mott and Gurney, 1948). For NaCl $x = 6$, so following Mott and Gurney and estimating v/v' as high as 2, we obtain for G the value 4×10^3. Thus the E which has been calculated is too low.

Another factor which was neglected is the temperature variation of E, which may be assumed to take the linear form

$$E = E_o - AT,$$

where E_o is the energy at absolute zero, and A is a coefficient related to the thermal expansion. Substituting for E in the above expression gives

$$N_z = (BGN_cN^4)^{1/5} \exp(-E_o/5kT),$$

where

$$B = \exp(A/k).$$

Mott and Gurney obtain a value of the order 10^2 for B, thus the estimated correcting factor, BG, is of the order 10^5.

It may be noted that none of the factors considered in this section have any effect on the slope of the $\log(N_c-N_z)$ versus $\log N_z$ plot; it is the intercept only which is affected.

8.10 The Corrected Value of E.

When the estimated corrections arising from considerations of the lack of uniformity of colouration, the effects on the vibrational frequency, and the temperature variation of E were applied it was found that E was raised from 1.78 eV to 1.93 eV. That is, the energy required to form a Ca^{++} ion centre in NaCl at absolute zero of temperature was found to be 1.9 eV.

That this value is reasonable may be seen from the following. The mechanism postulated in section 8.8 suggests that E is made up of three parts: (a) E_1, the energy required to remove one Ca^{++} ion and two Cl^- ions from a dislocation into the bulk; (b) E_2, the energy to form a positive ion vacancy; (c) E_3, the energy to form a Ca^{++} ion centre. It may be assumed that the Cl^- ions, apart from their elastic energy, do not change their energy.

According to Cottrel (1953) the elastic energy of a solute atom of radius r' at a distance

R from an edge dislocation is U, where

$$U = \frac{4}{3}G(r'-r)r^2 b \frac{\sin a}{R} \cdot \frac{(1+n)}{(1-n)}$$

Here, G = the shear modulus, r = radius of the solvent atom, b = the Burger's vector, a = the angle between R and the slip plane and n = Poisson's ratio. Putting $G = 3 \times 10^{11}$, r' (Ca^{++}) = 1.06Å, r = 0.98Å and n = 1/3, the maximum value for U (i.e. b/R = 1, sin a = 1) is about 0.04 eV, and this may be equated with E_1.

To the order of approximation at which we are working the Ca^{++} ion centre may be regarded as having the same energy of formation as a negative ion vacancy, since both carry an extra positive charge, electrostatic energy being the most important factor in NaCl lattice energy determinations. We can therefore equate $E_2 + E_3$ with the energy to form a pair of vacancies. In NaCl this has been estimated to be 1.86 eV, by Mott and Gurney (loc. cit.). Thus the total energy, E, is 1.90 eV. The close agreement between the two values is largely fortuitous, but the above considerations indicate that the value of E found from experiment is not unreasonable.

SUGGESTIONS FOR FURTHER WORK

(1) Investigation of the 345 mμ band in $NaCl.Ca^{++}$ with a view to determining its origin.

(2) Investigation of the relationship between the growth rates of the F- and Z-bands and the temperature from which a crystal is quenched. This should give a more accurate value for E.

(3) Purification of crystals by zone-melting techniques and subsequent investigation of the F-bandwidth and colouribility, taking dislocation densities into account.

(4) Investigation of the decay of the luminescence of quenched and coloured $NaCl.Mn^{++}$ with time; also the drop in the intensity of luminescence which can be induced, with time of annealing at various temperatures. This may throw light upon the electronic state of the Mn^{++} ion, and annealing mechanisms in the crystal. $NaCl.Ni^{++}$ is also a possible material for such work.

ACKNOWLEDGMENTS

It is a pleasure to acknowledge the help and supervision of this work given by Mr. J. E. Caffyn, and also the laboratory facilities provided by Professor J. E. P. Wagstaff, and his successor, Professor G. S. Rochester. Thanks are also due to Professor W. Curtis and Dr. E. E. Schneider of the Physics Department, King's College, Newcastle, for the loan of a grating monochromator; to Professor Coates and Mr. G. Martin of the Chemistry Department for permission to use a Unicam spectrophotometer, and also radioactive sources; to Professor Dunham and Mr. R. Phillips of the Geology Department for permission to use an X-ray unit; and to the Royal Society for a platinum crucible. The author is grateful to St. Cuthbert's Society, University of Durham, the Gateshead Borough Council, and the Department of Scientific and Industrial Research for maintenance awards. Finally, he would like to acknowledge the help and assistance given at various times by members of the Physics Department teaching staff, his fellow research students, Mr. F. Venmore of the laboratory workshop, and the members of the laboratory staff.

REFERENCES

Arsenjewa, A. Z. f. Phys. 57, 163 (1929).

Bassani, F. and Fumi, F.G. Phil. Mag. 45, 228 (1954).

Beale, R.N. and Roe, E.M.F. J. Sci. Inst. 28, 109 (1951).

de Boer, J.H. Recueil des Trav. Chim. d. Pays-Bas 56, 301 (1937).

Brauer, P. Z. Naturforsch 7a, 741 (1952).

Burstein, E. and Oberly, J.J. Phys. Rev. 79, 903 (1950).

Burstein, E. et al. Phys. Rev. 86, 255 (1952).

Camagni, P. et al. Phil. Mag. 45, 225 (1954).

Casler et al. J. Chem. Phys. 18, 887 (1950).

Chalmers, R. The Analyst, 79, 519 (1954).

Cottrel, A.H. "Dislocations and Plastic Flow in Crystals", Oxford Univ. Press (1953).

Dexter, D.L. Phys. Rev. 101, 48 (1956).

Dorendorf, H. Z. Physik, 129, 317 (1951).

Duerig, H. and Markham, J.J. Phys. Rev. 88, 1043 (1952).

Estermann et al. Phys. Rev. 75, 627 (1949).

Etzel, H.W. Phys. Rev. 87, 906 (1952).

Etzel, H.W. et al. Phys. Rev. 85, 1063 (1952).

Frenkel, Zeits. f. Phys. 35, 652 (1926).

Geiger, F. Phys. Rev. 99, 1075 (1955).

Goldstein, E. Zeits. f. Instrumentkunde 16, 211 (1896).

Goodfellow, T.L. Ph.D. Thesis, Univ. of Durham (1955).

Heiland, G. and Kelting, H. Z. Phys. 126, 689 (1949).

Herring, C. "Photoconductivity Conference, (Atlantic City)", p.81, Wiley (1956).

Hesketh and Schneider, E.E. Phys. Rev. 95, 837 (1954).

Hilsch, R. Z. f. Phys. 44, 860 (1927).

Hilsch, R. and Pohl, R.W. Z. f. Phys. 48, 384 (1928).

Hulme, Proc. Phys. Soc. B 68, 393 (1955).

Inui et al. Prog. Theoret. Phys. Jap. 8, 355 (1952).

Jahoda, E. Wien. Ber. IIa, 193, 675 (1927).

Kats, M.L.[(a)] Dolk. Akad. Nauk, S.S.S.R. 85, 539 (1952).

Kats, M.L.[(b)] Dolk. Akad. Nauk, S.S.S.R. 85, 757 (1952).

Kelting, H. and Witt, H. Z. Phys. 126, 697 (1949).

Kleinschrod, F.G. Ann. Physik, 27, 97 (1936).

Klick, C.C. and Shulman, J.H. J. Opt. Soc. Am. 42, 910 (1952).

Koref, F. Z. Elektrochem. 31, 249 (1925).

Kroger, F.A. Physica, 6, 369 (1939).

Kurtz, A.D. and Kulin, S.A. Acta Metallurg. 2, 353 (1954).

Kyropoulos, Z. anorg. Chem. 154, 308 (1926).

Kyropoulos, Z. f. Phys. 63, 849 (1930).

Larasch, S. and Turkevitch, J. Phys. Rev. 89, 1060 (1953).

Lax, M. J. Chem. Phys. 20, 1752 (1952).

Lehovac, K. Phys. Rev. 92, 253 (1953).

Leivo et al. Phys. Rev. 75, 627 (1949).

van Liempt, J.A.M. Z. Elektrochem. 31, 249 (1925).

Mador, I.L. et al. Phys. Rev. 91, 1277 (1953).

Mayence, J. and Vadar, B. C.R. Acad. Sci. Paris, 230, 634 (1950).

Mollwo, G. Ann. d. Physik, 29, 394 (1937).

Morton, C. J. Sci. Inst. 9, 289 (1932).

Mott and Gurney, "Electronic Processes in Ionic Crystals", Oxford Univ. (1940).

O'Rourke, R.C. Phys. Rev. 91, 265 (1953).

Petroff, S. Z. Phys. 127, 443 (1950).

Pick, H. Ann. d. Phys. 35, 73 (1939).

Pintsch, J. Gross. Jarhb. Radiotechn. v. Elektrotechnic. 15, 270 (1918).

Pohl, R.W. Proc. Phys. Soc. 49, 3 (1937).

Pohl, R.W. Phys. Z. 39, 36 (1938).

Pohl, R.W. Naturwissenschaften 39, 9 (1952).

Pringsheim, P. et al. Phys. Rev. 78, 293 (1950).

Pringsheim, P. et al. J. Chem. Phys. 21, 794 (1953).

Randall, J.T. Proc. Roy. Soc. Lond. 107 A, 272 (1939).

Randall, J.T. Trans. Farad. Soc. 25, 2 (1939).

Rothschild, S. Z. f. Phys. 108, 24 (1937).

Sauveur, A. Proc. Intern. Assoc. Testing Materials VI, Congr. 11, Sec. 1.

Schneider, E.E. and Caffyn, J.E. "Defects in Crystalline Solids", p.74, Physical Soc. (1955).

Scott, A.B. et al. J. Phys. Chem. 57, 757 (1953).

Seitz, F. J. Chem. Phys. 6, 150 (1938).

Seitz, F. Rev. Mod. Phys. 18, 384 (1946).

Seitz, F. Phys. Rev. 83, 134 (1951).

Seitz, F. Rev. Mod. Phys. 26, 7 (1954).

Shulman, J.H. et al. J. Opt. Soc. Amer. 40, 854 (1950).

Shulman, J.H. J. Phys. Chem. 51, 749 (1953).

Simpson, J.H. Proc. Roy. Soc. Lond. A 197, 269 (1949).

Smakula, A. Z. f. Phys. 45, 1 (1927).

Smakula, A. Z. Physik. 59, 603 (1930).

Spencer, E.G. et al. J. Chem. Phys. 20, 1177 (1952).

Stockbarger, D.C. Rev. Sci. Inst. 9, 426 (1938).

Thomas, T.B. M.Sc. Thesis, Univ. of Durham (1952).

Ueta, M. and Känzig, W. Phys. Rev. 94, 1390 (1954).

Verneuil, A. Ann. Chim. Phys. 8 ser. 3, 20 (1904).

Wagner and Schottky, Zeits. f. Phys. Chem. B 11, 163 (1930).

Willard and Greathouse, J. Am. Chem. Soc. 39, 2366 (1917).